

CLIPs regulate neuronal polarization through microtubule and growth cone dynamics

Dissertation zur Erlangung des Doktorgrades der Naturwissenschaften

an der Fakultät für Biologie
der Ludwig–Maximilians–Universität
München

Angefertigt am Max-Planck-Institut für Neurobiologie
in der Arbeitsgruppe 'Axonales Wachstum und Regeneration'

Vorgelegt von
Dorothee Neukirchen

München, 30. März 2010

Erstgutachter: PD Dr. Frank Bradke

Zweitgutachter: Prof. Dr. Rainer Uhl

Tag der mündlichen Prüfung: 19.Juli 2010

Ehrenwörtliche Versicherung:

Ich versichere hiermit ehrenwörtlich, dass ich die Dissertation mit dem Titel " CLIPs regulate neuronal polarization through microtubule and growth cone dynamics" selbständig und ohne unerlaubte Hilfe angefertigt habe. Ich habe mich dabei keiner anderen als der von mir ausdrücklich bezeichneten Hilfen und Quellen bedient.

Erklärung:

Hiermit erkläre ich, dass ich mich nicht anderweitig einer Doktorprüfung ohne Erfolg unterzogen habe. Die Dissertation wurde in ihrer jetzigen oder ähnlichen Form bei keiner anderen Hochschule eingereicht und hat noch keinen sonstigen Prüfungszwecken gedient.

München, 30.03.2010

Dorothee Neukirchen

Die vorliegende Arbeit wurde in der Arbeitsgruppe für „Axonales Wachstum und Regeneration“ von PD Dr. Frank Bradke am Max-Planck-Institut für Neurobiologie in Martinsried angefertigt.

Contents

List of figures.....	III
List of tables.....	IV
Abbreviations	V
1 Summary	- 1 -
2 Introduction	- 3 -
2.1 Neuronal polarity.....	- 3 -
2.2 The role of the cytoskeleton in neuronal polarity	- 5 -
2.2.1 Signaling pathways involved in neuronal polarization.....	- 5 -
2.2.2 The actin cytoskeleton.....	- 7 -
2.2.3 Microtubules.....	- 11 -
2.2.4 MAPs	- 13 -
2.2.5 Plus end tracking proteins (+TIPs).....	- 14 -
2.2.6 Cytoplasmic linker proteins 115 and 170.....	- 20 -
2.2.7 Hippocampal neurons as a model system for neuronal polarization	- 23 -
2.3 Objectives of this study.....	- 25 -
3 Results.....	- 26 -
3.1 CLIP function in hippocampal neurons.....	- 26 -
3.1.1 Localization of CLIP-115 and CLIP-170 in hippocampal neurons.....	- 26 -
3.1.2 Interference with CLIP function in hippocampal neurons.....	- 28 -
3.1.3 Interference with CLIP function inhibits axon formation.....	- 31 -
3.2 The microtubule-binding domain of CLIPs (MBD-CLIP)	- 34 -
3.2.1 Overexpression of <i>MBD-CLIP</i> leads to the formation of multiple axons.....	- 35 -
3.2.2 <i>MBD-CLIP</i> induced processes are differentiated axons	- 37 -
3.3 Microtubule dynamics after removal of CLIPs from microtubules	- 39 -
3.3.1 CLIPs organize the microtubule network in growth cones.....	- 39 -
3.3.2 Microtubule dynamics are impaired after <i>DN-CLIP</i> transfection	- 40 -
3.4 CLIPs influence the actin cytoskeleton of the growth cone	- 43 -
3.4.1 Growth cone structure and dynamics are impaired in <i>DN-CLIP</i> transfected neurons-	43 -
-	
3.4.2 Actin retrograde flow is not altered in DN-CLIP transfected neurons.....	- 45 -
3.4.3 Filopodia formation is impaired in <i>DN-CLIP</i> transfected neurons	- 46 -
3.5 Manipulation of the actin cytoskeleton rescues axon formation in <i>DN-CLIP</i> transfected neurons	- 47 -
3.6 A direct or indirect effect of CLIPs?.....	- 50 -
3.6.1 Destabilization of microtubules leads to a similar phenotype as the dominant negative construct of CLIPs.....	- 50 -

3.6.2	The actin cytoskeleton is also affected by destabilized microtubules.....	- 51 -
3.6.3	Inhibiting the interaction of CLIPs with the actin cytoskeleton results in the contrary phenotype of <i>DN-CLIP</i>	- 52 -
4	<i>Discussion</i>	- 56 -
4.1	CLIPs are key regulators during neuronal polarization	- 57 -
4.2	CLIPs and the microtubule network during neuronal polarization	- 59 -
4.3	CLIPs and the actin cytoskeleton during neuronal polarization	- 60 -
4.3.1	Microtubules as pushing force.....	- 61 -
4.3.2	Interaction of microtubules with the actin cytoskeleton.....	- 62 -
4.4	CLIPs for proper axon elongation	- 64 -
4.5	The “tug of war”	- 67 -
4.6	Concluding remarks	- 68 -
5	<i>Materials and Methods</i>	- 69 -
5.1	Materials	- 69 -
5.1.1	Chemicals.....	- 69 -
5.1.2	Drugs	- 70 -
5.1.3	Commercial kits	- 70 -
5.1.4	Equipment.....	- 71 -
5.1.5	Consumables.....	- 72 -
5.1.6	Media, buffers and standard solutions	- 73 -
5.1.7	Antibodies	- 77 -
5.1.8	Bacteria and Plasmids.....	- 79 -
5.2	Methods	- 80 -
5.2.1	Cell culture.....	- 80 -
5.2.2	Microscopy	- 81 -
5.2.3	Immunohistochemistry	- 83 -
5.2.4	Molecular Biology.....	- 84 -
5.2.5	Biochemistry.....	- 85 -
6	<i>References</i>	- 87 -
	<i>Acknowledgements</i>	- 100 -
	<i>Curriculum Vitae</i>	- 101 -
	<i>Publications</i>	- 102 -

List of figures

Figure 2-1: Neuronal network.....	- 4 -
Figure 2-3: Actin filaments.	- 8 -
Figure 2-4: Axonal growth cone.....	- 9 -
Figure 2-5: Axon elongation.	- 10 -
Figure 2-6: Microtubule polymerization.....	- 12 -
Figure 2-7: Mechanisms of microtubule plus-end tracking.	- 16 -
Figure 2-8: Structure of CLIP-115 and CLIP-170.	- 21 -
Figure 2-2: Development of hippocampal neurons in culture.	- 24 -
Figure 3-1: Localization of CLIPs in hippocampal neurons.	- 27 -
Figure 3-2: Downregulation of CLIP-115 and CLIP-170 in hippocampal neurons.....	- 29 -
Figure 3-3: Overexpression of <i>DN-CLIP</i> removes CLIPs from microtubules.....	- 31 -
Figure 3-4: Interference with the function of CLIPs impairs axon development.	- 32 -
Figure 3-5: Axons of <i>DN-CLIP</i> transfected neurons have less stable microtubules.	- 34 -
Figure 3-6: Overexpression of the microtubule-binding domain of CLIPs (<i>MBD-CLIP</i>) leads to the formation of functional multiple axons.....	- 35 -
Figure 3-7: Axons of <i>MBD-CLIP</i> transfected neurons do not show differences in microtubule-stability.....	- 37 -
Figure 3-8: MBD-CLIP transfected neurons develop differentiated axons.	- 38 -
Figure 3-9: Microtubule structure in <i>DN-CLIP</i> or <i>MBD-CLIP</i> transfected neurons.....	- 40 -
Figure 3-10: Microtubule growth speed is not altered in <i>DN-CLIP</i> transfected neurons	- 41 -
Figure 3-11: Overexpression of <i>DN-CLIP</i> impairs proper microtubule growth in the growth cone.	- 42 -
Figure 3-12: Growth cones are enlarged in <i>DN-CLIP</i> transfected neurons.....	- 44 -
Figure 3-13: Overexpression of <i>DN-CLIP</i> decreases growth cone dynamics.	- 45 -
Figure 3-14: Actin retrograde flow is not altered in <i>DN-CLIP</i> transfected neurons.	- 46 -
Figure 3-15: <i>DN-CLIP</i> transfected neurons provide less and immotile filopodia.	- 47 -
Figure 3-16: Modulating the actin cytoskeleton rescues axon formation in <i>DN-CLIP</i> transfected neurons.	- 49 -
Figure 4-1: CLIPs enable microtubule engorgement of the growth cone during axon formation.....	- 66 -

List of tables

Table 5-1: Chemicals used in this study.....	- 69 -
Table 5-2: Drugs used in this study.....	- 70 -
Table 5-3: Commercial kits.....	- 70 -
Table 5-4: Equipment.....	- 71 -
Table 5-5: Consumables.....	- 72 -
Table 5-6: Buffers and standard solutions.....	- 73 -
Table 5-7: Stock solutions.....	- 74 -
Table 5-8: N2 supplements.....	- 75 -
Table 5-9: Cell culture media.....	- 75 -
Table 5-10: Bacterial media.....	- 76 -
Table 5-11: Antibiotic stocks.....	- 76 -
Table 5-12: Primary antibodies used for immunohistochemistry.....	- 77 -
Table 5-13: Secondary antibodies.....	- 78 -
Table 5-14: Plasmids.....	- 79 -

Abbreviations

+TIP	Plus end tracking protein
ACF7	Actin cross-linking factor-7
ADF	Actin depolymerizing factor
ADP	Adenosin-diphosphat
APC	Adenomatous polyposis coli protein
Arp2/3	Actin related protein
ATP	Adenosin-triphosphat
CAP-Gly	Cytoskeleton-associated protein Gly-rich domains
Cdc42	Cell division cycle 42
C-domain	Central domain
CHO	Chinese Hamster Ovary cells
ChTOG	Colonic and hepatic tumor-overexpressed gene
CLASP	Cytoplasmic linker associated protein
CLIP	Cytoplasmic linker protein
DAPI	4',6-Diamidin-2'-phenylindol- dihydrochlorid
DIV	Days In Vitro
DN	dominant negative
E. coli	Escherichia coli
EB	End binding protein
ECL	Enhanced chemiluminiscence
EDTA	Ethylendiamin-tetraacetat
EGTA	Ethylenglykol-bis(aminoethylether)-N,N'-tetraessigsäure
Ena/VASP	Ena (enabled)/Vasp (vasodilator stimulated phosphoprotein)
FAP	Familial adenomatous polyposis
GAP	GTPase-activating proteins
GDI	Guanine nucleotide exchange inhibitors
GDP	Guaninediphosphate
GEF	Guanine nucleotide exchange factors
GFP	Green Fluorescent Protein

Gly	Glycin
GTP	Guanine-triphosphate
HC	Heavy chain
HEPES	2-(4-(2-Hydroxyethyl)- 1-piperazinyl)-ethansulfonsäure
IQGAP1	IQ motif containing GTPase activating protein
LIS1	Lissencephaly-1 protein
MACF	Microtubule actin cross-linking factor
MAP	Microtubule associated protein
MBD	Microtubule-binding domain
MCAK	Mitotic centromere-associated kinesin
MEM	Minimal essential medium
MgCl	Magnesiumchloride
MTOC	Microtubule organizing center
NaHCO ₃	Natriumhydrogencarbonat
Nap1	Nck-associated protein 1
NAV1	Navigator 1
PBS	Phosphate buffered saline
P-domain	peripheral domain
PFA	Paraformaldehyd
PIPES	Piperazin-N,N'-bis(2-ethansulfonsäure)
PSP	Postsynaptic potentials
Rac1	Ras-related C3 botulinum toxin substrate 1
Rap1b	RAS-related protein 1b
RhoA	Ras homolog gene family, member A
RT	Room Temperature
SDS	Dodecyl sulfat
shRNA	short hairpin RNA
siRNA	small interfering RNA
STIM1	Stromal interaction molecule-1
T-domain	Transitional domain
TEMED	N,N,N',N'-Tetramethylethylenediamine
WASP	Wiskott-Aldrich syndrome protein
WAVE	WASP-family verprolin-homologous protein

1 Summary

The formation of the axon is an initial event during the polarization of neurons (Barnes and Polleux, 2009), a critical process for a functioning nervous system. It relies on specific cytoskeletal changes that enable the growth of the axon, but restrain the growth of the remaining processes, the future dendrites (Craig and Banker, 1994). It has been shown that the actin cytoskeleton regulates neuronal polarization (Bradke and Dotti, 1999; Kunda et al., 2001). However, changes in actin dynamics alone are insufficient to preserve axon growth once growth is initiated (Bradke and Dotti, 2000). Recently, it was revealed that microtubules may play an active role in the formation of the axon in addition to their function as tracks for motor proteins and intracellular support of the sophisticated neuronal structure (Conde and Caceres, 2009). Microtubules of the subsequent axon were found to be more stable than microtubules of future dendrites in both cerebellar and hippocampal neurons (Arregui et al., 1991; Witte et al., 2008). Moreover, modest pharmacological stabilization of microtubules could transform both minor neurites and mature dendrites into growing axons (Gomis-Ruth et al., 2008; Witte et al., 2008). While these data suggest that microtubule stability may be a basic process that regulates neuronal polarity, we know relatively little about which molecules are important for its regulation (Conde and Caceres, 2009).

In my thesis, I investigated the role of a family of microtubule plus-end tracking proteins (+TIPs), the Cytoplasmic Linker Proteins (CLIPs) 115 and 170, during neuronal polarization. CLIPs are known to regulate microtubule stability and dynamics by binding to microtubule growing ends (Komarova et al., 2002). Here, I had aimed to investigate whether CLIPs are necessary and sufficient for the formation of an axon, and if so, which underlying cytoskeletal mechanisms would be involved in this process.

Using hippocampal neurons in culture, I addressed neuronal polarization after inhibition of CLIP function, which led to significantly impaired axon formation. In contrast, overexpression of the microtubule-binding domain of CLIPs induced the formation of supernumerary axons. Thus, I showed that CLIPs are necessary and sufficient to induce axon formation.

To examine the underlying changes of the cytoskeleton after inhibiting the function of CLIPs, I focused on changes of the microtubule and actin network. In neurons transfected with the dominant negative mutant of CLIPs, microtubules were less stable, splayed and did not grow into the peripheral domain of the growth cone in contrast to control neurons or neurons transfected with the microtubule-binding domain of CLIPs. Moreover, growth cones were enlarged, less mobile, and exhibited an increased number of actin arcs. Pharmacological increase of microtubule-stability or the dynamicity of the actin cytoskeleton led to the rescue of axon formation of CLIP-dominant negative transfected neurons. Taken together, impaired axon formation of neurons with non-functional CLIPs is based on affected microtubule and actin dynamics, as manipulation of the cytoskeleton leads to the rescue of axon formation.

To further characterize whether the microtubule-actin-interaction is important for neuronal polarization, I targeted the molecular interaction of CLIP-170 with its actin-binding partner IQGAP1. Inhibition of their interaction decreased microtubule catastrophe rates and enhanced axon growth. This suggests that capturing microtubules at the actin cytoskeleton is necessary for controlled microtubule growth.

In summary, my data show that CLIPs are necessary and sufficient for axon formation by regulating microtubule stability and actin arc formation. Moreover, the interaction of microtubules with the actin cytoskeleton is important for controlled microtubule growth.

2 Introduction

2.1 Neuronal polarity

Neurons are amongst the most polarized cell types. They are compartmentalized into two functionally and morphologically different domains – the axon and several dendrites - which both emerge from the cell body (**Figure 2-1**). Axons and dendrites are drastically different in their morphology, their cytoskeletal organization, physiological function and signaling properties.

Axons grow as long and thin processes, whereas dendrites are shorter and tapered, and appear branched. The polarization of a neuron into axons and dendrites during neuronal development is essential for their assigned functions, namely the transfer of information to other neurons or non-neuronal cells. Dendrites receive incoming information from other neurons (**Figure 2-1**). In contrast, axons are the main units for propagating these signals to other neurons. These signals of electrical origin are called action potentials and are initiated at a specialized trigger region, the initial segment or axon hillock. From there, the action potential is carried along the axon to its tip, where the axon divides into fine branches that establish sites of communication with other neurons. These communication sites are called synapses. An arriving action potential at the synapse promotes the release of neurotransmitters from the synaptic vesicles of the presynaptic cell into the synaptic cleft, which separates the pre- and postsynaptic cell. Most presynaptic cells establish synaptic contacts on neuron's dendrites, the cell body or also, but less often, on the proximal or distal end of the axon of the receiving cell. Receptors in the postsynaptic membrane of the receiving cell bind the released neurotransmitters, which then leads to the generation of postsynaptic potentials (PSPs). Depending on the type of the receptor, these potentials can be of an inhibitory or excitatory nature. By summing up these signals in the dendrite and the soma, a new action potential is generated.

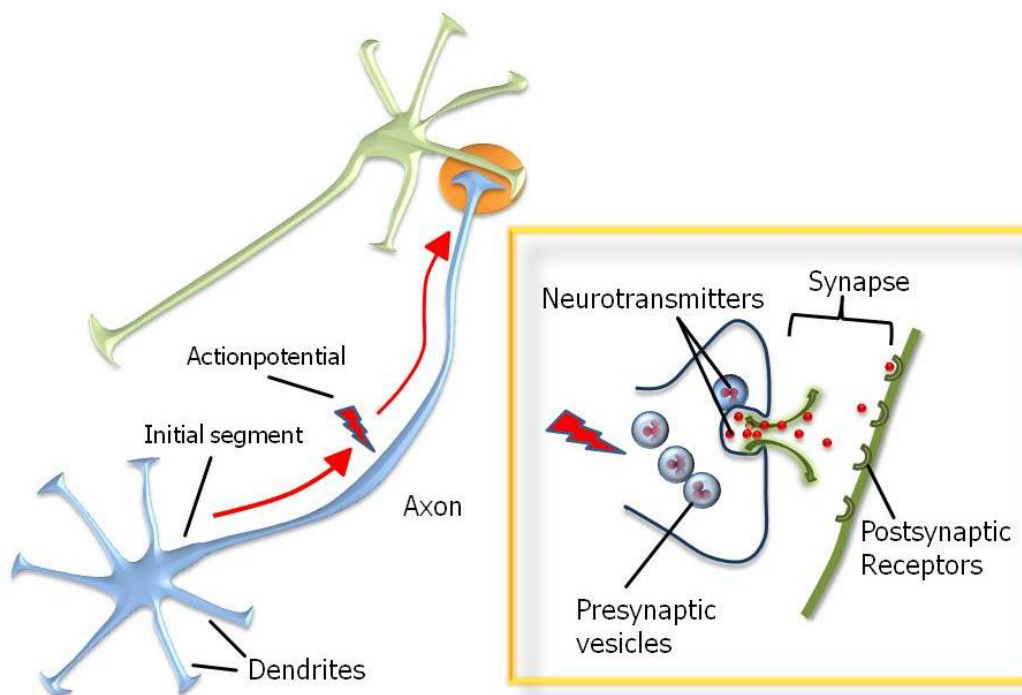


Figure 2-1: Neuronal network. Neurons generate action potentials at the initial segment of the axon, which are conducted down to the axon terminals. At the synapse, the action potential stimulates the release of neurotransmitters from the synaptic vesicles of the presynaptic cell into the synaptic cleft (blow up). Receptors in the postsynaptic membrane bind the released neurotransmitters, which then lead to the generation of postsynaptic potentials (PSPs).

The establishment and maintenance of neuronal polarity is seen as a segregation of protein and lipid repertoires that are specific for axons or dendrites, such as receptors, ion channels, transporters and adhesion molecules. Mechanisms regulating this selective arrangement of proteins include for example physical barriers for diffusion and transport of membrane proteins and lipids (Nakada et al., 2003; Song et al., 2009; Winckler et al., 1999), selective trafficking and membrane insertion of newly synthesized membrane components (Burack et al., 2000), selective retention of the components after initial nonselective transport (Sampo et al., 2003), and the transcytosis from dendrites to axons of axon-targeting proteins (Wisco et al., 2003; Yap et al., 2008).

However, the initial signals that establish cellular asymmetries and the underlying pathways are largely unknown.

2.2 The role of the cytoskeleton in neuronal polarity

2.2.1 Signaling pathways involved in neuronal polarization

In the last decades, a large number of studies have investigated the molecular players and pathways involved in neuronal polarization and improved our knowledge how neuronal polarity is established (reviewed in (Barnes and Polleux, 2009)). In order to examine the role of specific proteins in the establishment of neuronal polarity, different approaches have been used: the targeted genetic inactivation of one or more genes within an animal (Knock-out mice); mRNA and protein knockdown using RNAi; overexpression of mutated forms of specific proteins; pharmacological inhibition of proteins by drugs. These experiments brought many insights into the signaling pathways underlying neuronal polarization. I will focus on one group of signaling molecules known to be key regulators of neuronal polarity, the Rho GTPases.

Rho GTPases regulate various signal transduction pathways in all eukaryotic cells. Rho GTPases are implicated in the regulation of neuronal polarity, and are well known for their role in regulating the actin cytoskeleton. However, they also have an important role in the regulation of microtubule dynamics, membrane transport, and gene transcription. Their mode of operation depends on the cycling between an inactive GDP (guanine diphosphate)-bound state and an active GTP (guanine triphosphate)-bound state, which is controlled by GAPs (GTPase-activating proteins), GEFs (guanine nucleotide exchange factors) and GDIs (guanine nucleotide exchange inhibitors).

In total, there are about 22 mammalian Rho GTPases identified (reviewed in (Barnes and Polleux, 2009)), among which RhoA (ras homolog gene family, member A), Rac1 (ras-related C3 botulinum toxin substrate 1) and Cdc42 (cell division cycle 42) are the best studied members of this group. In general, active Cdc42 and Rac1 enhance neurite outgrowth, whereas RhoA activity counteracts the formation neurite formation.

Expression of a Cdc42 mutant, which autonomously cycles between its active and inactive state, leads to the formation of multiple axons (Schwamborn and Puschel, 2004). Moreover, genetic ablation of Cdc42 in mice, as well as the knockdown of Cdc42 by RNAi evoked a strong defect in axon specification (Garvalov et al., 2007; Schwamborn and Puschel, 2004). It was suggested that Cdc42 is subject to the control of Rap1b, a member of the Ras superfamily of GTPases, during neuronal polarization (Schwamborn and Puschel, 2004). Rap1b is found at the tip of the nascent axon and its overexpression is followed by the establishment of multiple axons. While RNAi against Rap1b leads to impaired axon formation, the expression of the Cdc42 mutant, which autonomously cycles between its active and inactive state, rescues this phenotype.

The function of Rac1 during neuronal polarization is still controversial, which may suggest a more complex role in this process. For example, Rac1 played a role in neurite outgrowth in *Drosophila* (Hakeda-Suzuki et al., 2002; Ng and Luo, 2004; Ng et al., 2002), whereas its loss in mammalian cells did not affect axon specification (Gualdoni et al., 2007). Other studies demonstrated a lack of polarization after using a dominant-negative form of Rac1. Yet another study showed that overexpression of a constitutively active Rac1-mutant did not affect axon formation (Schwamborn and Puschel, 2004).

In contrast, the role of RhoA is less profound than that of Rac1. While using a constitutive active form of RhoA led to the inhibition of neuritogenesis (Bito et al., 2000), the expression of a dominant negative RhoA mutant enhanced neurite outgrowth (Schwamborn and Puschel, 2004).

The Rho GTPases RhoA, Rac1 and Cdc42 have in common that their pathways merge at the level of LIM kinase, which phosphorylates its downstream effector cofilin, acting directly on actin nucleation and polymerization.

2.2.2 The actin cytoskeleton

Actin filaments (F-actin) are composed of two helical strands of polymerizing actin monomers (G (globular) -actin), and are about 6 nm in diameter. Globular actin exists in three versions: ATP-actin, ADP-Pi-actin and ADP-actin (**Figure 2-3**). During actin polymerization, ATP-actin binds to the barbed end of the actin polymer. After binding, ATP-actin undergoes two steps of hydrolysis, producing first ADP-Pi-actin and then ADP-actin. ADP-actin dissociates from the pointed end and is recycled before the cycle starts again. The binding of the different nucleotides occurs along the filament, resulting in different areas with ATP-actin at the barbed end, ADP-Pi-actin in the middle of the filament and with ADP-actin close to the pointed end. Although ATP-actin and ADP-actin can dissociate from both the barbed end (fast growing) and the pointed end (slow growing), dissociation of ADP-actin from the pointed end is favored (Pollard and Borisy, 2003). This leads to a polymerization at the barbed end and a fast dissociation from the pointing end, resulting in net growth of the filament at the barbed end (see Figure 2-3).

More than 60 classes of actin-associated proteins regulate the dynamics of actin filaments. These include WAVE (Wiskott-Aldrich syndrome protein [WASP]-family verprolin-homologous protein), ADF (actin depolymerizing factor)/Cofilin, profiling, Nap1 (Nck-associated protein 1) and the Ena (enabled)/Vasp (vasodilator stimulated phosphoprotein) family of proteins (Ishikawa and Kohama, 2007). By influencing actin dynamics in different manners, these proteins modulate the actin cytoskeleton to implement neuronal polarization.

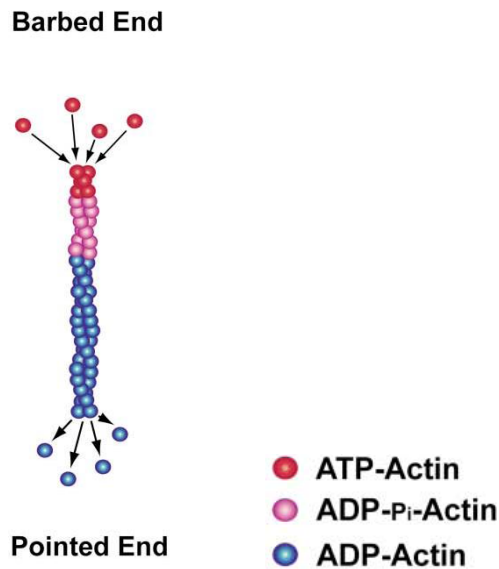


Figure 2-2: Actin filaments. Actin filaments consist of two helical strands of polymerizing globular actin monomers. Polymerizing globular actin is associated with ATP (red subunit), which undergoes two steps of hydrolysis, producing first ADP-P_i-actin (pink subunits) and then ADP-actin (blue subunit). ADP-actin dissociates from the pointed end and becomes recycled before the cycle starts again. At the so-called plus- or 'barbed' end addition of globular actin prevails (i.e. polymerization), making it the faster-growing end. Scheme from Dent and Gertler, 2003.

Highly dynamic actin structures compose the periphery of the neuronal growth cone, a specialized structure at the tip of growing axons. The growth cone is composed of three domains: the central (C) domain, the transition (T) domain, and the peripheral (P) domain (**Figure 2-4**). Filopodia, finger-like structures, are found both in the P and T domain, and mainly contain packed bundles of actin filaments (F-actin). In contrast, lamellipodia are localized within the P domain, and are organized as a flat network of actin filaments. Filopodia and lamellipodia both have a polarized organization within the growth cone with their barbed ends oriented to the distal membrane of the growth cone and the pointed ends facing toward the basal region. With the barbed ends pointing to the distal membrane, actin polymerization causes filopodia and lamellipodia to extend. Simultaneously, the actin polymerization creates a force that pushes the actin network and therefore also the closely linked membrane backwards. This process is called "retrograde flow". Moreover, myosin-II, a molecular motor that generates forces on F-actin, supports retrograde flow by contraction of actin filaments in the T domain. This results in the generation of actin

arcs in the T domain (**Figure 2-4**), orienting perpendicular to the axis of filopodia (Schaefer et al., 2002). Actin arcs prevent microtubules from invading the peripheral region (Burnette et al., 2008; Lee and Suter, 2008; Lowery and Van Vactor, 2009; Schaefer et al., 2008). During active growth phases, actin filaments disassemble in the transitional domain and actin arcs reorient towards the growth direction, creating an F-actin-free corridor into which microtubules protrude (Lee and Suter, 2008).

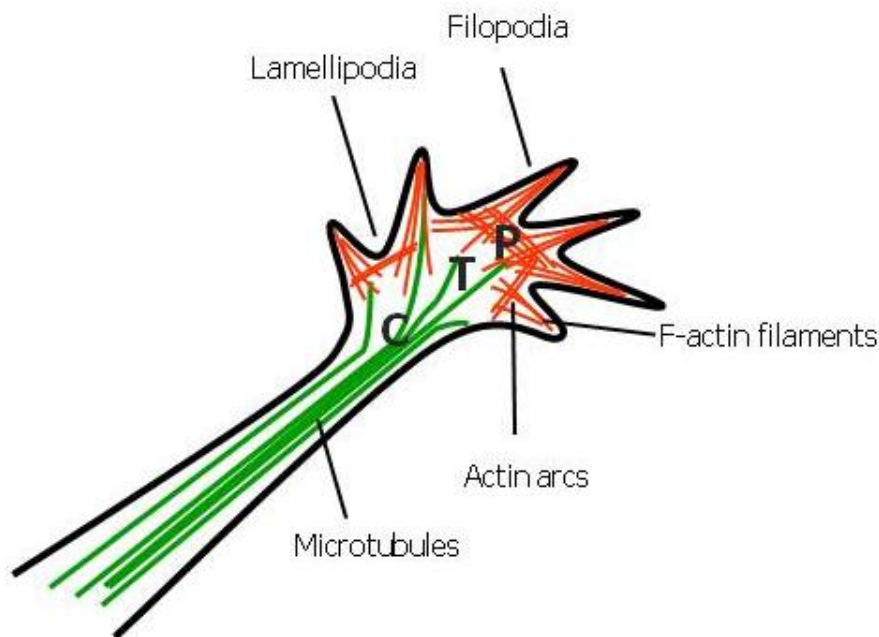


Figure 2-3: Axonal growth cone. The axonal growth cone exists of 3 different domains: the central (C) domain, the transition (T) domain and the peripheral (P) domain. Microtubules elongate along the axon, invade the C-domain of the axonal growth cone and sometimes extend into the P-domain along filopodia. Filopodia are found both in the P and T domain, and contain packed bundles of actin filaments. Lamellipodia are localized within the P domain and organized as a flat network of actin filaments. Actin arcs are generated by the contraction of actin filaments in the T domain via myosin-II, and orient perpendicular to the axis of filopodia.

For axonal extension, the growth cone repeatedly undergoes a cycle of specific steps (Goldberg and Burmeister, 1986; Lowery and Van Vactor, 2009) (**Figure 2-5**). First, filopodia and lamellipodia explore the cellular environment and protrude; the growth cone frequently expands at this stage. Then, dynamic microtubules engorge from the central growth cone area into the former transitional domain, in which then actin filaments are disassembled; the remaining actin arcs reorient towards the growth

axis. The protruding microtubules transport vesicles, organelles and, probably, actin-modulating proteins into the engorged area. The extension of the neurite becomes consolidated by the bundling of microtubules in the central domain of the growth cone. In this way, the proximal part of the growth cone resumes a cylindrical shape and becomes part of the axonal shaft. Repeated courses of these three events result in axon growth. In contrast, these processes do not operate in the minor neurites, thus growth is restricted to the axon.

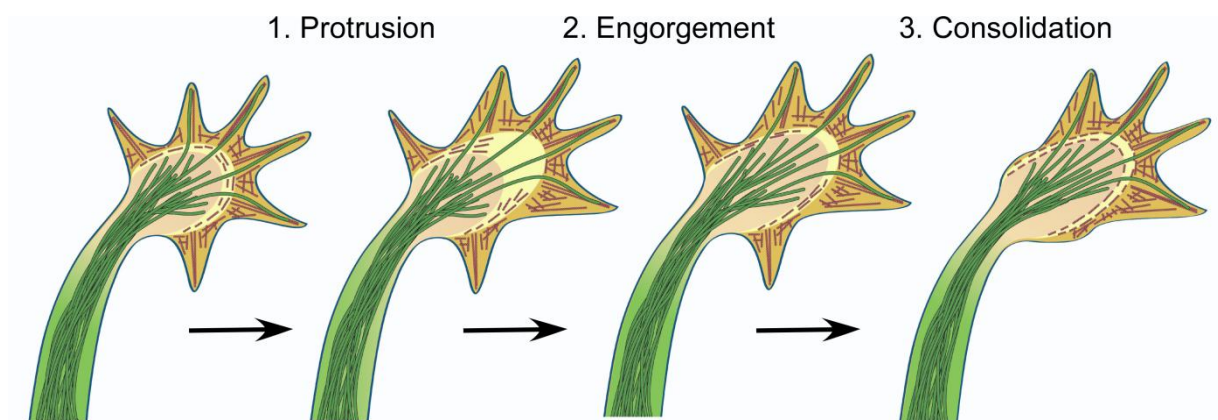


Figure 2-4: Axon elongation. Axon elongation consists of 3 repeating steps. First, filopodia and lamellipodia enable the growth cone to extend distally (*Protrusion*). Then, dynamic microtubules engorge from the central growth cone area into the former transitional zone, where actin filaments disassemble and the remaining arcs reorient towards the growth axis (*Engorgement*). Protruding microtubules transport vesicles and organelles into the engorged area. The extension of the neurite consolidates by the bundling of microtubules in the central domain; the proximal part of the growth cone resumes cylindrical shape and becomes part of the axonal shaft (*Consolidation*).

Actin filaments and their dynamics play an important role during neuronal polarization (Witte and Bradke, 2008). Two hallmarks of the actin cytoskeleton identify the future axonal growth cone of unpolarized neurons: on the one hand, the actin cytoskeleton exhibits decreased stability compared to the other minor neurites; and on the other hand, its dynamics are increased (Bradke and Dotti, 1999). Therefore, local actin instability reduces the impediment for protruding microtubules. This, in turn, could lead to the formation of an axon, which is supported by experiments using actin-destabilizing drugs (Bradke and Dotti, 1999). Hence, actin-modulating proteins, which influence actin dynamics or polymerization in neuronal

growth cones, have been revealed to play a pivotal role during the establishment of neuronal polarity.

2.2.3 Microtubules

Microtubules are hollow cylindrical polymers of 25 nm in diameter (**Figure 2-6**). On the lateral level, microtubules are assembled of 13 short protofilaments (Evans et al., 1985), which are, in turn, built up by head-to-tail associated α -/ β -tubulin-heterodimers (**Figure 2-6**) (Amos and Klug, 1974). Due to the specific assembly of tubulin heterodimers, microtubules are polar structures with a fast-growing end ("plus end"), terminated by the β -subunit, and a slow-growing end ("minus end"), terminated by the α -subunit (Allen and Borisy, 1974). The polymerization of microtubules is driven by the high affinity of tubulin-GTP dimers for the plus end of the microtubules. Shortly after assembly, tubulin can hydrolyze GTP when bound to β -tubulin. In contrast GTP, which is bound to the α -subunit of tubulin, is stable. GDP-tubulin is prone to depolymerization and will therefore fall off the tip of a microtubule. As only GTP-bound tubulin subunits bind to the growing end of microtubules, a cap of GTP-containing tubulin protects microtubules from disassembly.

In most mammalian cells, microtubules are controlled by microtubule organizing centers (MTOC) (reviewed in (Luders and Stearns, 2007)). The centrosome, one important MTOC, is the classical site to nucleate and anchor microtubule minus ends in a process that requires a γ -tubulin. This results in microtubule plus ends pointing outwards. However, in neurons, microtubule orientation was reported not to be uniform throughout all neuronal compartments. Microtubules exhibit a plus end distal distribution in the axon and a mixed polarity with both plus and minus end distal microtubules in dendrites (Baas, 1998; Baas et al., 1988).

Microtubules carry out a variety of essential functions within the cell. For example, microtubules form the mitotic spindle that is necessary for cell division, serve as tracks along which vesicles or organelles are transported through the cell tracks, or

also function as important factors of cell polarity. To fulfill these variety of functions, microtubules undergo different posttranslational modifications, including acetylation/deacetylation, tyrosination/detyrosination, generation of $\Delta 2$ -tubulin, polyglutamylation, polyglycylation, palmitoylation and phosphorylation (reviewed in (Westermann and Weber, 2003)). Subjects of these modifications are the carboxy-terminal tails of α - β -tubulin-heterodimers.

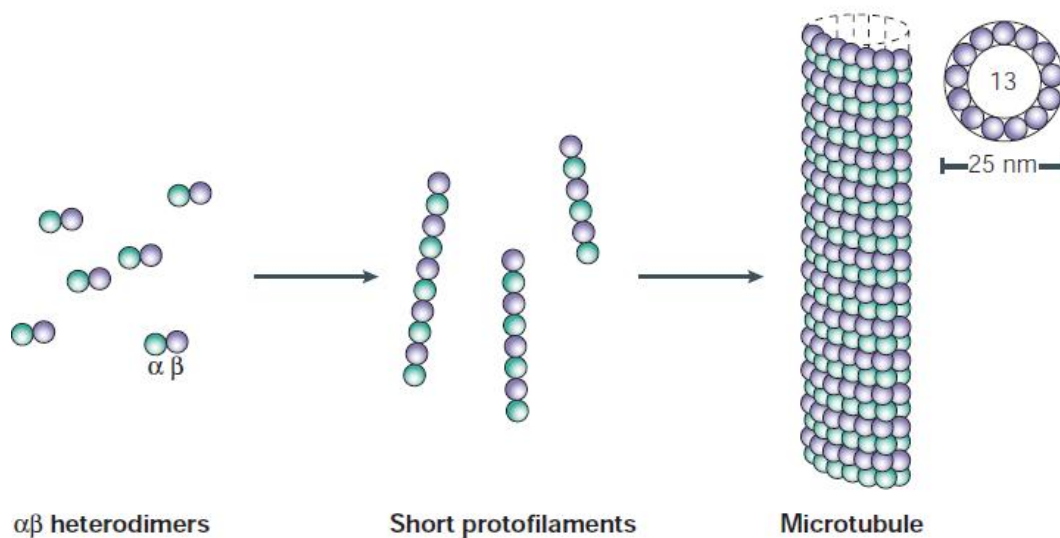


Figure 2-5: Microtubule polymerization. Microtubules are cylindrical polymers of 25 nm in diameter, assembled of 13 short protofilaments (Evans et al., 1985), which are, in turn, built up by head-to-tail associated α - β -tubulin-heterodimers (Amos and Klug, 1974). Scheme from Westerman and Weber, 2003.

So far, studies examining the mechanisms that regulate neuronal polarization have mostly focused on proteins influencing the actin cytoskeleton. However, microtubules also accomplish several important tasks during the development of neurons. They provide mechanical support for cell shape, or function as tracks along which molecular motors, such as kinesins or dyneins, move organelles to different compartments of the cells reviewed in (Goldstein and Yang, 2000). Moreover, microtubules are necessary for growth cone motility and axonal growth, growth cone steering, cell migration and branching (Buck and Zheng, 2002; Suter and Forscher, 1998). To deal with these tasks by efficiently probing the intracellular space, microtubules are highly dynamic structures. A fraction of microtubules frequently

undergoes switching between prolonged phases of growth and rapid shrinkage, a phenomenon called dynamic instability (Mitchison and Kirschner, 1984). The transition from growth to shrinkage is termed catastrophe, whereas the opposite transition is termed rescue. Microtubule instability is regulated by two different groups of factors: microtubule-stabilizing and microtubule-destabilizing factors. Microtubule-stabilizing factors act on microtubules by either preventing catastrophes of microtubules, by rescuing a depolymerizing microtubule or by decreasing shrinkage speeds. This group includes for example the tau protein, different microtubule-associated proteins (MAPs), doublecortin (DCX), or several members of the plus end tracking protein family (+TIPs). In contrast, microtubule-destabilizing factors regulate microtubule instability by inducing catastrophes, preventing rescues or increasing shrinkage speeds. Different members of the kinesin-13 family and the kinesin-8 family, as well as Op18/stathmin belong to the group of microtubule-destabilizing proteins.

2.2.4 MAPs

Microtubule instability and organization are regulated by a protein group called MAPs (Microtubule Associated Proteins; reviewed in (Cassimeris and Spittle, 2001)). MAPs are proteins that bind all the way along microtubules and, thereby, stabilize them and promote their assembly. A great effort of characterization has been performed on one family of MAPs, the MAP2/Tau-family. In neurons, MAPs were found to weakly increase the polymerization of microtubules, to strongly suppress catastrophes and to promote rescues (Drechsel et al., 1992; Pryer et al., 1992; Trinczek et al., 1995) by crosslinking adjacent tubulin subunits. Down-regulation of MAP2 inhibits neurite formation, whereas down-regulation of Tau using anti-sense inhibits axon formation (Caceres and Kosik, 1990; Caceres et al., 1992). However, knockout mice of MAP2 and Tau did not show any detectable polarity defects, suggesting a redundant effect by other MAPs (DiTella et al., 1996).

2.2.5 Plus end tracking proteins (+TIPs)

2.2.5.1 Subgroups of +TIPs

One specialized group of MAPs are the plus end tracking proteins (+TIPs), which are conserved in all eukaryotes and specifically accumulate at growing microtubule plus ends. Based on their structural elements, they can be classified into 5 different groups: EB family proteins, CAP Gly proteins, proteins containing basic and Ser-rich sequences, HEAT- and WD40-repeat proteins, and microtubule motor proteins (Table 1).

Table 2 - 1: +TIPs

+TIPs	Members
EB family proteins	EB1, EB2, EB3
CAP Gly proteins	CLIP-170, CLIP-115, p150 ^{Glued}
Proteins containing basic and Ser-rich sequences	CLASP1/2, APC, MACF/ACF7, STIM1
HEAT- and WD40-repeat proteins	LIS1, XMAP215/ChTOG
Microtubule motor proteins	MCAK, Dynein HC, kinesins

End binding (EB) proteins are composed of an N-terminus and a C-terminus, which are separated by a linker sequence. While the N-terminus is necessary and sufficient for the binding to microtubules (Hayashi and Ikura, 2003), the coiled-coil region of the C-terminus mediates the parallel dimerization of EB monomers (Honnappa et al., 2005). The coiled-coil region partially overlaps with the unique EB-like motif (end binding homology (EBH) domain), which is highly conserved.

Cytoskeleton-associated protein Gly-rich proteins contain cytoskeleton-associated protein Gly-rich (CAP-Gly) domains at their N-termini, which are responsible for their microtubule-attachment, EB- and dynactin-interaction (Goodson et al., 2003; Perez et al., 1999; Schroer, 2004). The adjacent coiled-coil region

mediates the homodimerization of CLIPs. In CLIP-170 the coiled-coil region is flexible and allows an intramolecular “folding back” of the protein, which results in the autoinhibition of CLIP-170 (Lansbergen et al., 2004). Its cargo-binding C-terminus contains two tandemly repeated metal-binding motifs, which is lacking in its close homologue CLIP-115 (De Zeeuw et al., 1997).

Proteins that contain basic and Ser-rich sequences are predicted to be flexible and to mediate interactions with microtubules and EB proteins. Adenomatous polyposis coli protein (APC; (Nathke, 2004), microtubule-actin crosslinking factor (MACF; (Sonnenberg and Liem, 2007), CLIP-associating proteins (CLASPs; (Galjart, 2005)) and the transmembrane protein stromal interaction molecule-1 (STIM1; (Grigoriev et al., 2008)) are a few members of this group.

HEAT- and WD40-repeat proteins contain several tumor-overexpressed gene (TOG) domains in their N-terminus, which, in turn, are comprised of several HEAT repeats (Al-Bassam et al., 2007; Slep and Vale, 2007). The N-terminal end also enables their binding to tubulin and microtubules (Gard et al., 2004). Lis1 (Lissencephaly-1 protein) is comprised of a WD40 repeat-containing domain which seems to enable the targeting of CLIP-170, dynein and dynactin (Coquelle et al., 2002; Tai et al., 2002).

Microtubule motor proteins include kinesins, mitotic centromere-associated kinesin (MCAK), and cytoplasmic dynein. The specific accumulation of kinesins and cytoplasmic dynein at microtubule plus ends involves regions outside their microtubule-interacting motor domains and relies on their association with other +TIPs.

2.2.5.2 Mechanism of plus end tracking

Although some +TIPs are able to bind along the entire lattice of microtubules (XMAP, Stu), most of them are known to exclusively decorate the plus end of polymerizing microtubules. How can the specific accumulation of +TIPs to the growing ends of microtubules be explained? The most likely reason is a preference for structural or

chemical properties of the plus end in contrast to the rest of the tube (**Figure 2-7**). The GTP cap at microtubule plus ends is too short to cover the area of +TIPs accumulation (0.5-2 μm). Therefore, specific structures of the tubulin sheet or individual protofilaments, or certain tubulin sites inside the tube might regulate the plus end tracking behavior of +TIPs (for example members of the EB-family).

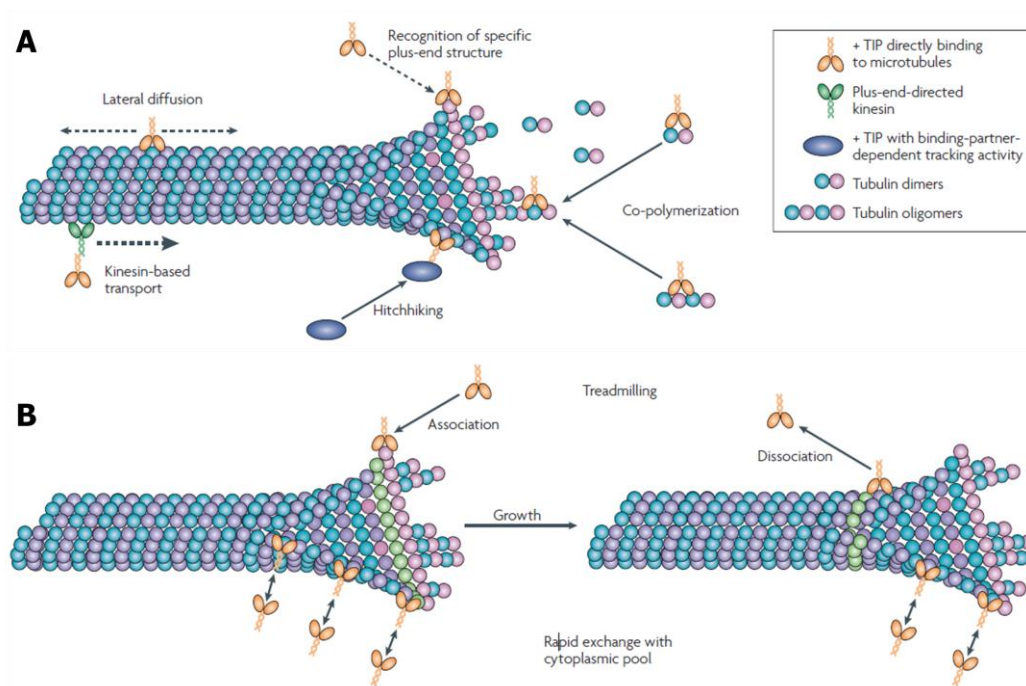


Figure 2-6: Mechanisms of microtubule plus-end tracking. A) +TIPs can reach the microtubule tips by diffusion in the cytoplasm or along the microtubule lattice, or can also be transported to microtubule plus ends by kinesins. +TIP accumulation at the microtubule ends can be caused by their preference for a specific structural or chemical property associated with microtubule polymerization. The affinity of some +TIPs for the microtubule end may depend on their binding partners. Some +TIPs might also co-polymerize with tubulin dimers or oligomers. **B)** +TIPs that recognize a specific structure at the growing microtubule end (or co-polymerize with tubulin) might be immobilized at the ends until this structure is converted into the regular microtubule lattice (tubulin dimers shaded in green). +TIPs may exchange rapidly at their binding sites at the microtubule ends, while these binding sites decay over time during microtubule lattice maturation. Scheme from Akhmanova and Steinmetz, 2008.

In vitro studies showed that some +TIPs also accumulate at microtubule plus ends by co-polymerizing with tubulin dimers or oligomers (e.g. mammalian CLIPs), and are then released from the older lattice (Folker et al., 2005; Perez et al., 1999). This mechanism implies that +TIPs redistribute in the cytoplasm by diffusion and achieve

high concentrations at growing microtubule tips. The following dissociation of +TIPs from microtubule ends can either occur spontaneously or can be stimulated by structural changes of the microtubule lattice. Other mechanisms, such as a kinesin-dependent transport of +TIPs in non-mammalian (Bik1 and Tip1, the CLIP homologues in budding and fission yeast (Busch and Brunner, 2004; Carvalho et al., 2004)) and mammalian cells (APC; (Jimbo et al., 2002)), or the transport of +TIPs via association with microtubule associated partners ("hitchhiking"; (Carvalho et al., 2004)) were recently described as well.

2.2.5.3 Regulation of microtubule dynamics by +TIPs

+TIPs are localized at the microtubule plus ends, so they are perfectly positioned to control the behavior of microtubules. Although +TIPs in general chose the same target, namely the plus ends of growing microtubules, they confer different effects on microtubule dynamics. While EB proteins decrease catastrophe events (Lansbergen and Akhmanova, 2006), and kinesin-13 family members destabilize microtubules and promote catastrophes (Moore and Milligan, 2006), CLIPs can stimulate rescue events and enable microtubules to switch from a shrinking mode into a growing mode (Komarova et al., 2002). In contrast, CLASPs or APC act as microtubule-stabilizing factors (Galjart, 2005; Lansbergen and Akhmanova, 2006).

Although the mechanisms of +TIPs on microtubule dynamics are under intensive investigation, it is still not completely clear how the individual +TIPs act. For CLIP-170, it was shown that its N-terminus induces the formation of tubulin rings, structures that were suggested to be involved in the process of microtubule assembly (Arnal et al., 2004). The generation of tubulin-rings would then generate conditions in which CLIP-170 could promote microtubule rescue. In contrast, CLASPs or APC could prevent catastrophe and promote rescue by binding the distal end of microtubules. EB proteins could positively influence microtubule growth by supporting to zipper the microtubule lattice (Sandblad et al., 2006). The identification of the exact mechanism and function of +TIPs is complicated by their direct interactions with many others +TIPs.

However, one interesting feature of +TIPs in general is that, although they provide a complex interaction-network, they seem to function through unique pathways and to influence microtubule dynamics independently from each other (Huisman and Segal, 2005; Wolyniak et al., 2006).

2.2.5.4 Functions of +TIPs in neurons

Most studies of +TIPs have been done in fibroblasts or non-polarized epithelial cells, where they play an important role in the formation and functioning of the mitotic apparatus (Maiato et al., 2004). In mammalian tissue, +TIPs play essential roles in cell differentiation as well as diverse aspects of cell functioning, including important developmental processes in neurons, as discussed below. The importance of +TIPs can be clearly seen in severe neuronal disorders, such as “familial adenomatous polyposis” (FAP), “Miller-Dieker lissencephaly”, or “Williams-Syndrome” (reviewed in (Jaworski et al., 2008), in which mutations of the encoding genes of APC, LIS1 or CLIP115 have been identified.

TIPs in neuronal migration

Lissencephaly, which literally means “smooth brain”, is a brain formation disorder caused by a mutation in the gene coding for Lis1. The mutation results in the failure of postmitotic neurons to migrate from the ventricular zone to the cortical plate during embryogenesis (Kato and Dobyns, 2003). By transfecting siRNA against Lis1 or dynein together with GFP-labeled EB3 *in utero*, the group of Vallee showed that both proteins are essential for neuronal migration by regulating centrosome and nuclear translocation (Tsai et al., 2007). Both proteins seemed to act on the microtubule network, and thus on the organization of centrosome and nuclear positioning. In line with these data, CLIP-170 was suggested to be also involved in this process, as it targeted Lis1 and dynein to microtubule plus ends (Coquelle et al., 2002; Kholmanskikh et al., 2006; Lansbergen et al., 2004). Moreover, Lis1 may also regulate the actin cytoskeleton via IQGAP and Cdc42 and by capturing microtubules to the cortical actin cytoskeleton (Kholmanskikh et al., 2006).

+TIPs in axonal growth cone dynamics

Several +TIPs have been studied in the context of growth cone dynamics and axon extension. For example, the orthologue of Clasp1 and 2 in *Drosophila* (Orbit or MAST) are involved in axon guidance in flies. It signals to the Slit-Robo pathway to modulate the extension of microtubules in the growth cone upon exposure to a chemorepellent cue (Lee et al., 2004). In *Xenopus* neurons, CLASP2 decorates a specific fraction of microtubules in the growth cone, which, in turn, penetrates into the leading edge of actin-rich filopodia. When overexpressed, microtubules formed loops and only a reduced number of microtubules reached the leading edge of the growth cone, suggesting that CLASP2 acts as a microtubule-stabilizer (Mimori-Kiyosue et al., 2005).

APC, which also acts as a microtubule-stabilizer, accumulates at microtubule plus ends in the growth cones (Zhou et al., 2004). This accumulation is lost when its upstream effector GSK3 β is blocked. As a result, the growth cone collapses. Moreover, the interaction with the end binding protein 1 (EB1) seems to be required for proper axon elongation, as APC mutants lacking the domains for EB-interaction inhibited axon elongation.

Interestingly, both CLASPs and APC seem to crosslink microtubules with the actin network, as both proteins feature, additionally to the microtubule-binding site, an actin-binding sequence (Tsvetkov et al., 2007; Moseley et al., 2007). Moreover, APC offers the ability to signal indirectly to the actin cytoskeleton through the interaction with IQGAP1, a Rac1 and Cdc42 activator (reviewed in (Nathke, 2006)).

Another +TIP, Lis1, was shown to be, together with dynein, an important player during axon remodeling. The inhibition of both proteins hindered microtubules to penetrate into the peripheral zone of growth cones, probably evoked by a reduced ability to resist the actin retrograde flow (Grabham et al., 2007).

Navigator1 (NAV1), a +TIP member only found recently, binds to the distal ends of microtubules and the peripheral domains of growth cones. Moreover, Nav1 was shown to be important for growth cone dynamics and neuronal migration (Martinez-Lopez et al., 2005).

2.2.6 Cytoplasmic linker proteins 115 and 170

CLIPs, the **C**ytoplasmic **L**inker **P**roteins 115 and 170, have a particular role among all +TIPs, because CLIP-170 was identified as the first member of the +TIP family in 1992 (Pierre et al., 1992). Following its structure, CLIP-170 can be divided into 3 main domains: the N-terminus, the coiled-coil domain and the C-terminus (**Figure 2-8**).

The N-terminus possesses two similar CAP-Gly motifs, which are responsible for its attachment to microtubules, as demonstrated *in vitro* (Pierre et al., 1992). The N-terminus is also responsible for the binding of CLIPs to EBs (Goodson et al., 2003; Ligon et al., 2006; Perez et al., 1999) and IQGAP1, an actin-binding protein (Fukata et al., 2002).

The potential metal binding domain at the C-terminus was shown to be involved in the autoinhibition of CLIP-170. Thereby, CLIP-170 is folding back on itself, owing to an intramolecular interaction between the N- and the C-terminal domain (Lansbergen et al., 2004). This was suggested to be a mechanism used by CLIP-170 to prevent any unwanted interactions of CLIP-170 with other proteins. The C-terminal domain binds to Lis1 and dynactin (Coquelle et al., 2002; Lansbergen et al., 2004) and is thus responsible for CLIP participation in the dynein pathway. Moreover, the C-terminal domain was shown to mediate the interaction between organelles and microtubules.

The N- and C-termini are separated by a coiled-coil region, which is important for the establishment of parallel homodimers, the conformation that allows CLIPs to be functional. Furthermore, the coiled-coil domain enables the interaction of CLIPs with CLASPs (Akhmanova et al., 2001).

Both CLIP-170 and CLIP-115 are expressed in the developing nervous system (Jaworski et al., 2009). However, unlike CLIP-170, CLIP-115 has a shorter coiled-coil domain and lacks the metal binding domain at the C-terminus, thus lacking the ability to bind organelles and vesicles.

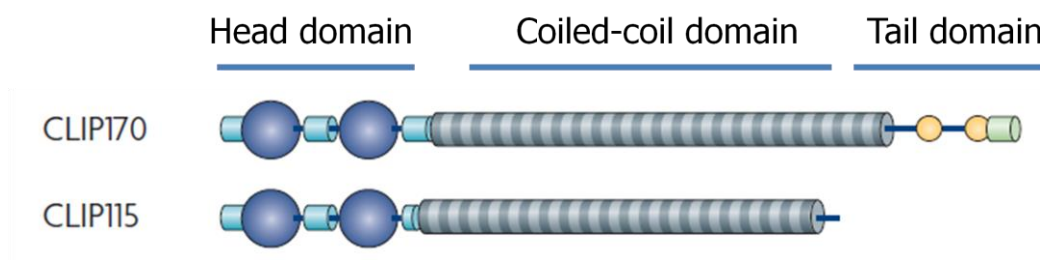


Figure 2-7: Structure of CLIP-115 and CLIP-170. CLIP-170 can be divided into 3 main domains: the N-terminus, the coiled-coil domain and the C-terminus. The N-terminus is comprised of two CAP-Gly motifs, which are responsible for its attachment to microtubules, and the binding of CLIPs to EBs and IQGAP. The interaction between the N-terminus and the metal binding domain of the C-terminus leads to the autoinhibition of CLIP-170, which might be a mechanism used by CLIP-170 to prevent unwanted interactions of its N- and C-terminal domains. The C-terminal domain binds to Lis1 and dynactin mediates the interaction between organelles and microtubules. The coiled-coil region is responsible for the establishment of parallel homodimers, and enables the interaction of CLIPs with CLASPs.

Functions of CLIPs

CLIPs carry out different functions during the development of various cell types by influencing microtubule organization and dynamics. In fission yeast for example, the homologue of CLIP-170 acts as an anticatastrophe factor for premature microtubules that had not yet reached the cell cortex. In contrast, in mammalian cells (e.g. CHO cells), CLIP-170 and CLIP-115 operate as rescue factors in a redundant way, supporting microtubules' switch from depolymerization to polymerization. This activity is located in the N-terminal domain of CLIPs (Komarova et al., 2002). Moreover, different studies interfering with CLIP-170-function in human cell lines revealed an essential role for CLIP-170 during mitosis where it localizes to the kinetochores of chromosomes (Dujardin et al., 1998; Wieland et al., 2004). The binding to the kinetochores is mediated through the C-terminus of CLIP-170 and might be enabled by regulators of dynein (Coquelle et al., 2002), in whose pathway CLIP-170 is suggested to be involved. Interestingly, there is also evidence that CLIP-170, together with different binding partners, is involved in the transport and localization of dynein and dynactin to the microtubule plus ends. Although the protein-protein interactions of CLIPs are conserved, different studies showed that

CLIP-170 is not necessary for dynein-dynactin localization in every cell type (Lansbergen et al., 2004; Niccoli et al., 2004).

CLIP-170 function on the dynamics of microtubules also draws attention to the polarization of cells. Brunner and Nurse demonstrated that CLIP-170 regulates microtubule dynamics in fission yeast and enables microtubules to discriminate cortical regions (Brunner and Nurse, 2000). However, when investigating the function of CLIP-170 in mice by genetic depletion, CLIP-170 seemed not to be necessary for the viability or the development of the nervous system (Akhmanova et al., 2005). CLIP-170 only affected the structural function in the male germ line, specifically in spermatid differentiation and sperm head shaping. In contrast, genetic depletion of CLIP-115 showed neurodevelopmental abnormalities (Hoogenraad et al., 2002), including an increased brain-ventricle volume or decreased size of the corpus callosum. However, these defects were not severe, as mice were viable and fertile.

Studies by the group of Kaibuchi suggested CLIP-170 can establish a link to the actin cytoskeleton by interacting with the actin-binding protein IQGAP1 (Fukata et al., 2002). Together with two important Rho GTPases Cdc42 and Rac1, CLIP-170 and IQGAP1 form a complex, which might capture microtubules to the actin cytoskeleton. Additionally, a complex involving these players was essential for the polarization of Vero cells (Fukata et al., 2002).

To summarize, CLIP-170 could provide an important link to the actin cytoskeleton by capturing microtubules to the cell cortex, alone or together with other +TIP-members, for potential delivery of actin-modulating proteins.

2.2.7 Hippocampal neurons as a model system for neuronal polarization

One main goal in the field of neuroscience is to identify the underlying mechanisms that specify the formation of the axon. Hippocampal neurons cultured from rat or mouse brain are among the best established systems to study this question (Craig and Banker, 1994; Dotti et al., 1988).

The hippocampus is located in the medial temporal lobe of the brain and belongs to the limbic system, which plays a vital role in several different functions such as long term memory, behavior, emotion and olfaction. The hippocampus itself is a structure essential for the formation of new memory. Damage of the hippocampus can lead to the lack of ability to form new memories or to the loss of memory that was achieved before damage.

In order to investigate the mechanisms underlying the establishment of neuronal polarity, culturing hippocampal neurons bears lot of advantages. First, under appropriate conditions, dissociated hippocampal cultures consist almost exclusively of neurons, with only a small fraction of contaminating interneurons or non-neuronal cells. Second, hippocampal neurons develop and mature *in vitro* without external cues which exist under natural conditions or in *in vivo*-slices. Therefore, this system is a representative model to study the function of specific extracellular signals on neuronal polarization and the cell-autonomous intracellular machinery regulating neuronal polarity. Third, as cultured hippocampal neurons can be maintained for up to one month, it is possible to observe living cells during their development.

Cultured hippocampal neurons reliably polarize *in vitro* by establishing one axon and several dendrites. Their development proceeds in a typical manner and is divided into five different developmental stages (Dotti et al., 1988); **Figure 2-2**). Directly after plating, neurons attach to the surface and appear as round spheres surrounded by dynamic membrane, the so called lamellipodia (stage 1). Within the next 12 hours, neurons start to form between 4-5 short and highly dynamic processes of same length, morphology and functionality, termed minor neurites (stage 2). At approximately day 1.5, only one of the minor neurites enriches with membrane,

organelles and cytosolic proteins (Bradke and Dotti, 1997). Only this minor neurite will undergo a boost of growth and elongation to become the axon (stage 3). At day 4 in culture, the other minor neurites begin to extend and differentiate into dendrites, while the axon continues to grow (stage 4). In this stage, proteins are segregated into axonal and dendritic compartments (Bradke and Dotti, 2000), indicating the molecular polarization of axons and dendrites.

After 7 days in culture, neurons start to establish synaptic contacts via their newly formed dendritic spines with their neighboring neurons to integrate into the neuronal network (stage 5). At this stage, neurons are functionally polarized.

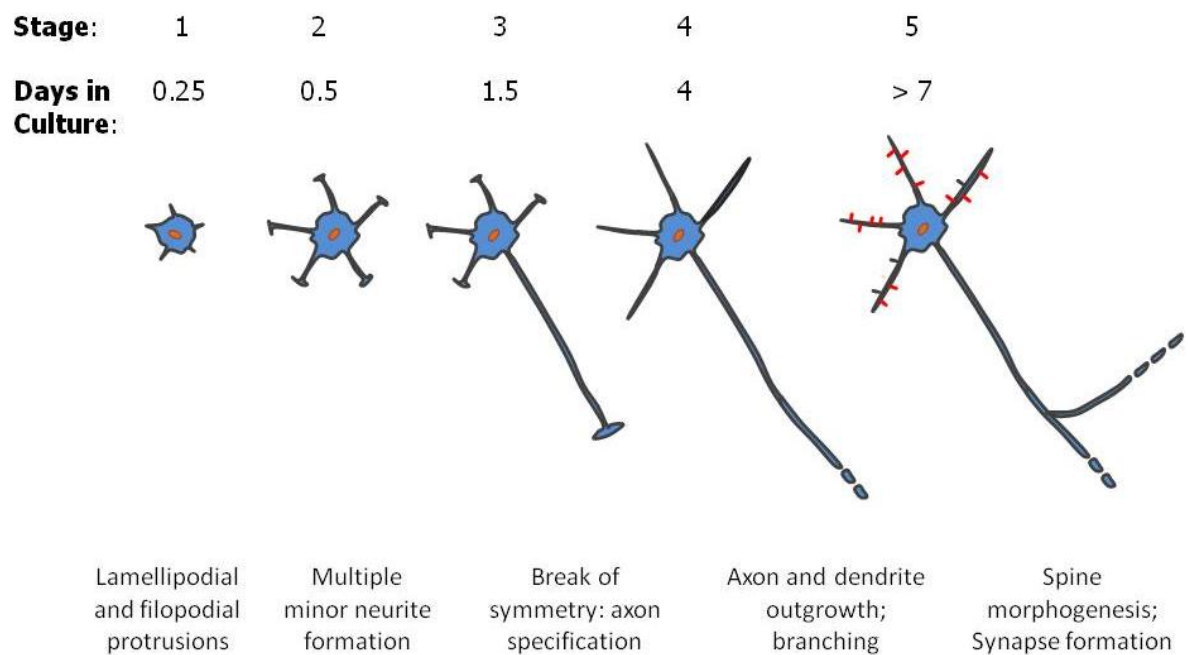


Figure 2-8: Development of hippocampal neurons in culture. Dissociated neurons typically undergo different stages of development, divided into stage 1 to 5 (Dotti et al., 1988).

2.3 Objectives of this study

Only recently, cytoskeletal dynamics emerged as a key process during neuronal polarization (Arimura and Kaibuchi, 2007; Witte and Bradke, 2008). In particular, pharmacological studies depicted microtubule stability as a putative determining factor for neuronal polarization (Witte et al., 2008). Interestingly, only modest stabilization of microtubules leads to axon formation, while strong microtubule stabilization results in the inhibition of the establishment of an axon (Witte et al., 2008). Therefore, I sought a microtubule-binding factor that only moderately changes the stability of microtubules by affecting their dynamics. I focused my investigation on a family of microtubule plus-end tracking proteins (+TIPs), the Cytoplasmic Linker Proteins 115 and 170 (CLIPs), as they were shown to regulate microtubule dynamics and polarity processes in other cell types (Brunner and Nurse, 2000; Fukata et al., 2002). To investigate the role of CLIPs during neuronal polarization, I asked whether the depletion of CLIPs or the overexpression of the microtubule-binding domain of CLIPs interferes with axon formation. Moreover, to investigate the underlying cytoskeletal mechanisms, I observed microtubule and actin dynamics after modifying the function of CLIPs. My data show that CLIPs are necessary and sufficient for axon formation. Furthermore, I show that CLIPs regulate axon formation by affecting microtubule stability and by positively regulating dynamics of the axonal growth cone and restraining actin arc formation. Thus, CLIPs regulate the polarization of neurons by affecting the microtubule and actin network in the axonal growth cone.

3 Results

Previous studies showed that both CLIP-115 and CLIP-170 are expressed in the developing nervous system (Jaworski et al., 2009). Besides its potential interaction with the actin cytoskeleton (Fukata et al., 2002), the CLIP-170 homologue tip1 is a critical regulator of cellular polarity in fission yeast (Brunner and Nurse, 2000) and known to interact with essential polarity effectors, such as the small Rho GTPases Rac1 and Cdc42. Moreover, CLIPs modulate microtubule stability by rescuing microtubule dynamics in macrophages and Chinese hamster ovary (CHO) cells (Binker et al., 2007; Komarova et al., 2002). However, the function of CLIPs during the development of neurons was never studied in detail. Taken together, these data make CLIPs interesting candidates to elucidate their function during neuronal polarity.

In my thesis, I investigated the role of a family of microtubule plus-end tracking proteins (+TIPs), the Cytoplasmic linker proteins 115 and 170 (CLIPs) during neuronal polarization. The most important finding in my thesis was that non-functional CLIPs led to the impairment of axon formation, not only by affecting microtubule stability and dynamics, but also by affecting the growth cone dynamics and actin contractility.

3.1 CLIP function in hippocampal neurons

3.1.1 Localization of CLIP-115 and CLIP-170 in hippocampal neurons

To gain a first insight how CLIPs could be involved in neuronal polarization, I first examined the localization of CLIPs in dissociated, cultured rat hippocampal neurons. Microtubules are present in both the minor neurites and the axon, and mainly grow from the cell body in direction to the tips of all processes. As CLIPs bind to the tips of growing microtubules (Perez et al., 1999), I expected CLIPs decorating growing

microtubule tips distributed throughout all compartments of the neurons. By immunohistochemistry, using an antibody that recognizes both CLIP-115 and CLIP-170, CLIP-comets were found within the cell body, the neurites and their tips of both unpolarized (stage 2; **Figure 3-1A**) and polarized (stage 3; **Figure 3-1B**) neurons. These patterns are reminiscent of CLIP structures at microtubule tips within non-neuronal cells, such as Chinese Hamster Ovary (CHO) cells or macrophages (Binker et al., 2007; Hoogenraad et al., 2000; Komarova et al., 2002; Pierre et al., 1992).

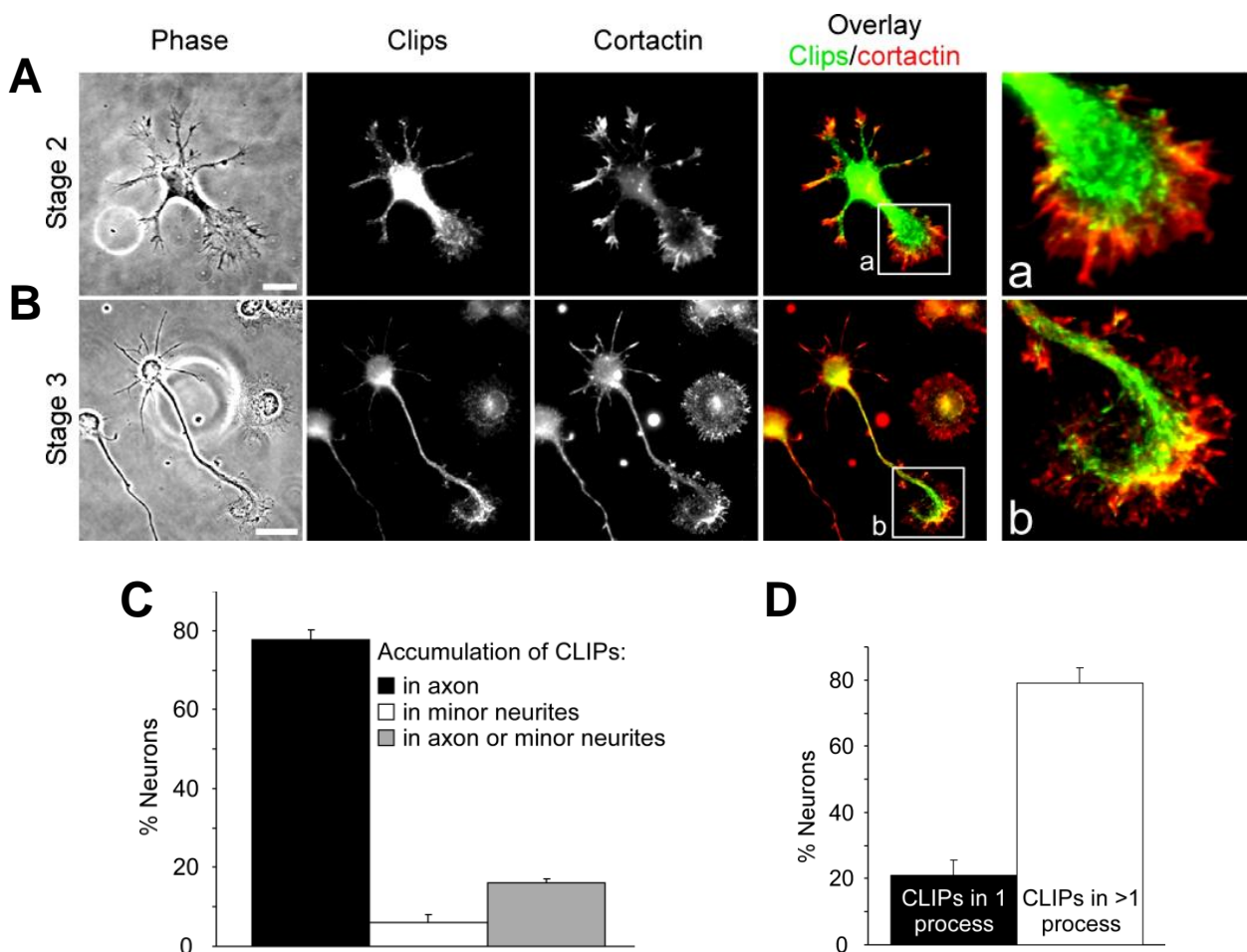


Figure 3-1: Localization of CLIPs in hippocampal neurons. Unpolarized stage 2 (**A**) and polarized stage 3 (**B**) rat hippocampal neurons were stained for CLIPs (CLIP-115 and 170) and cortactin. CLIPs bind to microtubule plus ends as comet-like structures. In stage 3 neurons (**A**), CLIPs are strongly enriched in growth cones, where they overlap with actin-rich regions. **A-a**, **B-b**, Blow ups of regions marked in A and B. Scale bars, 20 μ m. **C**, Quantification of CLIP-localization in stage 3 neurons (n=180 neurons from 3 independent cultures). **D**, Quantification of CLIP-localization in stage 2 neurons (n=200 neurons from 3 independent cultures).

In growth cones of both stage 2 and stage 3 neurons, CLIPs partially overlapped with the actin cytoskeleton (stained with anti-Cortactin) within the transitional zone (**Figure 3-1A, B**). In 79 ± 4.7 % of stage 2 neurons, CLIPs localized within multiple neurites and were only accumulated to one minor neurite in 21 ± 4.7 % of the cells (**Figure 3-1A, D**). In contrast, CLIPs were accumulated exclusively to the axonal growth cone in 77.8 ± 2.3 % of the neurons and rarely found gathered to one of the minor neurites (**Figure 3-1B, C**; 6.1 ± 1.9 %).

Hence, due to their localization, CLIPs could be potential candidates for regulating neuronal polarization by enabling the interaction between microtubules and the actin cytoskeleton.

3.1.2 Interference with CLIP function in hippocampal neurons

To assess whether CLIPs play a role during axon development, I interfered with the function of CLIPs in developing neurons. As a first approach, I depleted the endogenous proteins using RNA interference. To downregulate CLIPs, I transfected neurons with shRNA for CLIP-115, CLIP-170 or both proteins simultaneously before plating them (scrambled shRNA as a control). After 3 days of culturing the cells, western blot analysis showed that neurons transfected with CLIP-115/170-shRNA exhibited similar CLIP expression levels as neurons transfected with scrambled shRNA. However, after 5 days in vitro (DIV) CLIPs expression levels were significantly downregulated compared to scrambled shRNA transfected neurons (**Figure 3-2A**). An antibody against actin was used as a loading control.

Depletion of CLIPs led to a 60% reduction in axon growth from 3 to 5 DIV (**Figure 3-2B**) compared to control cells or neurons transfected with shRNA for either CLIP-115 or CLIP-170 alone (**Figure 3-2B**; data not shown for single shRNA-transfection). To test whether this effect on axon growth was specific to CLIP function, I reintroduced a vector containing the CLIP head domain (*MBD-CLIP*), which is sufficient for protein-microtubule attachment and reduction of catastrophe rates in CHO cells (Komarova et al., 2002). As the shRNA for CLIP-115 and CLIP-170

was targeted to regions of their coiled-coil domain, the *MBD-CLIP* construct could not be silenced by the shRNAs. As a result of overexpressing *MBD-CLIP*, the axon growth defect was compensated in CLIP-115/170-shRNA expressing neurons (**Figure 3-2C**) to an axon length comparable with control conditions (**Figure 3- 2C**; $222 \pm 2.1 \mu\text{m}$ for sh-CLIPs + *MBD-CLIP*, $251 \pm 9.3 \mu\text{m}$ for sh-scrambled + GFP).

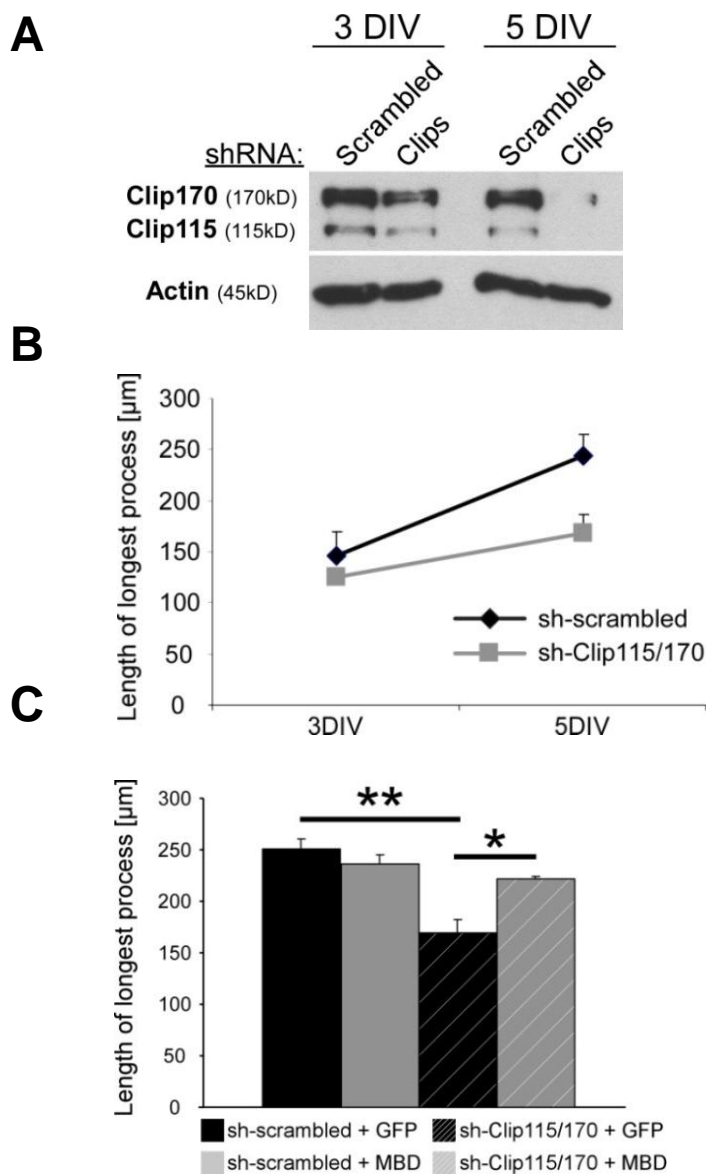


Figure 3-2: Downregulation of CLIP-115 and CLIP-170 in hippocampal neurons. **A**, Cells were transfected with either scrambled shRNA or shRNA for CLIP-115 and CLIP-170 and lysates taken at 3 and 5 DIV. Antibodies against CLIPs and actin were used. **B**, Quantification of length of longest process of neurons transfected with scrambled shRNA or shRNA for CLIP-115 and CLIP-170 after 3 and 5 DIV. Neurons, knocked down for CLIP-115 and CLIP-170, show shorter axons than the control cells after 5 DIV. **C**, Quantification of length of longest process of neurons transfected with scrambled shRNA or shRNA for CLIP-115 and CLIP-170 together with either GFP or GFP-tagged *MBD-CLIP*. Overexpression of *MBD-CLIP* rescues axon development in neurons knocked down for CLIP-115/170 ($n > 236$ neurons from 4 independent cultures; * $p < 0.05$, ** $p < 0.01$).

Depletion of CLIP proteins was not achieved during neuronal polarization within the first 24 hours, which was probably due to shRNA expression timing or to the half-life of CLIP proteins. Therefore, I chose a different approach to interfere with CLIP function. To examine whether CLIPs indeed play a role during this process, I used a dominant negative (DN) CLIP-170 mutant form fused to GFP (*DN-CLIP*). This mutant was lacking the microtubule-binding head domain, which enables CLIPs' attachment to microtubules. The mode of operation of this dominant mutant of CLIPs can be explained by its feature of autoinhibition. In the wild type situation, the tail domain exhibits an affinity to the head domain of CLIP. By folding back on itself, CLIPs enable the interaction of the tail domain with the head domain, which results in their inhibition. When overexpressed, the dominant negative mutant of CLIPs, which contains the coiled-coil region and the tail domain (**Figure 3-3A**), binds to the head domain of endogenous full length CLIPs. Thereby, endogenous CLIPs are inhibited to attach to microtubules, as their head domain is occupied with the tail-domain of the CLIP mutant. Consistent with previous studies in fibroblasts (Komarova et al., 2002), I found that expression of this dominant negative CLIP mutant removed endogenous CLIP-comets from the microtubules in 60% of the neurons (**Figure 3-3B, C**).

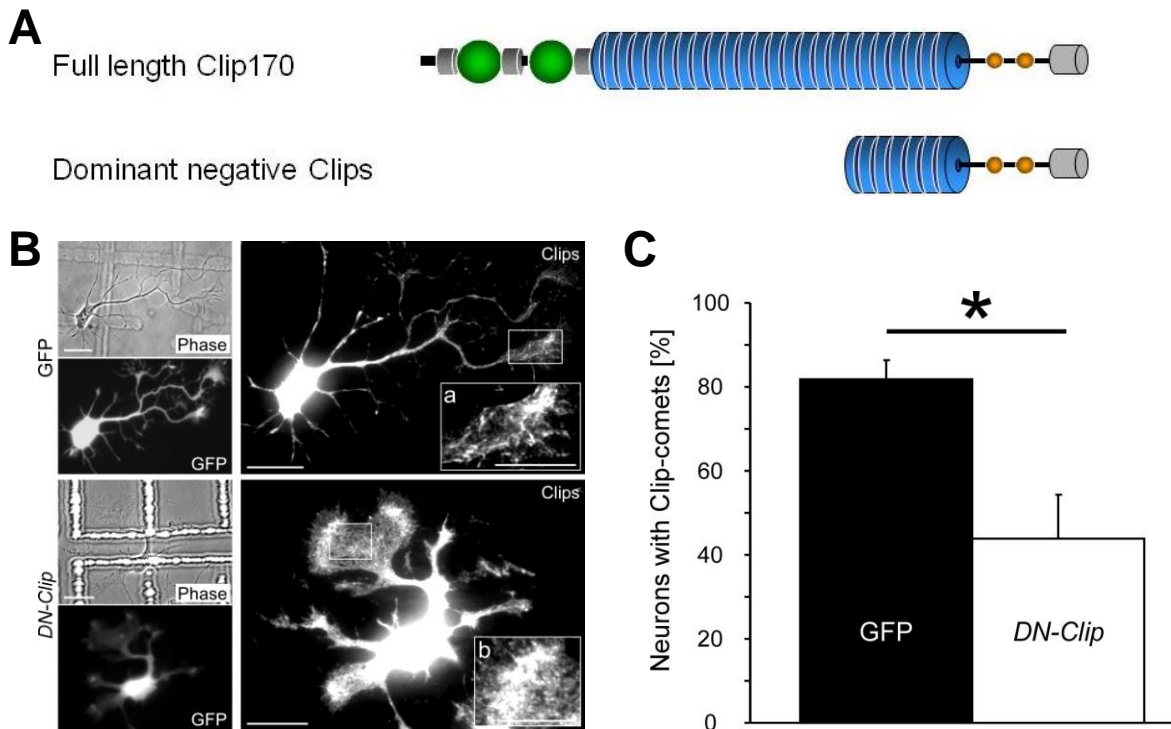


Figure 3-3: Overexpression of *DN-CLIP* removes CLIPs from microtubules. **A**, Model of full length and dominant negative CLIP-170. **B**, Neurons were transfected with GFP or GFP-tagged *DN-CLIP*, fixed at 2 DIV and stained for CLIPs. **B (a, b)**, Higher magnifications of the regions marked in **B**. *DN-CLIP* transfected neurons do not show the typical comet-like CLIP-staining. Scale bars, 20 μm . **C**, Quantification of GFP (black bar) or *DN-CLIP* (white bar) transfected neurons showing regular CLIP-170-comets ($n > 167$ cells from 4 independent cultures; $*p < 0.05$).

3.1.3 Interference with CLIP function inhibits axon formation

Next, I wanted to assess axon formation in neurons where I interfered with the function of CLIPs. To this end, I fixed *DN-CLIP* transfected cells after 2 days in culture and stained them with the axonal marker Tau-1. Only 33% of these neurons exhibited processes that were positive for Tau-1, a 50% reduction compared to GFP transfected control neurons (**Figure 3-4A, B**). The major fraction of transfected cells, however, was arrested either in developmental stage 1 ($30.4 \pm 6.8 \%$) or 2 ($38.4 \pm 6.7 \%$). Consistently, *DN-CLIP* transfected neurons, which still carried the capacity to develop into later stages, established axons which were significantly reduced in length compared to control cells (**Figure 3-4C**; $121 \pm 12.2 \mu\text{m}$ for GFP

and $73 \pm 2.9 \mu\text{m}$ for *DN-CLIP* transfected neurons). These data show that CLIPs play a role in the initial neuronal polarization and axon elongation.

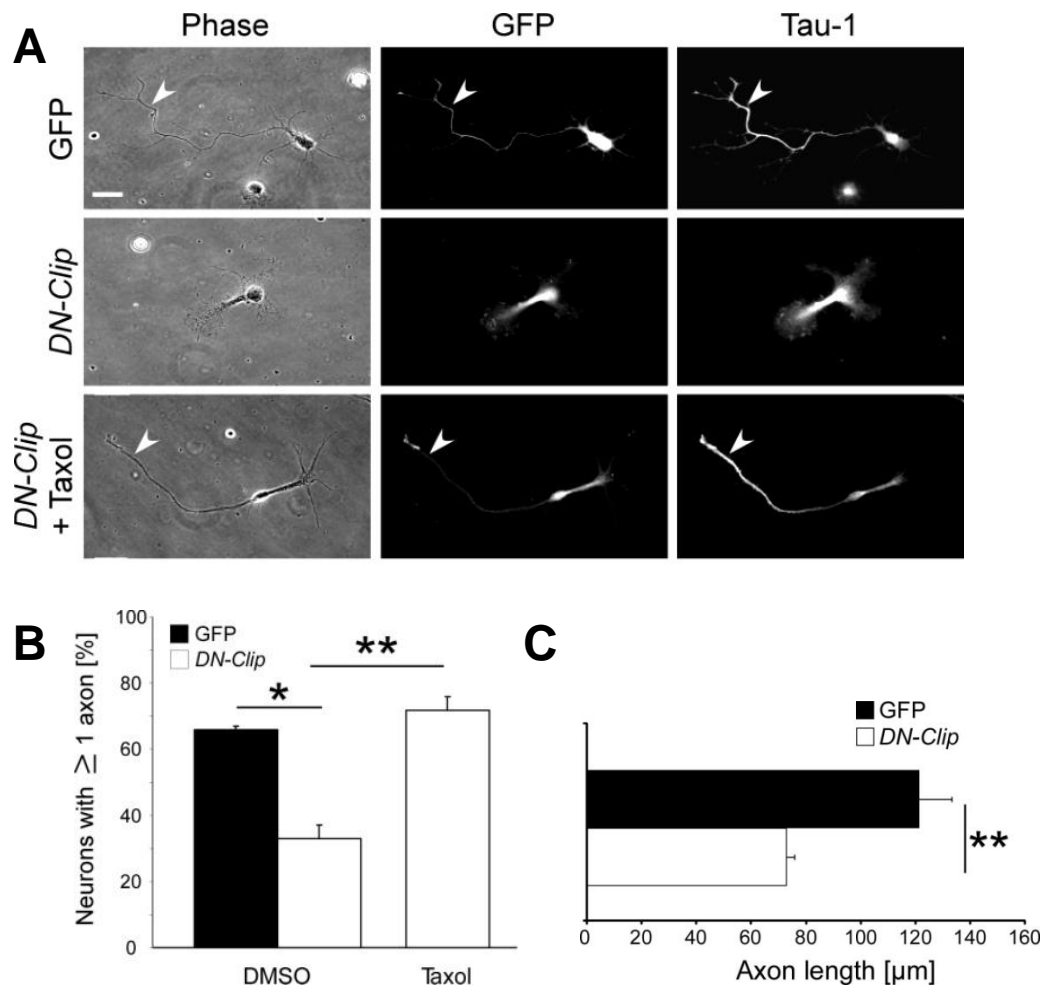


Figure 3-4: Interference with the function of CLIPs impairs axon development. A, Neurons were transfected with GFP or a GFP-tagged dominant negative form of CLIP (*DN-CLIP*), treated with DMSO or 3 nM taxol, fixed at 2 days in vitro (DIV), and stained for the axonal marker Tau-1. In *DN-CLIP* transfected neurons, axon formation is impaired, but can be rescued by taxol-treatment. Arrowheads indicate axons. Scale bar, 20 μm . **B,** Quantification of GFP (black bar) or *DN-CLIP* (white bars) transfected neurons having ≥ 1 Tau-1 positive processes in cultures treated with DMSO or taxol ($n > 281$ cells from 3 independent cultures, $*p < 0.05$, $**p < 0.01$). **C,** Quantification of length of longest process in neurons transfected with GFP (black bar) or *DN-CLIP* (white bar) that were fixed at 2 DIV ($n > 331$ cells from 6 independent experiments; $**p < 0.01$).

Previous work of other cell types showed that the removal of CLIPs from microtubules reduces the stability of microtubules (Binker et al., 2007; Komarova et al., 2002). Therefore, I asked whether the impairment of axon formation in *DN-CLIP* transfected neurons was also due to changes of microtubule stability, as a result of inhibiting the attachment of CLIPs to microtubules. To address this question, I used antibodies against acetylated and tyrosinated tubulin as markers for posttranslational modifications of microtubules, to indicate stable and dynamic microtubules, respectively. Using immunocytochemistry, I measured the fluorescence intensity of acetylated and tyrosinated tubulin in the medial part of the minor neurites and axons. In wild type neurons, stable acetylated microtubules are found in the axon, whereas minor neurites exhibit dynamic tyrosinated microtubules (**Figure 3-5**) (Witte et al., 2008). The distribution of stable acetylated microtubules and dynamic tyrosinated neurons in *DN-CLIP* transfected neurons resembled the distribution in control neurons (**Figure 3-5**). However, the acetylated signal in established axons in *DN-CLIP* transfected neurons was reduced compared to microtubules of control neurons. I also found a decrease in the ratio of acetylated versus tyrosinated tubulin of the axonal microtubules, which may indicate that these microtubules were less stable compared to the axonal microtubules of control cells (**Figure 3-5A, B**; 40% reduction of stability from control to *DN-CLIP* transfected neurons) (Westermann and Weber, 2003; Witte et al., 2008). In contrast, minor neurites of *DN-CLIP* transfected or control neurons showed the same microtubule stability.

To test whether the loss of axon formation was linked to a loss in microtubule stability, I treated *DN-CLIP* transfected neurons with low doses of taxol (Witte et al., 2008) to modestly stabilize microtubules and monitor any rescue of axon formation. After 24 hours of taxol treatment, 72 ± 4.2 % of *DN-CLIP* transfected neurons formed at least one process that was positive for the axonal marker Tau-1, reaching a level of axon-bearing cells similar to control cells (**Figure 3-4 B**; 66 ± 1.0 % of ≥ 1 Tau-1 positive process). Together, these data show that CLIPs are necessary for axon growth, and that they regulate neuronal polarization by affecting microtubule stability.

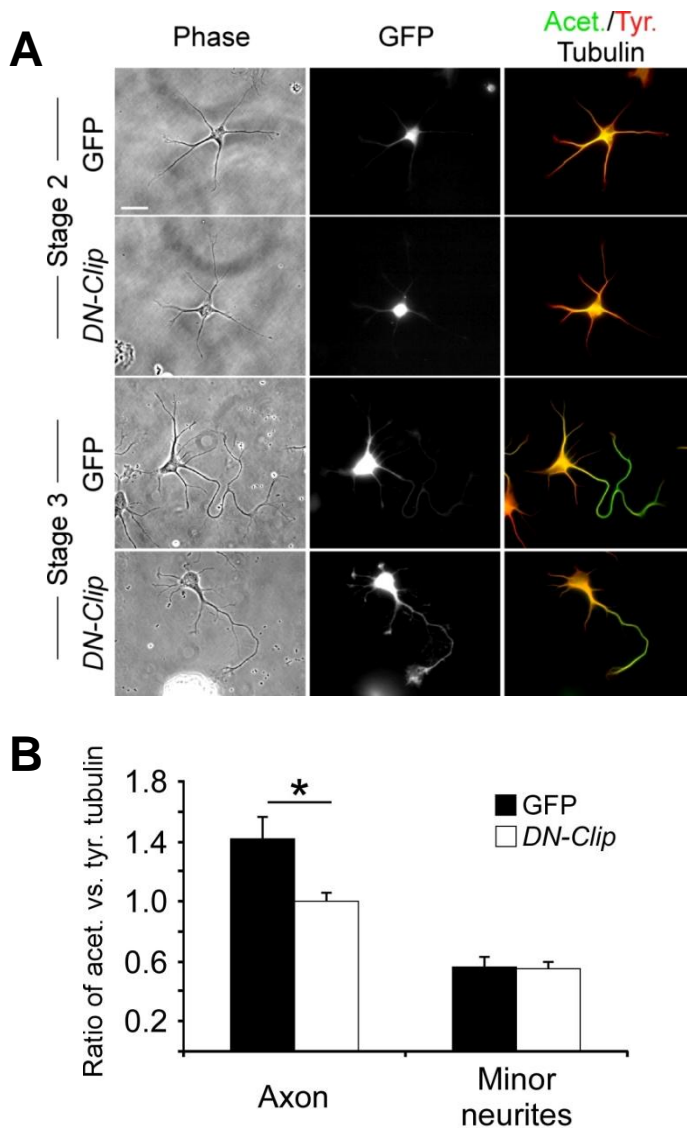


Figure 3-5: Axons of *DN-CLIP* transfected neurons have less stable microtubules. **A**, Neurons were transfected with GFP or GFP-tagged *DN-CLIP*, fixed at stage 2 or stage 3, and stained for acetylated and tyrosinated α -tubulin. Scale bar, 20 μ m. **B**, Ratio quantification of fluorescence intensities of acetylated and tyrosinated α -tubulin in microtubules of GFP (black bars) or *DN-CLIP* (white bars) transfected stage 3 neurons (2DIV). Axons of GFP-transfected neurons show a higher ratio of acetylated versus tyrosinated tubulin compared to *DN-CLIP* transfected neurons ($n > 133$ neurons from 3 independent experiments; $*p < 0.05$). Values are normalized to the mean of *DN-CLIP* axons (red line).

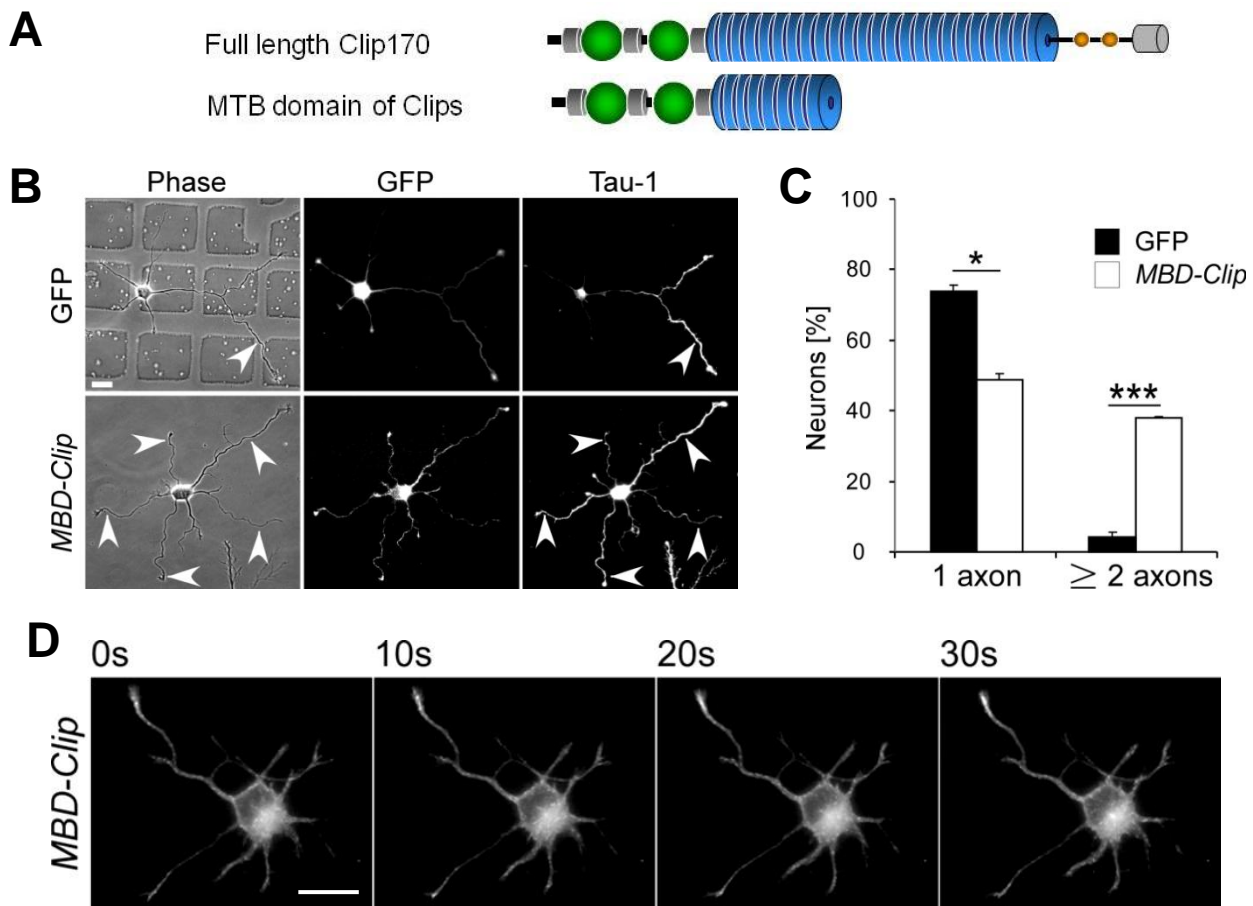
3.2 The microtubule-binding domain of CLIPs (*MBD-CLIP*)

My data so far suggested that CLIPs play an important role during neuronal polarization and that they are necessary for axon formation. Therefore, I hypothesized that they may also have the potential to turn immature minor neurites, which would later differentiate into dendrites, into axons. Hence, following my hypothesis, they could be sufficient to induce axon formation.

3.2.1 Overexpression of *MBD-CLIP* leads to the formation of multiple axons

To test this hypothesis, I used a mutant form of CLIPs, which was composed of the microtubule-binding domain of CLIPs fused to GFP (*MBD-CLIP*) (**Figure 3-6A**). This domain is sufficient for CLIP-microtubule attachment and the increase of rescue events in CHO cells (Komarova et al., 2002). Cultured hippocampal neurons develop in a homogenous way, so that one can find different stages of development in one culture. Usually, only about 5-10% of the cultured hippocampal neurons establish more than one axon. However, overexpressing *MBD-CLIP* shifted this distribution to the fraction of neurons bearing more than one Tau-1 positive axon from 4.2 ± 1.7 % in control cells to 37.9 ± 2.0 % at 2 DIV (**Figure 3-6B, C**). *MBD-CLIP* decorated microtubules as comet-like structures along the shafts of all processes (**Figure 3-6D**). Interestingly, I found a strong accumulation of *MBD-CLIP* at the tips of the induced supernumerary axons, which indicates that the majority of polymerizing microtubules extended into the growth cone.

Figure 3-6: Overexpression of the microtubule-binding domain of CLIPs (*MBD-CLIP*) leads to the formation of functional multiple axons. **A**, Model of full length CLIP-170 and the microtubule-binding domain (MBD) CLIP construct. **B**, Neurons were transfected with either GFP or GFP-tagged *MBD-CLIP*, fixed at 2 DIV, and stained for the axonal marker Tau-1. Scale bar, 20 μ m. Arrowheads indicate axons. **C**, Quantification of GFP (black bars) or *MBD-CLIP* (white bars) transfected neurons having one and multiple Tau-1 positive processes (n > 247 cells from 3 independent cultures; *p < 0.05, ***p < 0.001). **D**, Time series of *MBD-CLIP* transfected neurons over 30 s. *MBD-CLIP* accumulates mainly in the axonal growth cone. Scale bar, 20 μ m.



To test microtubule stability in these newly formed axons, I stained *MBD-CLIP* transfected neurons with antibodies against acetylated and tyrosinated tubulin at 2DIV (**Figure 3-7A**). Axons of *MBD-CLIP* transfected neurons exhibited stable acetylated tubulin along the shaft with a dynamic tyrosinated process tip, a distribution of posttranslational modifications as in control axons. By plotting the ratio of acetylated versus tyrosinated tubulin of the longest processes of the control cells and cells transfected with *MBD-CLIP*, I could show that processes of *MBD-CLIP* transfected neurons displayed the same ratio as axons of control neurons of the same length (**Figure 3-7B**). This suggested that these axons exhibit the same microtubule stability as control axons.

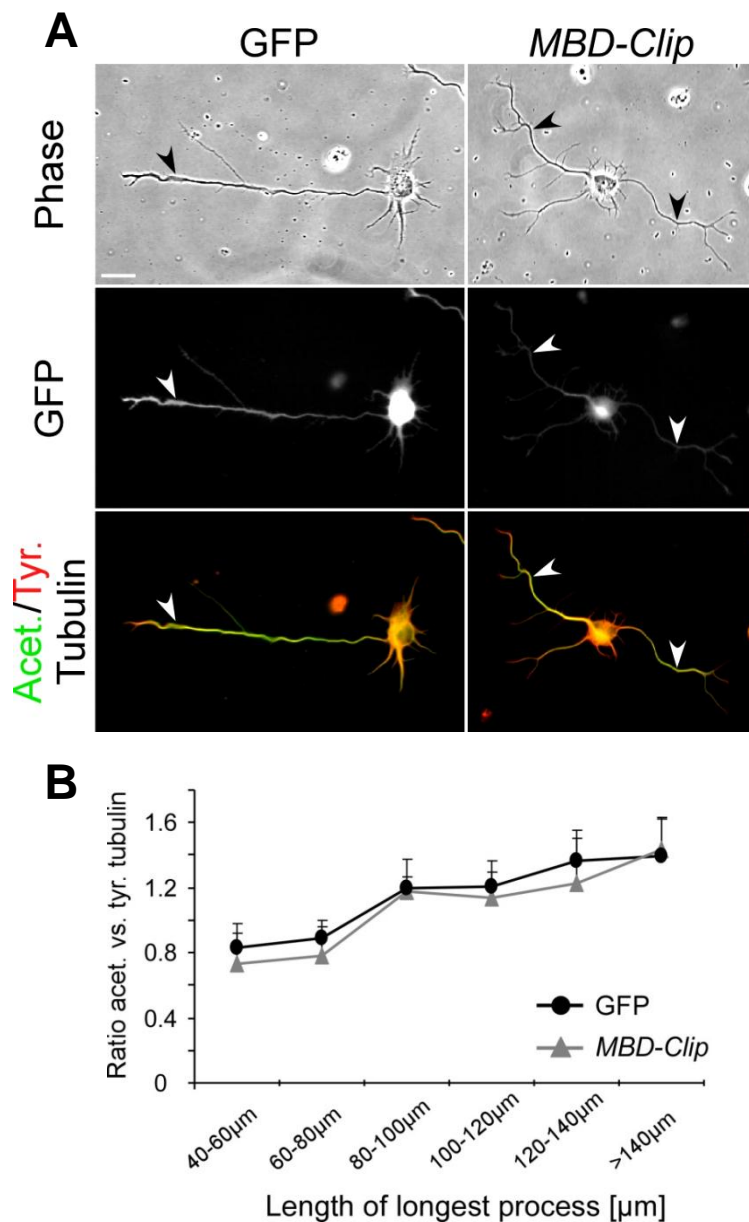


Figure 3-7: Axons of *MBD-CLIP* transfected neurons do not show differences in microtubule-stability. **A**, Neurons were transfected with either GFP or GFP-tagged *MBD-CLIP*, fixed at 2 DIV, and stained for acetylated and tyrosinated α -tubulin. Scale bar, 20 μm . **B**, Ratio of acetylated versus tyrosinated tubulin plotted against the length of longest process of neurons transfected with GFP (black line) or *MBD-CLIP* (grey line) ($n > 118$ cells from 3 independent cultures).

3.2.2 *MBD-CLIP* induced processes are differentiated axons

After I demonstrated above that the newly formed processes in *MBD-CLIP* transfected neurons were positive for Tau-1, I further wanted to know whether these axons could mature and become fully integrate into the neuronal network of the surrounding cells.

Therefore, I stained 11 day old neurons with an antibody against the Microtubule associated protein-2 (MAP-2), which is a well established marker for dendrites, and the synaptic vesicle protein Synapsin I, which stains vesicles in presynaptic regions. As shown in Figure 8b and 8c, processes, which were negative for the dendritic marker MAP-2 showed a clear staining of Synapsin I, giving evidence that these processes were mature axons loaded with presynaptic vesicles. In contrast, depicted in **Figure 3-8a**, MAP-2-positive dendrites did not show any Synapsin I staining. Thus, overexpression of the microtubule-binding domain of CLIPs is sufficient to induce axon formation.

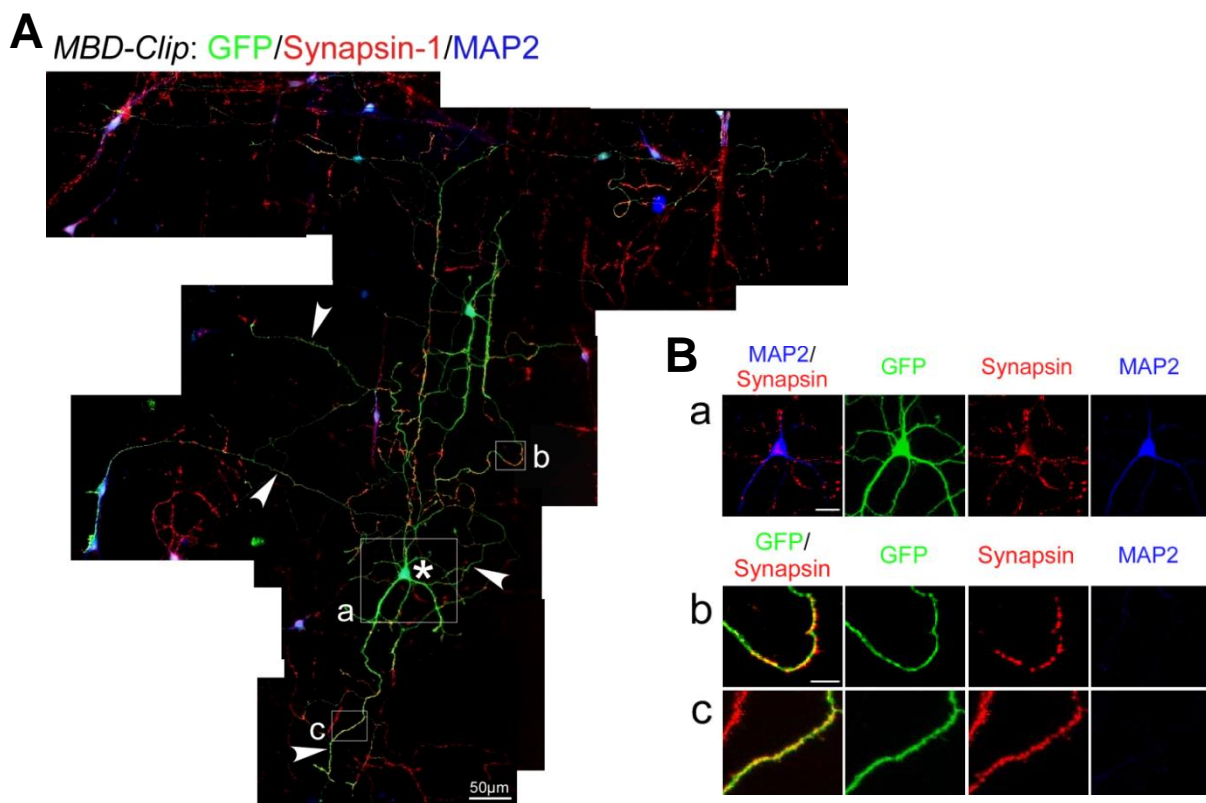


Figure 3-8: MBD-CLIP transfected neurons develop differentiated axons. **A**, MBD-CLIP transfected neurons at 11 DIV, stained for GFP, Synapsin and MAP2. Asterisk label a GFP-positive neuron; arrowheads indicate axons. Scale bar, 50 μ m. **B (a – c)**, Blow ups of regions marked in A. Scale bar, 20 μ m (a) and 10 μ m (b, c).

3.3 Microtubule dynamics after removal of CLIPs from microtubules

3.3.1 CLIPs organize the microtubule network in growth cones

As CLIPs change microtubule stability in the shaft of neurites and are enriched in the growth cones of polarized hippocampal neurons. I hypothesized that CLIPs may also organize the microtubule network in growth cones.

To test whether the microtubule network is altered in neurons without functional CLIPs, I first visualized microtubules by immunocytochemistry. In order to achieve a clear staining of polymerized microtubules, I fixed and permeabilized 2 day old cells at the same time to remove free tubulin monomers. In control neurons, microtubules of minor neurites and axons of stage 2 and stage 3 neurons appeared bundled in the transitional zone of the growth cone and reached into the tips of the processes in a linear manner (**Figure 3-9A, B**). In contrast, microtubules of *DN-CLIP* transfected neurons failed to coalesce within the minor neurites of stage 2 neurons as well as both minor neurites and axons in stage 3 neurons (**Figure 3-9C, D**). For quantification, I measured the length of splayed microtubules from the tips of microtubules until the region where they bundled. In axons, the length of splayed microtubules increased from $9.7 \pm 0.5 \mu\text{m}$ in GFP-transfected control neurons to $21.7 \pm 0.4 \mu\text{m}$ in *DN-CLIP* transfected neurons (**Figure 3-9F**). The splayed microtubule length in minor neurites also increased from $7.0 \pm 0.9 \mu\text{m}$ (GFP) to $12.5 \pm 1.1 \mu\text{m}$ (*DN-CLIP*). By contrast, *MBD-CLIP* transfected neurons exhibited strongly bundled microtubules at the tips of all processes (**Figure 3-3E, F**; $2 \pm 0.2 \mu\text{m}$ length of displayed microtubules). This confirmed my hypothesis that CLIPs regulate the microtubule network at the neurite tips, mainly in the axonal growth cones.

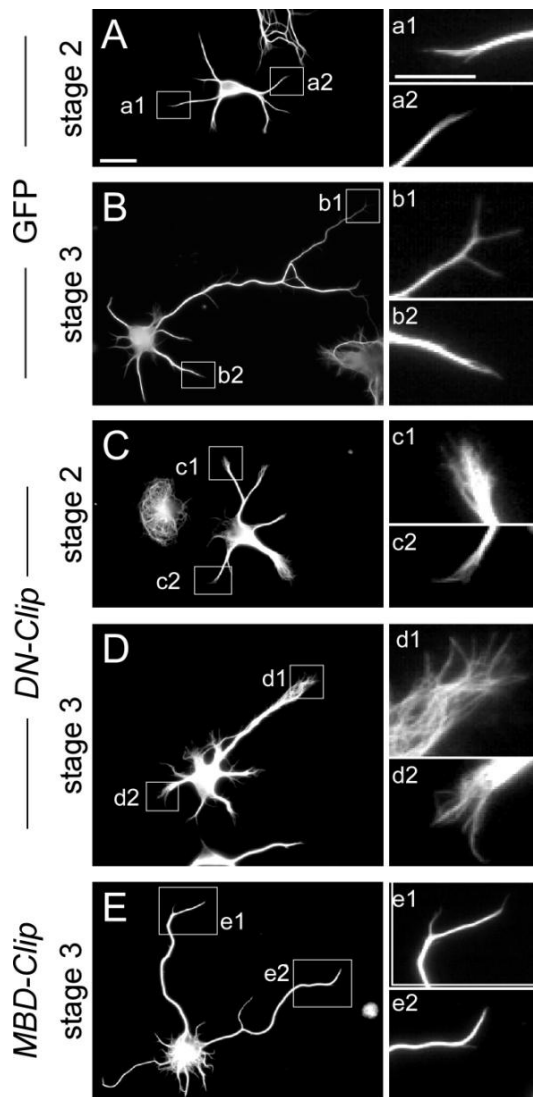
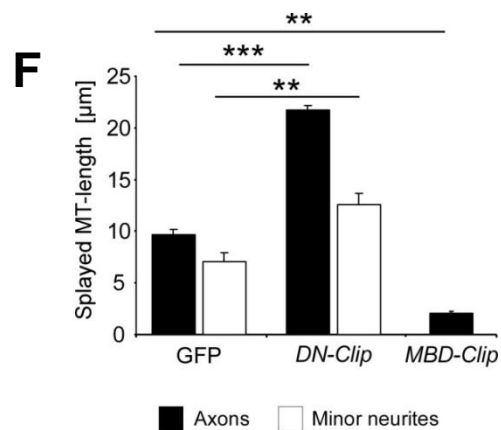


Figure 3-9: Microtubule structure in *DN-CLIP* or *MBD-CLIP* transfected neurons. **A**, Neurons were transfected with GFP (**A - B**), GFP-tagged *DN-CLIP* (**C - D**) or GFP-tagged *MBD-CLIP* (**E**), fixed at 2 DIV, and stained for α -tubulin. Microtubules of *DN-CLIP* transfected neurons are splayed out at the process tips, both in axons and in minor neurites of stage 2 (**C**) and stage 3 (**D**) neurons. *MBD-CLIP* transfected neurons contain strongly bundled microtubules (**E**). **a - e**, Higher magnifications of regions marked in **A - E**. Scale bars (**A - E**), 20 μ m, (**a - e**) 10 μ m. **F**, Quantification of splayed microtubule-length in axons (black bars) and minor neurites (white bars) of GFP, *DN-CLIP* or *MBD-CLIP* transfected neurons. Splayed microtubule-length was defined as distance from microtubule-tip to area of bundled microtubules ($n > 160$ cells from 3 independent cultures; ** $p < 0.01$, *** $p < 0.001$).



3.3.2 Microtubule dynamics are impaired after *DN-CLIP* transfection

To test whether these changes of the microtubule network affect the dynamics of microtubules within the growth cone, I analyzed the growth rates of microtubules in control as well as in *DN-CLIP* and *MBD-CLIP* transfected neurons.

Therefore, I transfected GFP, *DN-CLIP* or *MBD-CLIP* additionally with mCherry-End binding protein 3 (mCherry-EB3), a well established marker to examine microtubule dynamics (Hasaka et al., 2004; Stepanova et al., 2003) by visualizing polymerizing ends of microtubules. By analyzing kymographs of live imaging series over 90 s, I

could demonstrate that in GFP alone, *DN-CLIP*, or *MBD-CLIP* transfected neurons, EB3 comets moved with the same speed along the entire shaft of the axon (**Figure 3-10A**). This indicated that microtubules grew with similar rates (**Figure 3-10A, B**; 125 ± 4 nm/s for GFP, 125 ± 4 nm/s for *DN-CLIP*, and 120 ± 5 nm/s for *MBD-CLIP* transfected neurons).

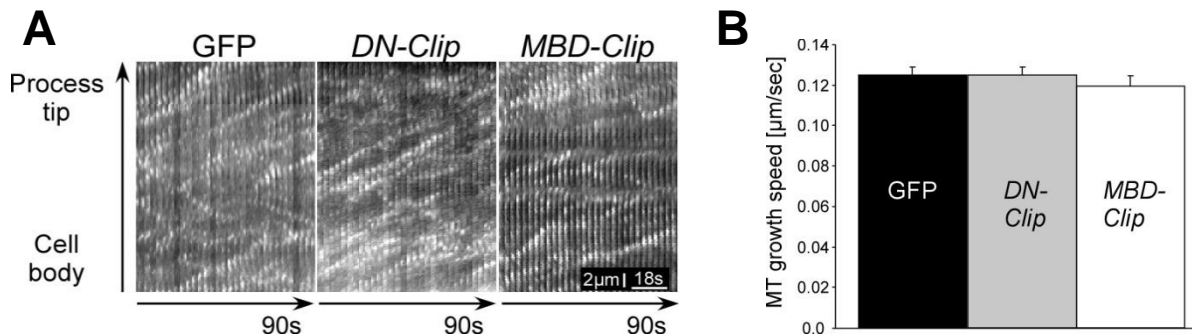


Figure 3-10: Microtubule growth speed is not altered in *DN-CLIP* transfected neurons. Neurons were double-transfected with GFP, GFP-tagged *DN-CLIP*, or GFP-tagged *MBD-CLIP* and mCherry-EB3 to visualize microtubule-growing ends. Living neurons were imaged at 2 DIV. **A**, Kymographs of single processes of neurons transfected with GFP, *DN-CLIP* or *MBD-CLIP* together with mCherryEB3. Scale bars: 2 μm; 18 s. **B**, Quantification of microtubule growth speed in neurons transfected with GFP (black bar), *DN-CLIP* (grey bar) or *MBD-CLIP* (white bar) ($n > 61$ EB3-particles from 2 separate cultures).

Although microtubules did not show any defects in their growing speed along the neurite shaft, differences in microtubule dynamics were visible within the growth cones. By observing the growth behavior of microtubule plus ends highlighted with mCherry-EB3, I found that microtubules moved into the growth cone in control conditions and in neurons transfected with *MBD-CLIP*, and polymerized until they reached the membrane of the leading edge (**Figure 3-11C, Ca and Cc**). In *DN-CLIP* transfected neurons, the majority of microtubules grew into the transitional domain of the growth cone, but not further. More precisely, around 50% of the relative EB-3 fluorescence intensity of GFP or *MBD-CLIP* transfected neurons was located within 0.4 μm (*MBD-CLIP*) and 1.3 μm (GFP) from the growth cone tip. By contrast, in *DN-CLIP* transfected neurons 50% of the relative EB3-fluorescence intensity was only found within a distance of more than 5 μm to the membrane edge

of the growth cones (**Figure 3-4C, D**). Microtubules of *DN-CLIP* transfected neurons were affected in their growth behavior, presumably due to the lack of microtubule stability. Thus, I conclude that CLIPs support the directed growth of microtubules to the peripheral domain of the growth cone.

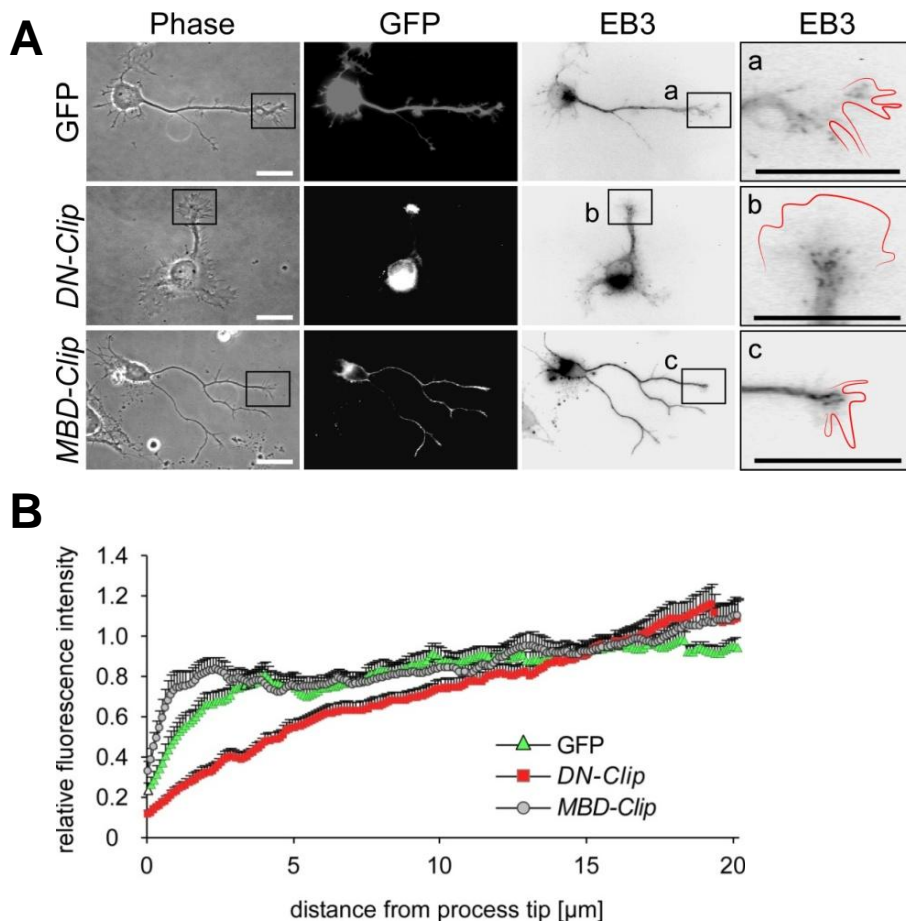


Figure 3-11: Overexpression of *DN-CLIP* impairs proper microtubule growth in the growth cone. **A**, Images show neurons transfected with GFP, GFP-tagged *DN-CLIP*, or GFP-tagged *MBD-CLIP* and mCherry-EB3. Higher magnifications of the growth cones marked in **A**. Microtubule plus ends of GFP or *MBD-CLIP* transfected neurons show a shift towards the process tips, whereas overexpression of *DN-CLIP* abolishes such a shift. Scale bar, 20 μm . Red line indicates the membrane edge. **B**, Quantification of relative fluorescence intensity in neurons transfected with GFP (green triangle), *DN-CLIP* (red box) or *MBD-CLIP* (grey circle) together with mCherry-EB3. *DN-CLIP* transfected neurons are lacking microtubule dynamic ends in the growth cones ($n > 33$ processes from 2 independent cultures). Values are normalized to the mean of fluorescence intensity of the single processes.

3.4 CLIPs influence the actin cytoskeleton of the growth cone

Growth cones are important structures for growth cone steering and axon elongation. Although growth cone morphology and dynamics are mainly determined by actin filaments (Chien et al., 1993; Marsh and Letourneau, 1984), it was shown that also microtubules are playing a vital role in growth-cone mediated axon-extension (Tanaka et al., 1995; Tanaka and Kirschner, 1991; Williamson et al., 1996). This is presumably mediated by the interaction with the actin cytoskeleton in the P-domain, into which microtubules extend.

3.4.1 Growth cone structure and dynamics are impaired in *DN-CLIP* transfected neurons

Because I showed that CLIPs regulate microtubules to grow into the P-domain of the growth cone, I wondered whether CLIPs also influence growth cone structure and dynamics, both known to affect axon growth.

First, by examining the morphology of control or *DN-CLIP* transfected neurons after 2 DIV, I found that growth cones of *DN-CLIP* transfected neurons were enlarged from $90 \pm \mu\text{m}^2$ in control cells to $224 \pm \mu\text{m}^2$, a 2.5-fold increase (**Figure 3-12**). Next, I hypothesized, according to the changes in the growth cone size, that also growth cone dynamics could be affected.

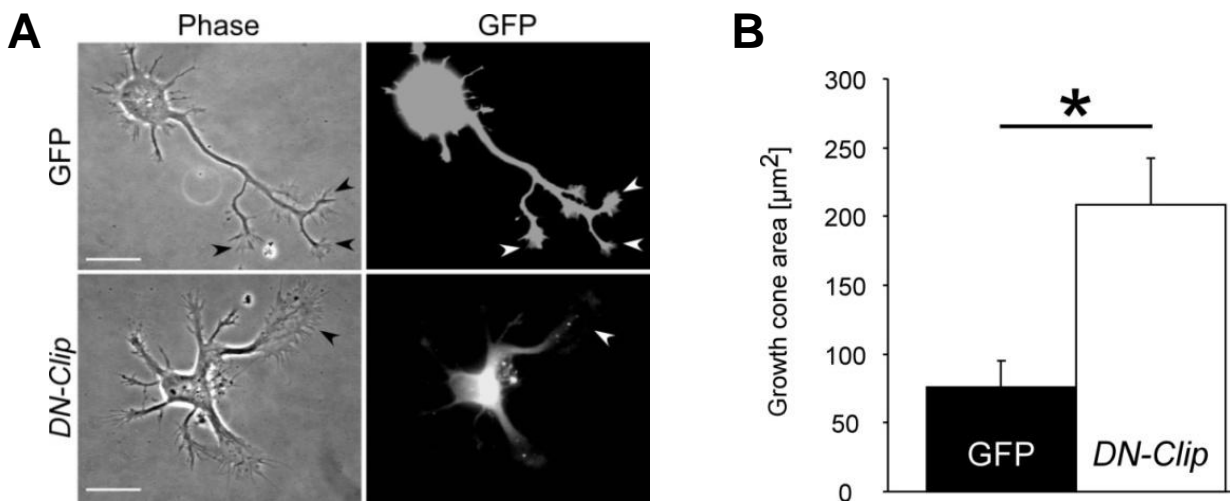
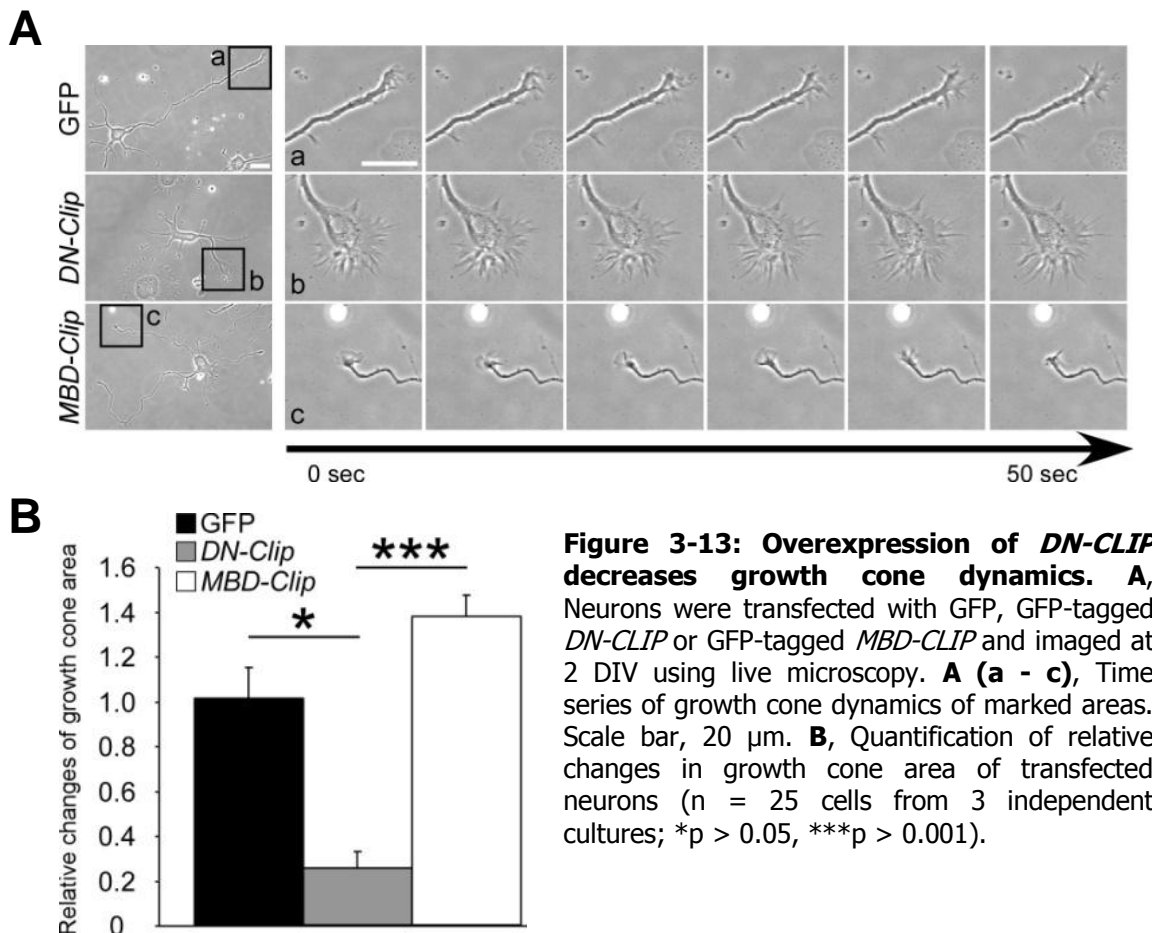


Figure 3-12: Growth cones are enlarged in *DN-CLIP* transfected neurons. **A**, Neurons were transfected with GFP or *DN-CLIP* and fixed at 2 DIV. Scale bars, 20 μm. Arrowheads indicate growth cones. **B**, Quantification of the growth cone area in GFP- (black bar) or *DN-CLIP* (white bar) transfected neurons (n > 200 cells from 4 independent cultures; *p < 0.05).

In order to analyze growth cone dynamics, I performed phase contrast live cell-imaging of neurons transfected with GFP alone, *DN-CLIP* or *MBD-CLIP* after culturing the cells for 2 days. Live imaging of the cells displayed that axonal growth cones of GFP or *MBD-CLIP* transfected neurons were highly dynamic and motile, here depicted for a time period of 50 s (**Figure 3-13Aa and 3-13Ac, B**). In contrast, growth cones of *DN-CLIP* transfected neurons showed very little dynamics and appeared strongly attached to the surface (**Figure 3-13Ab, B**). Quantifying relative changes of growth cone area over a time period of 50 s demonstrated not only that growth cones of *DN-CLIP* transfected neurons were significantly decreased, but also that growth cones of *MBD-CLIP* transfected neurons were even more mobile than control growth cones.



3.4.2 Actin retrograde flow is not altered in *DN-CLIP* transfected neurons

To further elucidate the underlying CLIP-mediated changes in growth cone dynamics, I studied actin dynamics using *Lifect-RFP* as live marker for the actin cytoskeleton (Riedl et al., 2008). Although the overall growth cone dynamics were significantly impaired after removing CLIPs from the microtubules, the actin retrograde flow speed was not altered in *DN-CLIP* and GFP overexpressing control cells (**Figure 3-14B, D**; $0.13 \pm 0.02 \mu\text{m/s}$ for *DN-CLIP* and $0.11 \pm 0.01 \mu\text{m/s}$ for GFP transfected neurons). However, in *DN-CLIP* expressing neurons, prominent actin arcs, which are known to prevent microtubule protrusion in the peripheral growth cone (Lee and Suter, 2008; Lowery and Van Vactor, 2009; Schaefer et al., 2002), surrounded the central domain of the growth cone perpendicular to the filopodia projection axis (**Figure 3-14Bb**). By contrast, in control neurons (**Figure 3-14Aa**) or neurons

expressing *MBD-CLIP* (data not shown) these arcs were not found. Instead, the bases of filopodia reached close to the central, microtubule-rich domain of the growth cone (**Figure 3-14A**). Hence, I conclude that CLIPs affect growth cone structure and dynamics and influence actin arc formation in growth cones.

3.4.3 Filopodia formation is impaired in *DN-CLIP* transfected neurons

Filopodia are actin based structures of the growth cone composed of parallel actin filaments and different actin-associated proteins. Besides their tasks to act as sensors of the local environment, they are necessary for neurite outgrowth and initial neurite formation in cortical neurons (Dent et al., 2007). Therefore, I asked whether filopodia-formation or behavior was altered in neurons transfected with *DN-CLIP*.

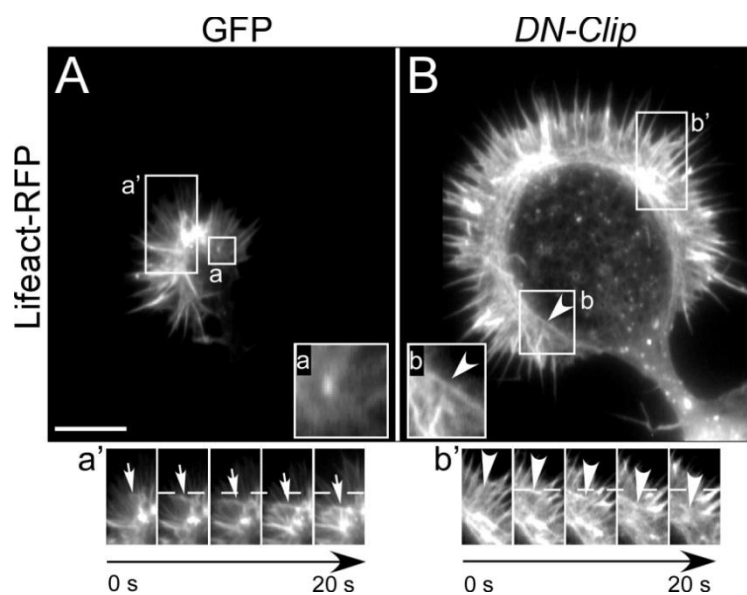
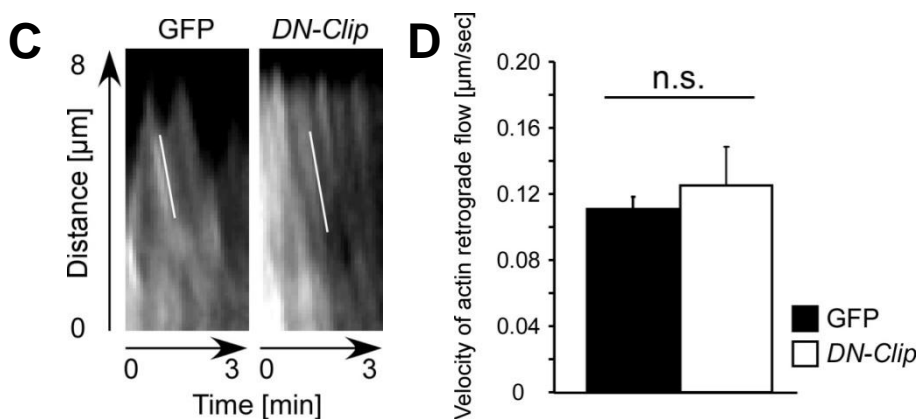


Figure 3-14: Actin retrograde flow is not altered in *DN-CLIP* transfected neurons. **A** and **B**, Neurons were transfected with GFP (**A**) or GFP-tagged *DN-CLIP* (**B**) together with Lifeact-RFP. Living neurons were imaged at 2 DIV. Scale bar, 10 μm . **A (a)** and **B (b)**, Higher magnifications of marked regions of growth cones in **A** and **B**, showing actin arcs in *DN-CLIP* transfected neurons (**b**). **A (a')** and **B (b')**, Time series of actin retrograde flow of marked areas in **A** and **B**. **C**, Kymographs of actin retrograde flow for GFP and *DN-CLIP* transfected neurons. **D**, Quantification of actin retrograde flow-velocity of GFP (black bar) and *DN-CLIP* (white bar) transfected neurons ($n > 26$ cells from 3 independent cultures; $p = 0.5$).



To this end, I quantified neurons that were double-transfected with either GFP or *DN-CLIP* together with Lifeact to observe filopodia behavior of 2 day old neurons by live cell imaging. First, in *DN-CLIP* transfected neurons, the filopodia number per $10 \mu\text{m}^2$ of growth cone area was significantly reduced compared to GFP transfected control neurons (**Figure 3-15A**; 2.4 ± 0.1 filopodia/ $10 \mu\text{m}^2$ growth cone area in control neurons; $1.2 \pm 0.1 \mu\text{m}^2$ in *DN-CLIP* transfected neurons). Moreover, overlaying images of 2 different time points demonstrated a lack of filopodia dynamics in *DN-CLIP* transfected cells, seen by a clear alignment of filopodial structures (**Figure 3-15B**).

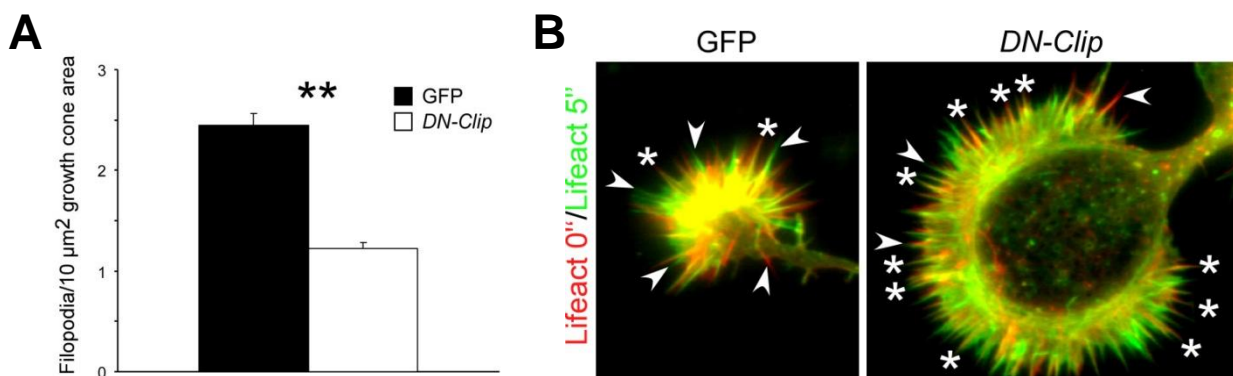


Figure 3-15: *DN-CLIP* transfected neurons provide less and immotile filopodia. Neurons, transfected with either GFP or *DN-CLIP* and Lifeact were imaged by live microscopy. **A**, Quantification of filopodia per $10 \mu\text{m}^2$ growth cone area. *DN-CLIP* transfected neurons exhibit less filopodia ($n > 28$ of 3 independent cultures; $**p < 0.01$). **B**, Overlay of 2 time points (0 and 5 s) of Lifeact-images of growth cones of control or *DN-CLIP* transfected neurons. Filopodia of *DN-CLIP* transfected neurons are less motile than control filopodia. Asterisks, overlaying filopodia; arrowheads, non-overlapping filopodia.

3.5 Manipulation of the actin cytoskeleton rescues axon formation in *DN-CLIP* transfected neurons

Actin arcs prevent microtubules from protruding to the peripheral region of the growth cone (Lee and Suter, 2008; Lowery and Van Vactor, 2009; Schaefer et al., 2002). Therefore, a disassembly of the actin cytoskeleton or an inhibition of the myosin II-mediated actin arc compression could also cause microtubules to protrude further distally to the growth cone, even if CLIPs are non-functional. Hence, I

postulate that actin manipulation may be able to rescue axon formation in *DN-CLIP* expressing neurons.

In order to test this, I treated *DN-CLIP*-expressing neurons co-transfected with mCherry-EB3 with cytochalasin D, an actin-depolymerizing drug that in wildtype neurons converts non-growing neurites into growing axons (Bradke and Dotti, 1999; Kunda et al., 2001). Directly after applying cytochalasin D to *DN-CLIP* transfected neurons, growth cone dynamics ceased and the actin cytoskeleton depolymerized (data not shown). Before cytochalasin D application, microtubules, decorated with EB3-comets, grew only close to the growth cone edge. However, immediately after treatment, I observed EB3-comets appearing close to the cortex and subsequently thin processes containing EB3-comets emerged out of the former growth cone and continued growing in a straight manner (**Figure 3-16A**).

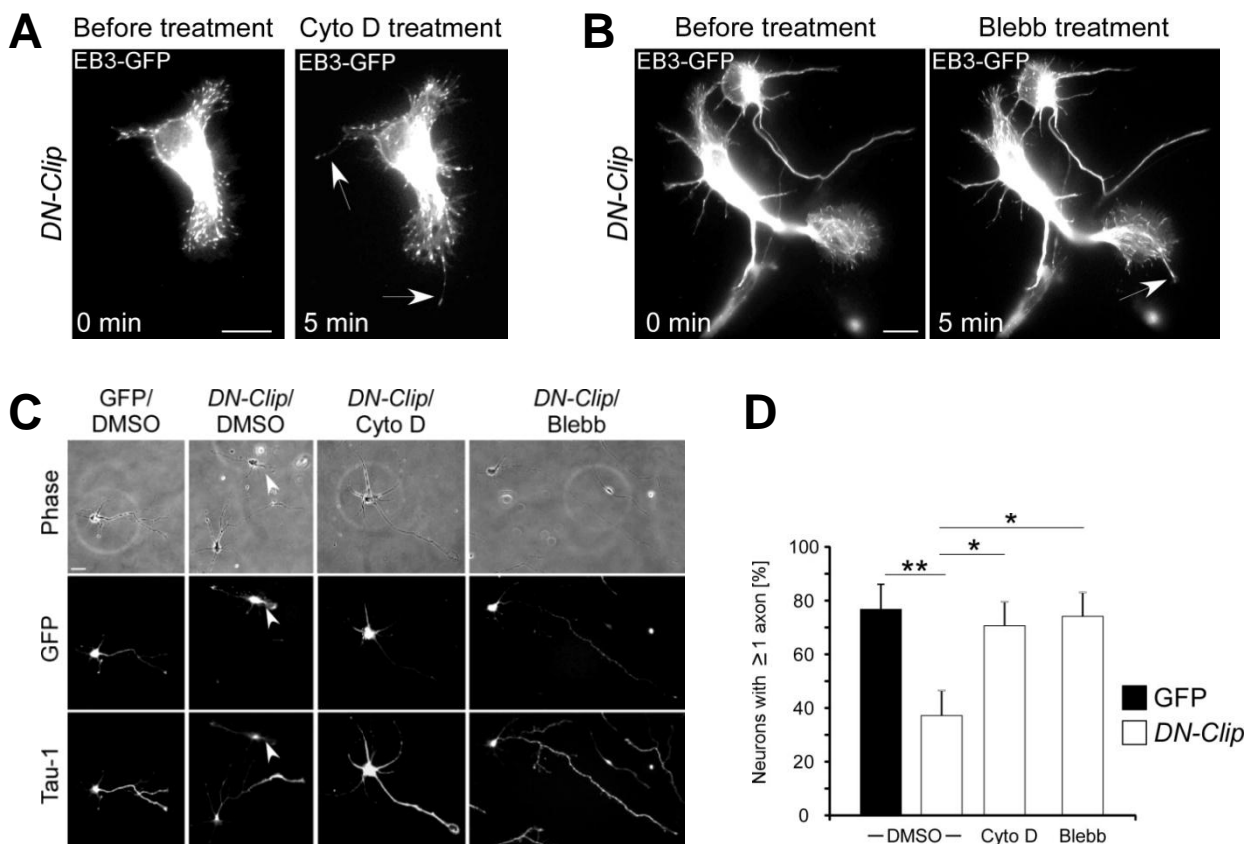


Figure 3-16: Modulating the actin cytoskeleton rescues axon formation in *DN-CLIP* transfected neurons. **A** and **B**, Neurons, doubletransfected with *DN-CLIP* and mCherry-EB3, were treated with cytochalasin D (**A**) or blebbistatin (**B**) at 2 DIV. 5 min after drug application, EB3-comets appeared closer to the membrane and a thin process containing EB3 emerged out of the growth cone (arrows) (n = 12 neurons treated with cytochalasin D; n = 6 for neurons treated with blebbistatin). Scale bar, 20 μ m. **C**, Neurons were transfected with GFP or GFP-tagged *DN-CLIP*, treated with DMSO, 1 μ M cytochalasin D or 1 μ M blebbistatin, fixed at 2 DIV and stained for the axonal marker Tau-1. Scale bar, 20 μ m. Arrowheads indicate axons. **D**, Quantification of GFP (black bar) or *DN-CLIP* (white bars) transfected neurons having ≥ 1 Tau-1-positive processes in cultures treated with DMSO, cytochalasin D or blebbistatin (n > 184 cells from 3 independent cultures; *p < 0.05, **p < 0.01).

Similarly, when I applied the myosin II inhibitor blebbistatin to *DN-CLIP* expressing neurons, EB3-comets reached the growth cone tip and neurites started to grow into new protrusions (**Figure 3-16B**).

Furthermore, the assessment of axon formation after longer treatments with cytochalasin D or blebbistatin showed that *DN-CLIP* expressing neurons formed at least one Tau-1 positive axon (70.8 ± 7.4 % for cytochalasin D treated and 74.1 ± 10.8 % for blebbistatin treated neurons) (**Figure 3-16C, D**). Similar results were obtained when I treated the cells with another actin-depolymerizing drug, latrunculin B, and the inhibitor of the myosin light chain kinase ML7 (32.6 ± 3.1 % of ≥ 1 Tau-1 positive processes for DMSO treated *DN-CLIP* transfected neurons and 79.8 ± 6.0 % of ≥ 1 Tau-1 positive processes for latrunculin B treated *DN-CLIP* transfected neurons; 30.5 ± 3.5 % of ≥ 1 Tau-1 positive processes for DMSO treated *DN-CLIP* transfected neurons and 82.2 ± 4.1 % of ≥ 1 Tau-1 positive processes for ML7 treated neurons).

Thus, these data show that in the absence of CLIP-microtubule interaction, axon formation can be rescued by manipulating the actin cytoskeleton. Overexpression of *DN-CLIP* induced the destabilization of microtubules and thereby mediated a loss of protrusive force. This loss of function can be counteracted by disassembling the actin cytoskeleton of the growth cone or by releasing the myosin II-mediated compression of actin arcs.

3.6 A direct or indirect effect of CLIPs?

So far, my data demonstrated the effect of CLIPs on axon formation by affecting microtubule and growth cone dynamics. However, the underlying mechanisms are still unclear. One could imagine two possible scenarios how the loss of CLIPs from the microtubules could lead to the given phenotype. On the one hand, CLIPs could affect neuronal polarization in a mechanistic way by decreasing microtubule stability. This decrease could then, in turn, influence the formation of axons. On the other hand, the phenotype could be caused by the interaction of CLIPs with the actin cytoskeleton. As CLIP-170 was shown to bind via its N-terminus to the actin-binding molecule IQGAP1 in Vero cells, CLIPs could also directly link microtubules to the actin-cytoskeleton in hippocampal neurons via IQGAP. This interaction could, for example, lead to the delivery of actin modulating molecules to the periphery of the growth cone.

3.6.1 Destabilization of microtubules leads to a similar phenotype as the dominant negative construct of CLIPs

To clarify which scenario could be valid for the function of CLIPs, I affected microtubule stability by using nocodazole, a microtubule destabilizing drug. This should imitate the putative effect of CLIPs on microtubules. Neurons were treated with nocodazole for 2 DIV and afterwards stained with an antibody against α -tubulin. Under these pharmacological conditions, microtubules did not coalesce at the tips of processes when compared to control conditions (**Figure 3-17A, B**). The length of splayed microtubules increased from $11.1 \pm 2.6 \mu\text{m}$ (DMSO treatment) to $26.8 \pm 3.0 \mu\text{m}$ (nocodazole treatment). Furthermore, processes of nocodazole-treated neurons showed an overall reduction in length of about $46.5 \mu\text{m}$ (**Figure 3-17C**; $151 \mu\text{m} \pm 15.1 \mu\text{m}$ of axon length for DMSO treated neurons and $104.5 \pm 7.9 \mu\text{m}$ of axon length for nocodazole treated neurons). Thus, nocodazole-treated neurons exhibit a

very similar phenotype to *DN-CLIP* transfected neurons regarding the microtubule network.

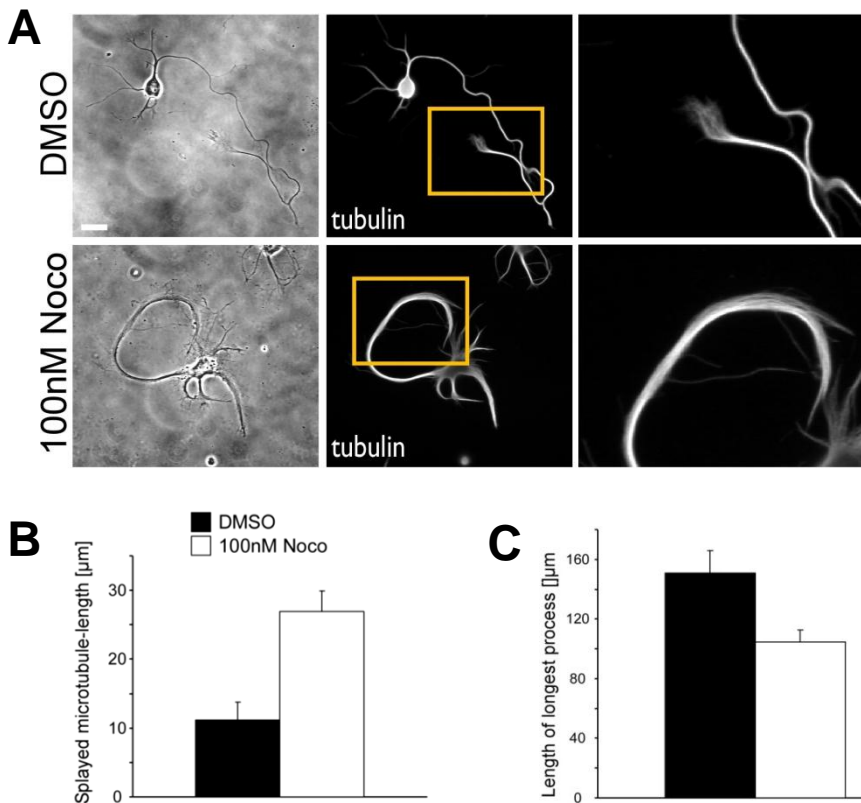


Figure 3-17: Pharmacological destabilization of microtubules resembles the phenotype of *DN-CLIP* transfected neurons. **A**, Neurons were treated with DMSO or 100 nM nocodazole for 2 DIV and stained with α -tubulin. Scale bar, 20 μm . **B**, Quantification of the length of processes of control and nocodazole-treated cells ($n > 167$ neurons from 3 independent cultures). **C**, Quantification of the length of splayed microtubules after treatment with DMSO or 100 nM nocodazole ($n > 167$ neurons from 3 independent cultures).

3.6.2 The actin cytoskeleton is also affected by destabilized microtubules

To further investigate the effect destabilized microtubules on the actin cytoskeleton, I questioned whether growth cone dynamics were altered in the same manner as in neurons after CLIP removal.

Therefore, I transfected neurons with the actin marker Lifeact, treated the neurons with low doses of nocodazole and followed growth cones dynamics by live imaging at day 2 after plating. In nocodazole-treated neurons, most of the growth cones were

enlarged in size compared to DMSO treated neurons (**Figure 3-18**) and showed decreased dynamics. Furthermore, treated cells also exhibited actin arcs, which were established perpendicular to the basis of filopodia and moved towards to the center of the growth cone (**Figure 3-18**).

Overall, the phenotype of neurons with pharmacologically altered microtubule stability, resembled that phenotype of *DN-CLIP* transfected neurons in respect to cytoskeletal dynamics and structure as well as axon elongation. Thus, CLIPs could affect axon formation by generally affecting the microtubule network.

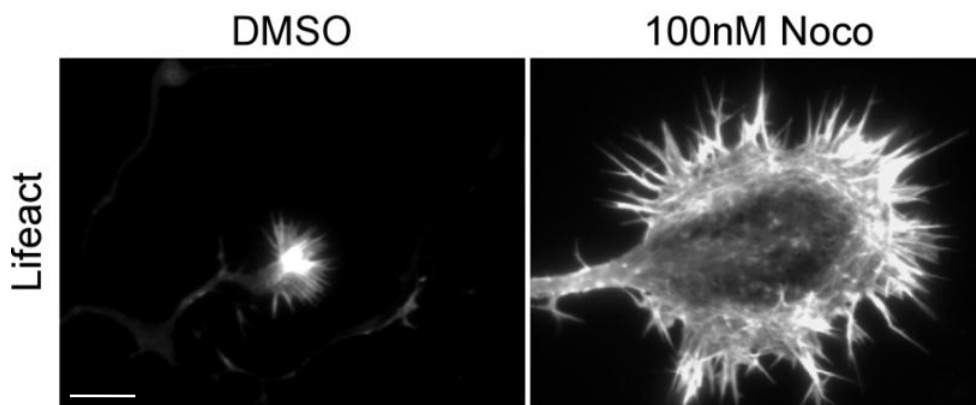


Figure 3-18: Growth cones are enlarged and form actin arcs after nocodazole-treatment. Neurons were transfected with Lifeact and treated with 100 nM nocodazole and observed after 2 DIV. Growth cones of nocodazole-treated neurons are enlarged and show actin arcs forming perpendicular to the center of the growth cones. Scale bar, 20 μ m.

3.6.3 Inhibiting the interaction of CLIPs with the actin cytoskeleton results in the contrary phenotype of *DN-CLIP*

CLIP-170 is known to function together with IQGAP1, an actin-binding molecule (Hart et al., 1996) and effector of Rac1 and Cdc42 (Hart et al., 1996; Kuroda et al., 1996), as a linker between the plus ends of microtubules and the cortical actin meshwork in Vero cells (Fukata et al., 2002). It has been hypothesized that this connection is necessary to capture microtubules to the cortex of the growth cone to allow the

delivery of actin-modulating molecules. Continuous actin turnover is necessary to enable growth cone dynamics, which are necessary for growth cone steering and axon elongation. Hence, inhibiting the CLIP-IQGAP1 interaction in hippocampal neurons by using the dominant negative mutant of CLIPs could lead to the loss of protein delivery and therefore to the impairment of axon elongation.

In order to analyze whether this interaction is indeed necessary for axon elongation, I interfered with the interaction of CLIPs with IQGAP1 by overexpression an IQGAP mutant that is comprised of only the CLIP-binding site fused to GFP (IQGAP-1537)(Brandt et al., 2007). Therefore, overexpression of the IQGAP mutant would interfere with the binding of endogenous CLIPs to the actin-bound IQGAP1. Inhibition of the IQGAP-CLIP interaction would show whether this interaction is indeed necessary for proper axon elongation.

To this end, I transfected hippocampal neurons with IQGAP-1537 and analyzed their development at 2 DIV compared to GFP transfected control neurons by staining for the axonal marker Tau-1. IQGAP-1537 transfected neurons did not show any impairment in their development. To the contrary, their development seemed to be accelerated (**Figure 3-19A, C**). Compared to control neurons, not only were less neurons transfected with the IQGAP mutant still in stage 1 (3.0 ± 1.9 % stage 1 IQGAP-1537-transfected neurons; 20.6 ± 5.3 % stage 1 control neurons), but there was also an increase in the fraction of neurons with multiple axons (10.0 ± 4.7 % for control neurons and 26.1 ± 14.4 % for IQGAP-1537 transfected neurons). Moreover, the analysis of the length of the longest process after 3 DIV demonstrated a significant increase (**Figure 3-19B, C**).

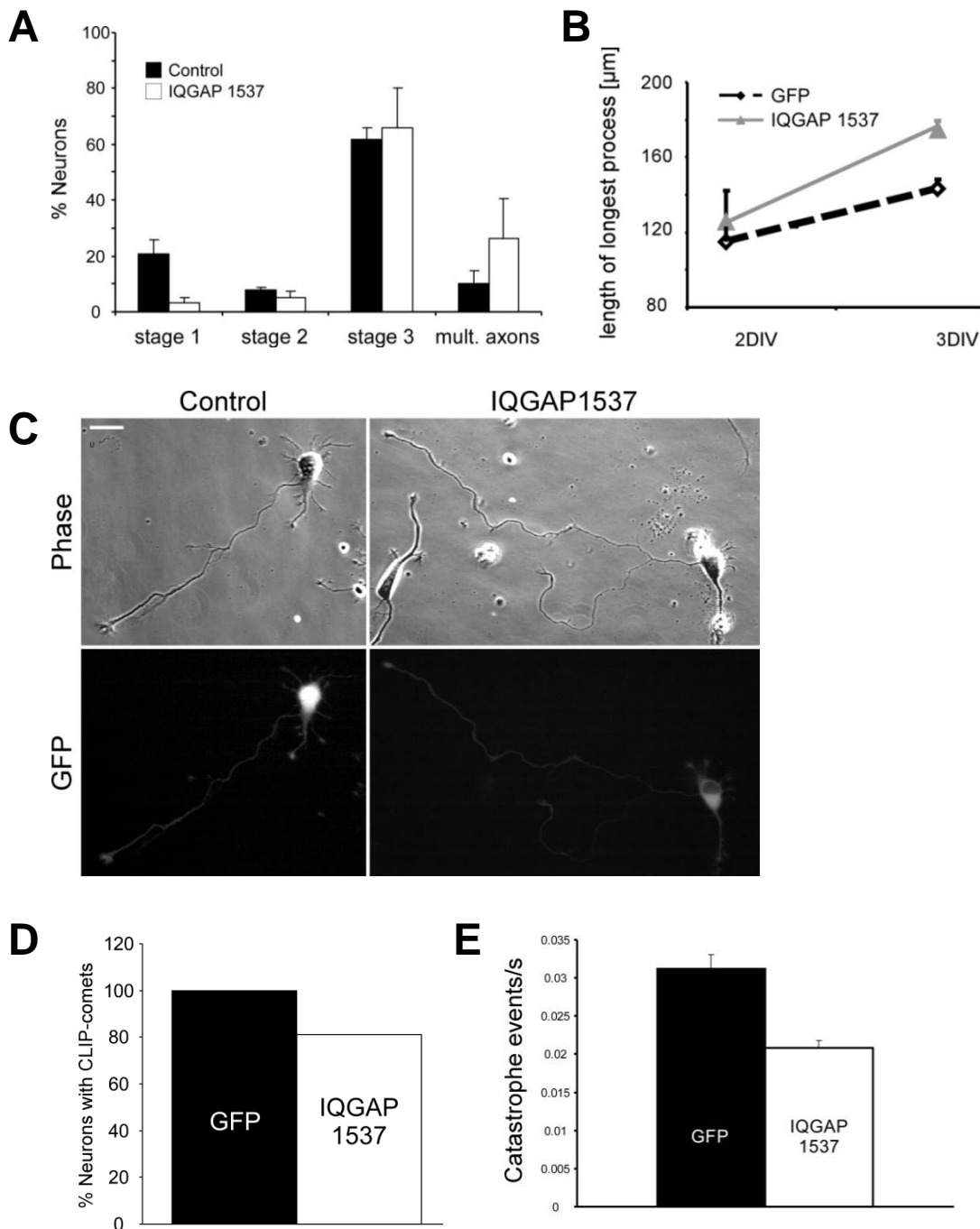


Figure 3-19: Inhibiting the interaction of CLIPs with the cytoskeleton leads to an increase in axon establishment, elongation and a decrease of catastrophe events. **A and B**, Neurons were transfected with IQGAP-1537 and stained with Tau-1 on 2 and 3 DIV. **A**, Neurons, transfected with IQGAP-1537, show a decrease in the formation stage 1 cells and an increase in the formation of multiple axons ($n > 153$ from 3 independent cultures). **B**, Neurons, transfected with IQGAP-1537, display an increase in axon length on 3DIV ($n > 153$ from 3 independent cultures). **C**, Neurons transfected with GFP and IQGAP1537. Scale bar, 20 μm . **D**, GFP- or IQGAP-1537 transfected neurons stained for CLIP after 2 DIV. CLIPs are still prominent in transfected neurons. **E**, Quantification of catastrophe events/s in GFP and IQGAP-1537 transfected neurons ($n > 15$ neurons from 2 independent experiments; *** $p < 0.001$).

In Vero cells, it was shown that the IQGAP mutant was acting in a dominant negative fashion for CLIP-170 (Fukata et al., 2002). They showed that after transfection, CLIP-170 was dislocalized from microtubules. To test whether also in hippocampal neurons the transfection of this mutant would lead to the removal of CLIPs from the microtubules, I stained transfected neurons with an antibody against CLIPs. However, I could not repeat this effect. In about 81.1 % of IQGAP-1537 transfected neurons, a clear comet-like staining for CLIPs was visible (**Figure 3-19D**).

Being aware that CLIPs are not removed from microtubules after the transfection with IQGAP-1537, I wondered whether the increase of axon length was due the modification of microtubule dynamics, induced by the binding of the IQGAP-mutant to microtubule-bound CLIPs. CLIPs are known to affect microtubule dynamics in wild type conditions as either anti-catastrophe factors, as reported in yeast cells, or as rescue factors, as observed in mammalian cells. To investigate catastrophe events of microtubules, I double-transfected neurons with GFP or IQGAP-1537 in combination with mCherry-EB3 and quantified the frequency of catastrophe events during their total growing time. Neurons, transfected with IQGAP-1537 showed less catastrophe events compared to GFP transfected control neurons (**Figure 3-19E**; 0.031 ± 0.001 catastrophe events/s for GFP transfected neurons and 0.021 ± 0.001 catastrophe events/s for IQGAP 1537 transfected neurons). Thus, microtubules exhibited longer growing cycles compared to control neurons, as they have less frequent catastrophe events.

Taken together, the interaction between CLIPs and IQGAP1 seems to contribute to axon elongation by regulating guided microtubule extension into growth cones and by modifying microtubule catastrophe events. This supports the hypothesis that CLIPs regulate axon formation by enabling the direct interaction between microtubules and the actin cytoskeleton.

4 Discussion

In the last decades, significant progress has been made to identify cellular and molecular mechanisms underlying the establishment of this polarity. Cytoskeletal dynamics have emerged as a key process during neuronal polarization (Arimura and Kaibuchi, 2007; Witte and Bradke, 2008), in addition to several pathways and different cellular events (reviewed in (Barnes and Polleux, 2009). Enhanced actin dynamics (Bradke and Dotti, 1999) as well as modest microtubule stabilization, in particular, has been shown to be a determining factor for neuronal polarization (Witte et al., 2008). However, detailed analysis of molecules potentially involved in the modest microtubule stabilization necessary for axon specification still remains elusive.

In my thesis, I investigated the role of a family of plus end tracking proteins including the cytoplasmic linker proteins (CLIPs), CLIP-115 and 170, during neuronal polarization. CLIPs are known to regulate microtubule stability by acting as rescue factors (Komarova et al., 2002), and are involved in polarization events of different cell types (Brunner and Nurse, 2000). My data show for the first time that CLIPs play an instructive role during the specification of axonal fate in early neuron development. They exert this by acting both on the microtubule network and the actin cytoskeleton. On the one hand, my data suggest that the polarizing activity of CLIPs is mediated by stabilizing the microtubule network in the axon to allow microtubules to protrude to the growth cone's leading edge. On the other hand, I demonstrate that the role of CLIPs during neuronal polarization is also due to the regulation of axonal growth cone dynamics and actin arc formation. Finally, I provide evidence that CLIPs play an important role in capturing microtubules to the actin cortex, which might be a fundamental event for controlled microtubule growth, and therefore for proper axon formation.

In summary, I present evidence that the cytoplasmic linker proteins 115 and 170 are necessary and sufficient for axon formation by influencing the microtubule network and actin cytoskeleton during neuronal polarization.

4.1 CLIPs are key regulators during neuronal polarization

Recently, it was shown that only modest, but not strong stabilization of microtubules led to axon formation (Witte et al., 2008). To identify molecules that regulate polarization of neurons by directly affecting microtubules, I sought a microtubule-binding factor that could modestly affect the stability of microtubules and that had been involved in other polarity processes. The members of the CLIP family were primary candidates, as CLIPs regulate microtubule dynamics (Komarova et al., 2002), and as the CLIP homologue tip1 is involved in the polarized growth of fission yeast (Brunner and Nurse, 2000).

Here, I have demonstrated that CLIPs are indeed necessary for axon growth. Using siRNA-mediated downregulation of CLIPs in neurons, I established a role of CLIPs in positively regulating axon length, but not a role in impairment of axon formation. This observation could have been due to either the timing of expression of the siRNA-machinery, or due to the half life of CLIPs. Therefore, I made use of a dominant negative CLIP construct that removed CLIPs from the microtubules immediately after expression. In these experiments, a large fraction of neurons had impaired axon formation. However, modest stabilization of microtubules by taxol rescued axon formation, which is consistent with the observation that axon formation is linked to microtubule-stability (Witte et al., 2008).

Besides several specialized polarity-regulating proteins (reviewed in (Barnes and Polleux, 2009)), it has been suggested that microtubule end binding proteins, including APC, Lis1, EB3, or Navigator1 (Nav1) may also be involved in various polarity processes. These include the migration of neuronal cells (Bai et al., 2008), axon guidance in invertebrates (Lee et al., 2004), and also neurite growth (Geraldo

et al., 2008; Muley et al., 2008; Zhou et al., 2004). However, overexpression of these molecules neither led to enhanced axon growth, nor to the inhibition of axon formation (Muley et al., 2008; Shi et al., 2004; Stepanova et al., 2003). As this contrasted my results, I investigated whether overexpression of CLIPs could, unlike other plus end tracking proteins, lead to enhanced axon growth and thereby regulate neuronal polarization.

My data show that overexpression of only the microtubule-binding domain (MBD) of CLIPs was sufficient to change a neurite into an axon. The microtubule-binding domain appeared as comet-like structures at the growing ends of microtubules and accumulated at the tips of the axons. The newly established axons exhibited characteristics of differentiated, mature axons. Moreover, microtubules of *MBD-CLIP* transfected axons were as stable as axonal microtubules in control neurons.

Taken together, I demonstrate that the microtubule-binding activity of CLIPs is sufficient to induce axon formation. Although my data support the hypothesis that CLIPs exhibit a direct role in the establishment of neuronal polarity, I consider this a less likely scenario. Like the overexpression of *MDB-CLIP*, modest microtubule stabilization using low concentrations of taxol can transform non-growing neurites into growing axons and lead to an accumulation of polymerizing microtubule tips in the growth cone. Microtubules in taxol-induced axons also had the same stability as of control axons (Witte et al., 2008). In contrast, I show that neurons treated with low doses of nocodazole, a microtubule depolymerizing drug, resembled the phenotype of *DN-CLIP* transfected neurons: microtubules splayed out, the growth cones enlarged in size, and axon formation was inhibited.

Therefore, the similarities between *MBD-CLIP* evoked axons and taxol-induced axons suggest that the formation of axons in *MBD-CLIP* transfected neurons is regulated by modest stabilization of microtubules through CLIPs, likely by acting as microtubule rescue factors (Komarova et al., 2002).

Consistent with the idea that other microtubule-regulating molecules could also regulate axon formation, is that the microtubule-binding domain of CLIPs is

comprised of sequences that enable the interaction with other proteins. These are for example IQGAP1, or the +TIPs EB1 and EB3. In general, +TIPs accumulate in a complex at the tips of growing microtubules. Therefore, one could imagine that +TIPs have to interact with other +TIPs, organized in a complex, to influence microtubule dynamics. Therefore, other microtubule regulating proteins could also orchestrate axon formation (Witte and Bradke, 2008). These molecules could mediate microtubule stabilization through different molecular mechanisms, including inhibition of microtubule severance or enhancement of microtubule polymerization. The fundamental criterion, however, is that these putative molecules need only to modestly enhance microtubule stability in the axon, as this is critical for axon growth (Dehmelt et al., 2003; Witte et al., 2008).

4.2 CLIPs and the microtubule network during neuronal polarization

CLIPs regulate microtubule dynamics by regulating rescue frequencies and thereby support microtubule-growth (Komarova et al., 2002). Removal of CLIPs from microtubule plus ends leads to the equal shrinking and growing events of microtubules. This can result in a lack of net microtubule-growth, as demonstrated in CHO cells (Komarova et al., 2002), and a decrease of microtubule stability in macrophages (Binker et al., 2007).

However, I found that microtubule growth speed was not altered in developing hippocampal neurons after depleting CLIPs from microtubules. Thus, the impaired neuronal development is unrelated to microtubule growing events. However, the ultimate destination of microtubules was affected in that they failed to reach the peripheral zone of the growth cone when CLIPs were non-functional. By measure of posttranslational microtubule modifications, I also found that microtubules were less stable after inhibiting the CLIP-attachment to microtubules. Hence, while their growth rates are unchanged, microtubules may not provide the appropriate rigidity or strength to accommodate directional growth in the growth cone.

On the other hand, microtubules also failed to coalesce within the growth cone of neurons transfected with the dominant negative mutant of CLIPs. The same phenotype was found when Lis1 was knocked down in hippocampal neurons (Grabham et al., 2007). Lis1, a member of the +TIP family, composes together with dynactin, a regulatory unit of dynein. By using siRNA against Lis1, growth cone organization and axon elongation were altered. The distal axon was abnormally wide with spread microtubules, which were less resistant to the actin retrograde flow (Grabham et al., 2007). Therefore, in the absence of CLIPs, the combined loss of microtubule-stability and -bundling might result in microtubules that are less resistant to the actin retrograde flow. This in turn may cause the lack of axon growth, as microtubule stability is necessary for axon formation.

Supporting this hypothesis, when the microtubule-binding domain of CLIPs was overexpressed, microtubules appeared tightly bundled, exhibited the same stability as control microtubules, and extended in a directed manner up to the membrane edge of growth cones. These changes in microtubule organization resulted in the formation of supernumerary axons.

Thus, these data indicate that CLIPs are key regulators for the directed growth of microtubules into the growth cone and for the stabilization of microtubules to extend into the actin-rich area of the growth cone. In turn, these effects on the microtubule network are necessary and sufficient for axon growth.

4.3 CLIPs and the actin cytoskeleton during neuronal polarization

I provide evidence that CLIPs modulate not only microtubule dynamics during neuronal polarization, but also affect the actin cytoskeleton as well as growth cone dynamics. My data demonstrate that *DN-CLIP* transfected neurons have less motile, but enlarged growth cones with a reduced number of filopodia. However, the actin retrograde flow was not affected in these cells. Furthermore, the number of actin arcs in *DN-CLIP* transfected neurons increased, while pharmacologically induced actin

depolymerization or inhibition of actin arc contractibility caused the rescue of axon formation.

4.3.1 Microtubules as pushing force

Although there is evidence that microtubules interact with the actin cytoskeleton, it is still unclear how the former affect the latter. Microtubules are known to control the cell shape. For proper axon growth, both organized dynamic microtubules and a dynamic actin-rich growth cone are essential (Dent and Gertler, 2003). It was hypothesized that microtubules may therefore function as a “pushing force” for the axon to grow, whereas the actin cytoskeleton acts as a “steric hindrance” for uncontrolled microtubule-growth at the cortex of the growth cones (Witte and Bradke, 2008). In this context, dynamic microtubules were shown to be necessary to create an actin-free corridor within the T domain of the growth cone by pushing against the myosin-II generated actin arcs (Schaefer et al., 2008). Actin arcs prevent microtubules to invade the peripheral domain of the growth cone (Burnette et al., 2008; Lowery and Van Vactor, 2009; Schaefer et al., 2008). Therefore, unstable microtubules, as for example in neurons transfected with *DN-CLIP*, would fail to induce the disassembly of actin arcs, which leads to the continuous increase in the formation of these arcs. In accordance with this enhanced formation, unstable microtubules are not able to invade the area engorged by actin polymerization, which is essential for axon extension (Goldberg and Burmeister, 1986; Lowery and Van Vactor, 2009). Moreover, *DN-CLIP* transfected neurons miss the microtubule pushing force, which is essential for the axon to grow. Thus, the growth cone stalls. In addition, as the protrusion of the growth cone is only dependent of the actin dynamics (Goldberg and Burmeister, 1986; Lowery and Van Vactor, 2009), which are not affected in *DN-CLIP* transfected neurons, the growth cone increases in size.

This hypothesis is supported by the observation that the attenuation of steric hindrance by depleting the actin cytoskeleton or inhibiting the actin arc contractibility

in *DN-CLIP* transfected neurons re-enabled them to form an axon. Thus, even less organized and less stable microtubules seem to have the ability to push axonal growth, if the opposing actin filaments and arcs are lacking.

4.3.2 Interaction of microtubules with the actin cytoskeleton

Interactions between microtubules and the actin cytoskeleton play an important role in various fundamental processes, including cell motility, neuronal path finding, cellular wound healing, cell division and cortical actin flow (reviewed in (Rodriguez et al., 2003)). Already in 1988, *Forscher and Smith* demonstrated that actin filaments may play an important role in determining the spatial distribution of microtubules (Forscher and Smith, 1988). After applying the actin-depolymerizing drug cytochalasin D to *Aplysia* neurons, microtubule distribution within the growth cone was altered and immediately extended into the peripheral domain of the growth cone. Moreover, *Tanaka and Kirschner* demonstrated the importance of functional dynamic microtubules in the persistent forward movement of the actin-rich growth cones of *Xenopus* neurons (Tanaka et al., 1995). A study in fibroblasts showed that induced microtubule growth by either the washout of the microtubule-depolymerizing drug nocodazole or the local application of taxol activated the Rho GTPase Rac1. The induced microtubule growth resulted in actin-polymerization in lamellipodia protrusions, an essential event for cell migration (Waterman-Storer et al., 1999). Hence, manipulation of either component of the cytoskeleton results in the adaptation and reorganization of the opposing cytoskeletal component. This suggests the existence of an indirect interaction between microtubules and the actin cytoskeleton. After the discovery of +TIPs and their unique localization at the ends of microtubules, they have been suggested to link microtubules to the actin cytoskeleton. However, it is still unclear whether the actin cytoskeleton and microtubules is necessary for neuronal polarization.

In this study, I demonstrated that CLIPs specifically accumulate at the axonal tips of hippocampal neurons and get in close contact with the actin cytoskeleton within the

axonal growth cone. Due to their localization, CLIPs could directly affect the actin cytoskeleton by enabling the microtubule-actin interaction. To manage an interaction between microtubules and the actin cytoskeleton in the event of neuronal polarization, CLIPs would need to interact with proteins that are involved in regulating the actin cortex. In support of this, CLIP-170 is known to bind the actin-binding protein IQGAP1 via its N-terminal domain in Vero cells (Fukata et al., 2002). This interaction seems to capture and recruit microtubules to the actin cytoskeleton. In this scenario, the arrest of microtubules at the actin cortex could be an essential tool to deliver actin-modulating proteins, such as ADF/cofilin, Arp2/3 (Actin related protein 2/3) or also IQGAP, to alter actin dynamics. Along these lines, *Minc et al.* could show that the forced change of microtubule-shape in fission yeast resulted in the establishment of new sites of microtubule-cortex-interaction. This, in turn, led to the recruitment of polarity factors to these new sites of the cell, which, in turn, induced localized cell growth (Minc et al., 2009). Thus, increasing the number of potential CLIP-IQGAP interaction sites in unpolarized hippocampal neurons, leads to the recruitment of actin-regulatory factors to new sites of the neuron. This in turn results in the establishment of new sites of polarization. It thus stands to reason from the above observations that attenuating the capturing of microtubules to the actin cytoskeleton via the CLIP-IQGAP interaction, should lead to the loss of polarity spots. Indeed, when I overexpressed the microtubule-binding domain of CLIPs, which permits binding of CLIP-170 to IQGAP1, multiple axons were established. In contrast, when CLIPs were removed from microtubules, thereby inhibiting the link from the microtubules to IQGAP and the actin cytoskeleton, neuron development was impaired. Therefore, the capture of microtubules to the actin cytoskeleton via CLIP-170-IQGAP1 interaction might be of importance to allow the delivery of actin-modulating proteins.

My work also argues for the role of CLIP-170-IQGAP1 interactions in the regulation and control of microtubule growth. I mimicked the interaction of CLIP-170 and IQGAP1 using a mutant form of IQGAP1, that consisted only of the CLIP-170-binding domain. In this way, the IQGAP1-mutant only interacts with endogenous CLIP-170,

while endogenous IQGAP1 still binds to the actin cytoskeleton – thus dissociating the microtubule-actin link (Hart et al., 1996). Neurons, transfected with the IQGAP1-mutant, exhibited axons of increased length compared to control neurons. Moreover, they showed an unusually enlarged number of neurons with supernumerary axons. This could be due to a prolonged phase of microtubule growth, as the frequency of microtubule catastrophe events was significantly decreased. This observation is contrary to the knowledge that mammalian CLIPs do not affect microtubule catastrophe, but rather microtubule rescue. However, it is possible that the binding of the IQGAP-mutant to endogenous CLIP-170 led to conformational changes of CLIP-170 in a way that influenced the duration of subsequent CLIP-microtubule interactions and thereby delayed the dissociation from microtubules. This, in turn, might have affected microtubule catastrophe events in neurons that were transfected with IQGAP-1537.

Therefore, I hypothesize that the interaction of CLIP-170 with IQGAP1 plays a prominent role in regulating microtubule polymerization. Capturing microtubules at the actin cortex could therefore avoid uncontrolled growth of microtubules by arresting them at the actin cytoskeleton.

Along these lines, the linkage of microtubules to the actin cytoskeleton, which could be enabled through the CLIP-IQGAP interaction, may be essential for proper neuronal development on the one hand by allowing the delivery of proteins necessary for actin dynamics and on the other hand by regulating microtubule growth.

4.4 CLIPs for proper axon elongation

Taken together, my data indicate that CLIPs play an important role during neuronal polarization by affecting microtubule and growth cone dynamics. I propose the following model how CLIPs could be involved during neuronal polarization.

During initial neuronal polarization, a single neurite rapidly extends to become the axon (see introduction "Neuronal polarity"). For the extension, the axonal growth cone repeatedly undergoes a cycle of specific steps (Goldberg and Burmeister, 1986; Lowery and Van Vactor, 2009) (**Figure 4-1**). First, filopodia and lamellipodia, actin based structures at the growth cone periphery, explore the cellular environment and protrude; the growth cone frequently expands at this stage. Then, dynamic microtubules engorge from the central growth cone area into the former transitional domain, where actin filaments are then disassembled; the remaining actin arcs reorient towards the growth axis. The protruding microtubules transport vesicles, organelles and probably actin-modulating proteins into the engorged area. The extension of the neurite becomes consolidated by the bundling of microtubules in the central domain of the growth cone. Thereby, the proximal part of the growth cone resumes a cylindrical shape and becomes part of the axonal shaft. The repeat of these three events results in axon growth. As these processes do not operate in the minor neurites, only the axon grows.

My data suggest that CLIPs have an important function during this cycle of events in the future axonal growth cone leading to neuronal polarization. By modestly stabilizing microtubules, CLIPs enable microtubules to protrude to the growth cone tip. This, in turn, enables the microtubules to interact with the actin cytoskeleton, either by physically pushing against the actin network or by inducing actin related signaling. Weakening these features by removing CLIPs from microtubules could decrease rescue frequencies. Consequently, the microtubules fail to engorge the area already protruded by actin filaments, thus interrupting the growth cycle. Instead, the splayed microtubules cannot create a corridor free of actin arcs, which is formed when microtubules are bundled (**Figure 4-1**). As a result, the growth cone increases in size and the axon fails to extend.

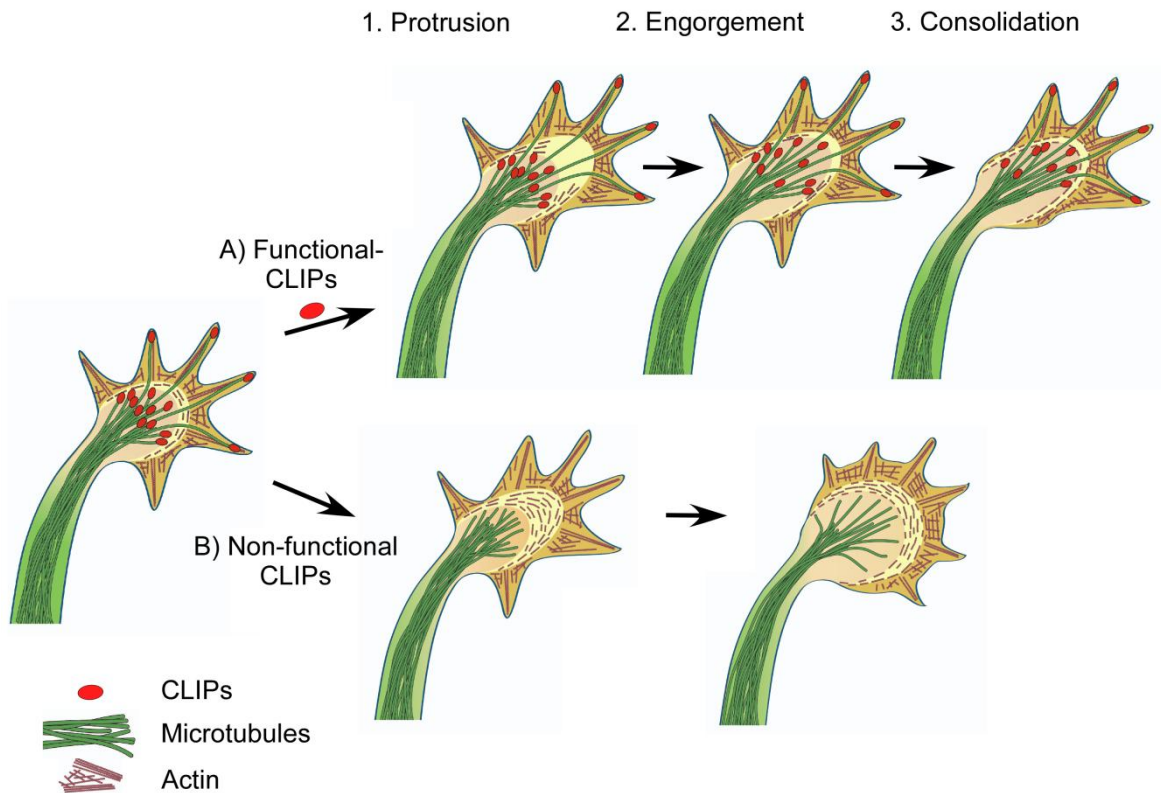


Figure 4-1: CLIPs enable microtubule engorgement of the growth cone during axon formation. **A**, Axon elongation consists of 3 repeating steps. First, filopodia and lamellipodia enable the growth cone to extend distally (*Protrusion*). Then, dynamic microtubules engorge from the central growth cone area into the former transitional zone, where actin filaments disassemble and the remaining arcs reorient towards the growth axis (*Engorgement*). Protruding microtubules transport vesicles and organelles into the engorged area. The extension of the neurite consolidates by the bundling of microtubules in the central domain; the proximal part of the growth cone resumes cylindrical shape and becomes part of the axonal shaft (*Consolidation*). **B**, Non-functional CLIPs lead to a decrease in microtubule-stability. Hence, while filopodia and lamellipodia still protrude, microtubules fail to subsequently engorge into the actin rich area. As a result, the growth cone area increases, but the axon fails to grow.

4.5 The “tug of war”

Initial neuronal polarization has been described as a “tug of war”, in which each neurite aims to become the axon (Craig and Banker, 1994). In this model, an intracellular re-enhancing feedback loop singles out one neurite to become the axon, while intrinsic inhibitory cues repress the growth of the others (Andersen and Bi, 2000; Witte and Bradke, 2008). The mutual influence of the actin network and the microtubule cytoskeleton could be part of this proposed positive feedback loop in the future axon. Consistently, a brief local microtubule stabilization (Witte et al., 2008) or actin depolymerization (Bradke and Dotti, 1999) can bias the fate of a neurite of a still unpolarized cell to become an axon. It suggests that a transient manipulation of either the actin or microtubule cytoskeleton is sufficient to promote axon specification by activating reinforcing events that promote sustained axonal outgrowth. Thus, CLIPs could regulate neuronal polarization by enhancing microtubule stability, in turn affecting growth cone dynamics and the underlying actin cytoskeleton. Changes in the actin network can then enable microtubules to protrude further distally into the growth cone (Schaefer et al., 2002; Schaefer et al., 2008), thereby generating a positive feedback loop.

A reinforcement of polarized growth might be further provided by vectorial membrane and cytoplasmic flow into the future axon, which may rely on stable microtubules (Bradke and Dotti, 1997). Consistent with this possibility, specific microtubule-dependent motor proteins, including kinesin-1, transport vesicles preferentially on stable microtubules and enrich before morphological polarization (Jacobson et al., 2006; Konishi and Setou, 2009; Reed et al., 2006). If the transported cargo contains limiting factors for axon growth, for example microtubule stabilizers, including CLIPs, or actin regulators, such as the Wiskott-Aldrich syndrome protein (WASP)-family verprolin-homologous protein (WAVE) (Kawano et al., 2005; Yokota et al., 2007), the axon would be enriched for those factors while the minor neurites would become depleted of them. Hence, CLIP mediated stabilization of microtubules may be one entry site to induce a re-enhancing loop to form an axon.

4.6 Concluding remarks

Modest microtubule stabilization has been shown to play an instructive role in the initial polarization of neuronal cells (Witte et al., 2008). I present here for the first time to the best of my knowledge, that CLIPs, a group of microtubule end-binding proteins, modestly enhance microtubule stability to generate an axon. This establishes microtubule stabilization as a key process during neuronal polarization on a molecular level. By affecting microtubules, CLIPs also influence dynamics of the actin cytoskeleton, suggesting the prominent role of direct microtubule-actin-interaction during the establishment of neuronal polarity. As the microtubule network and the actin cytoskeleton mutually influence each other, it implies that these cytoskeletal elements reinforce their changes to sustain axon growth. The molecular dissection of this putative enhancement loop is now the challenge ahead.

5 Materials and Methods

5.1 Materials

5.1.1 Chemicals

Table 5-1: Chemicals used in this study

Chemicals	Supplier
Acetone	Merck
Agarose	Biomol
Apo-transferrin, human	Sigma
Borax	Sigma
Boric acid	Merck
Bovine serum albumin, powder	Sigma
Copper (II) sulfate pentahydrate	Merck
Dimethyl sulfoxide	Roth
EDTA	Sigma
EGTA	Sigma
Ethanol absolute	Sigma
Fetal bovine serum	Invitrogen
Fish gelatin	Sigma
Gelmount mounting medium	Sigma
D(+)-Glucose monohydrate	Merck
L-Glutamine 200 mM	Invitrogen
Glycerol	Roth
Hank's balanced salt solution (HBSS) with Calcium and Magnesium	Invitrogen
HEPES (N-2-Hydroxyethylpiperazine-N'-2-ethane sulfonic acid)	Biomol
Horse serum	Sigma
Hydrochloric acid (HCl; 1M)	Merck
Insulin	Sigma
Magnesium chloride hexahydrate (MgCl ₂ *6H ₂ O)	Merck
MEM 10x	Invitrogen
MEM essential amino acids 50x	Invitrogen
MEM non-essential amino acids 100x	Invitrogen
Nitric acid (HNO ₃ ; ≥65 %)	Roth
Ovalbumin (albumin from chicken egg white)	Sigma
Paraffin	Merck
Paraformaldehyde	Merck
PIPES (1,4-Piperazinediethanesulfonic acid)	Sigma
Poly-L-lysine	Sigma
Progesteron	Sigma
Putrescine-dihydrochloride	Sigma
Pyruvate (piruvic acid)	Sigma
Selenium-dioxide	Sigma
Sodiumhydrogencarbonate (NaHCO ₃)	Merck
Sodium hydroxide	Merck

Sucrose	Merck
TEMED	Sigma
Tris(hydroxymethyl)-aminomethane	Merck
Tris base	Sigma
Triton X(TX)-100	Roth
Trypsin-EDTA (1x, 0.05 % Trypsin, 0.53 mM EDTA*4Na)	Invitrogen

5.1.2 Drugs

Table 5-2: Drugs used in this study

Drug	Stock [mM]	Solvent	Supplier	Function
Cytochalasin D	10	DMSO	Sigma	Destabilization of F-actin
Taxol	5	DMSO	LC laboratories	Microtubule stabilization
Blebbistatin	50	DMSO	Sigma	Myosin-II inhibition
ML7	10	DMSO	Sigma	Myosin light chain kinase inhibition
Latrunculin B	1	DMSO	Mo Bi Tec	Inhibition of actin polymerization
Nocodazole	6.67	DMSO	Sigma	Microtubule destabilization

5.1.3 Commercial kits

Table 5-3: Commercial kits

Name	Supplier & Product number
EndoFree Plasmid Maxi Kit	Quiagen
Rat Neuron Nucleofector Kit	Amaya

5.1.4 Equipment

Table 5-4: Equipment

Equipment	Model	Supplier
<u>Primary Cell Culture</u>		
Incubator (with CO ₂)	HERAcell®240	Kendro
Dissection stereomicroscope	Stemi SV6	Zeiss
Forceps	Straight forceps Dumon #5, 11 cm, Biological tips	Fine Science Tools
	Curved forceps Dumont #7, 11.5 cm, Biological tips	Fine Science Tools
Scissors	Vannas-Tübingen spring scissors, 8.5 cm, straight tips	Fine Science Tools
	Hardened fine iris scissors, 11 cm, straight tips	Fine Science Tools
	Extra fine scissors, model "Bonn", 8.5 cm, straight tips	Fine Science Tools
<u>Eletroporation</u>		
<i>In vitro</i>	Nucleofector™ II	Amaxa
<i>in vivo</i>	BTX ECM830	VWR
<u>Microscope</u>		
CCD Camera	4912-5000 or 4912-5100	Cohu
Camera control panel	C 2741	Hamamatsu
Image acquisition hardware for PC	LG3 image grabber	Scion Corp.
Inverted epifluorescence microscopes	Axiovert 135TV	Zeiss
	AxioObserver.D1	Zeiss
Inverted bright field microscope	Wilovert ^R	Will
Mechanical microscope shutters	Uniblitz-Shutter for phase light (incl. adapter) VS25S 2 ZM 0-21	Vincent Associates
	Uniblitz-Shutter for fluorescence light (incl. adapter) VS25S 2 ZM 0 R1-21 (with high temperature modification)	Vincent Associates
Shutter driver	VMM-D1 or VCM-D1	Vincent Associates
<u>Western Blotting</u>		
Western Blot Electrophoresis Cell	XCell Surelock™	XCell
Spectrophotometer	Ultrospec 3000	Amersham-Biosciences
<u>Surgical Instruments (in vivo)</u>		
Forceps		Fine Science Tools
Scissors		Fine Science Tools

5.1.5 Consumables

Table 5-5: Consumables

Material	Type	Supplier
<u>Filtration Systems</u>		
Bottle top filters	Steritop™ bottle top filter 250 ml/500 ml (0.22 µm)	Millipore
Filtration systems	Stericup™ filter unit 250 ml/500 ml (0.22 µm) Filter System 250 ml/500 ml (0.22 µm)	Millipore Corning Inc.
Syringe driven filter units	MillexR-GV, 0.22 µm (sterilization) or MillexR-HA, 0.45 µm (clarification)	Millipore
<u>Microscopy and immunohistochemistry</u>		
Cover glasses for microscopy	No. 1, ø 15 mm	Marienfeld
Cover glasses with relocation grid	Custom-made glass coverslips with 4x4 mm relocation grid	Laserzentrum Hannover
Glass bottom dishes	Custom-made 6 cm dishes, 13 mm hole size, with coverslip glued on bottom	Custom-made
Microscope slides	76x26 mm, with frosted end	Menzel-Gläser
<u>Tissue culture</u>		
Tissue culture flasks	Nunclon™ Delta surface, 75 cm ²	Nunc
Tissue culture plastic dishes	Nunclon™, ø 3 cm or 6 cm Falcon®, ø 10 cm	Nunc Becton and Dickinson
<u>Western Blotting</u>		
Western Blot gel cassettes	Gel cassettes, 1.5 mm	Invitrogen
Semi-dry transfer system		Custom-made
Membrane for protein transfer	PVDF membrane, Hybond-P	GE Healthcare
Western Blotting Detection System	ECL Plus Detection System	GE Healthcare
Molecular Weight Marker	Full range rainbow marker; range from 12K-225KDa	GE Healthcare

5.1.6 Media, buffers and standard solutions

5.1.6.1 Buffers and standard solutions

Table 5-6: Buffers and standard solutions

Solution	Ingredients and preparation	
<u>Cell culture</u>		
Borate Buffer, pH 8.5	1.24 g Boric acid 1.90 g Borax	Dissolve in 390 ml of distilled water. Adjust pH to 8.5 with 1 M HCl or NaOH if necessary. Adjust volume to 400 ml and filter-sterilize. Store at RT.
16 % PFA	16 % (w/v) PFA 16 % (w/v) Sucrose	PFA should be handled under the fume hood. Heat 650ml water to ~60 °C, add 3 pellets of NaOH and 160 g PFA powder. Continue heating until PFA is fully dissolved. Add 160 g sucrose and stir until fully dissolved. Add 100ml 10x PBS. Adjust pH 7.4 with HCl and adjust volume to 1 l with 1xPBS. Filter solution through paper filter and store aliquots at -20 °C.
5x PHEM buffer, pH 6.9	300 mM PIPES 125 mM HEPES 50 mM EGTA 10 mM MgCl ₂	<p><u>For 250ml:</u> 4.54 g PIPES powder 1.49 g HEPES powder 5 ml EGTA (500mM) 0.5 ml MgCl₂ (1M)</p> <p>Dissolve all ingredients in 200 ml of distilled water. Adjust pH to 6.9 with 1/10 of the final volume of 5N NaOH. Adjust volume to 250 ml with distilled water and check pH again. Filter solution through 0.45 µm filter and store at RT.</p>
Phosphate-buffered saline (PBS)	137 mM NaCl 2.7 mM KCl 8 mM Na ₂ HPO ₄ 1.5 mM KH ₂ PO ₄	<p><u>For 1 l:</u> 8 g NaCl 0.2 g KCl 1.15 g Na₂HPO₄ 0.24 g KH₂PO₄</p> <p>Dissolve all ingredients in 800 ml of distilled water. Adjust to pH 7.4 with HCl and adjust volume to 1 l with distilled water. Sterilize by autoclaving and store at RT. For 10x PBS use the 10-fold amount of salts in 1 l of distilled water.</p>
<u>Western Blotting</u>		
1 M Tris-HCl, pH 7.4 or 8.0		Dissolve 121.1 g Tris base in 800 ml of distilled water.

		Adjust pH to the desired value by adding HCl. Adjust volume to 1 l. Sterilize by autoclaving and store at RT.
Running buffer	50 ml 1 M Tris-HCl 0.1 % SDS	Mix 50 ml of Tris-HCl with 1 l H ₂ O. Add 0.1 % SDS and mix. Store at RT.
Transfer buffer	100 ml 1 M Tris-HCl 100 ml MeOH	Mix 100 ml Tris-HCl with 100 ml MeOH in 1 l H ₂ O.
4x Tris-Cl/SDS, pH 6.8	6.05 g Tris base (Trizma)	Dissolve Tris base in 40 ml distilled water. Adjust pH to 6.8 with 1 N HCl (37 %). Add distilled water to 100 ml total volume. Filter solution through 0.45 µm filter and add 0.4 g SDS. Store at RT.
4x Tris-Cl/SDS, pH 8.8	91 g Tris base (Trizma)	Dissolve Tris base in 300 ml distilled water. Adjust pH to 8.8 with 1 N HCl. Add distilled water to 500 ml total volume. Filter solution through 0.45 µm filter and add 2 g SDS. Store at RT.
Blocking solution	25 g Milk powder 0.1 % Tween	Dissolve milk powder in 500 ml PBS, add 0.1 % Tween and stir until fully dissolved.
PBS-Tween	0.1 % Tween	Dissolve 0.1 % Tween in 500 ml PBS until fully dissolved.
5x Laemmli buffer	250 mM Tris-HCl, pH6.8 1 M β-Mercaptoethanol 10 % (w/v) SDS 30 % (v/v) Glycerol	Handle SDS under the fume hood. Store aliquots at -20°C.

5.1.6.2 Media and supplements for primary cell culture

Table 5-7: Stock solutions

Solution	Ingredients	Preparation
5.5 % (w/v) NaHCO ₃	27.5 g NaHCO ₃	Dissolve NaHCO ₃ in distilled water and filter-sterilize. Store at 4 °C.
20 % (w/v) Glucose	20 % (w/v) D(+)-glucose	Warm up distilled water and add glucose stepwise under constant stirring. Do not autoclave but rather filter-sterilize. Store at 4 °C.
L-glutamine (100x)	200 mM glutamine	Dissolve glutamine in warm distilled water. Store 5 ml aliquots at -20 °C.
Pyruvate (100x)	1.1 g pyruvate	Dissolve pyruvate in 100 ml distilled water. Filter-sterilize and store at 4 °C for up to ~3 months.

Table 5-8: N2 supplements

Supplement	Preparation
Insulin (1.000x)	Dissolve 50 mg insulin in 10 ml 0.01 N HCl, store aliquots at -20 °C.
Progesteron (1.000x)	Dissolve 63 mg Progesteron in 100 ml ethanol, add 1 ml of this solution to 99 ml distilled water. Store aliquots at -20 °C.
Putrescine-dihydrochloride (1.000x)	Dissolve 161 mg putrescine-dihydrochloride in 10 ml distilled water, store aliquots at -20 °C.
Selenium-dioxide (1.000x)	Dissolve 33 mg selenium-dioxide in 100 ml distilled water, add 1 ml of this solution to 99 ml distilled water. Store aliquots at -20 °C.
N2 supplement stock (10x)	Mix 5 ml of each insulin, progesteron, putrescine-dihydrochloride and selenium-dioxide 1.000x-stocks with 500 mg human apo-transferrin in a total volume of 500 ml N-MEM. Store aliquots for up to ~6 months at -20 °C.

Table 5-9: Cell culture media

MEM-HS (Minimal essential medium supplemented with 10 % (v/v) horse serum)	300 ml	distilled water
	50 ml	10x MEM
	20 ml	5.5 % NaHCO ₃
	15 ml	20 % (w/v) glucose
	5 ml	L-glutamine (100x)
	10 ml	50x MEM essential aminoacids
	10 ml	100x MEM non-essential aminoacids
50 ml	horse-serum	
Adjust pH to 7.3 with 1 M NaOH, add distilled water to 500 ml. Filter-sterilize and store at 4 °C for up to ~2 weeks.		
N-MEM	50 ml	10xMEM
	20 ml	5.5 % NaHCO ₃
	15 ml	20 % (w/v) glucose
	5 ml	L-Glutamine (100x)
	5 ml	Pyruvate (100x)
Mix all ingredients in a total volume of 500 ml distilled water. Filter-sterilize and store at 4 °C for up to ~2 weeks.		

N2 medium	450 ml	N-MEM
	50 ml	N2 supplement stock (10x)
	100 mg	Ovalbumin
<p>Check pH, adjust to 7.3 if necessary. Filter-sterilize and store at 4 °C for up to ~2 weeks.</p>		

5.1.6.3 Media and antibiotics for bacterial culture

Table 5-10: Bacterial media

LB (Luria-Bertani-) media	1 % (w/v)	Bacto-Trypton
	0.5 % (w/v)	Yeast extract
	0.5 % (w/v)	NaCl
<p>Add distilled water to final volume, Adjust pH to 7.5 if necessary. Sterilize by autoclaving and store at RT.</p>		
LB-plates	<p>Like LB media, but supplemented with 1.5 % Bacto-Agar before autoclaving. Store at 4 °C.</p>	

LB-Agar was cooled to 55 °C, LB-media to RT before the addition of antibiotics. After addition of antibiotics selection media and plates were stored at 4 °C.

Table 5-11: Antibiotic stocks

Ampicillin	100 mg/ml
Kanamycin	50 mg/ml

Dissolve antibiotics in distilled water (1.000x stock solutions), filter-sterilize and store aliquots at -20 °C.

5.1.7 Antibodies

5.1.7.1 Primary antibodies

Table 5-12: Primary antibodies used for immunohistochemistry

Antibody	Dilution	Type	Supplier & Product number
anti-acetylated tubulin (clone 6-11B-1)	1:50.000	mouse monoclonal, ascites fluid	Sigma, #T-6793
anti-GFP (goat)	1:5.000	goat polyclonal	USBiological, #G8965-05
anti-GFP (rabbit)	1:2.000	rabbit polyclonal	RDI Research Diagnostics Inc., #RDI-GRNFP4abr
anti-MAP2 (goat)	1:2.000	goat polyclonal	Santa Cruz, #sc-5357
anti-MAP2 (mouse)	1:5.000	mouse monoclonal	Sigma, #M-4403
anti-MAP2 (rabbit)	1:6.000	rabbit polyclonal	Chemicon, #AB5622
anti-Synapsin 1	1:200	rabbit polyclonal	Chemicon, #AB1543
anti-α-tubulin (clone B-5-1-2)	1:20.000	mouse monoclonal	Sigma, #T-5168
anti-tyrosinated tubulin (YL1/2)	1:40.000 1:200 to 1:3.000	rat monoclonal	Abcam, #ab6160 (purified) gift from M. Schleicher (supernatant of hybridoma cells)
anti-Tau-1	1:5.000	mouse monoclonal	Chemicon, #MAB 3420
anti-CLIP	1:1.000	rabbit polyclonal	Gift from S. Kandel-Lewis
anti-cortactin	1:500	mouse monoclonal	clone 4F11; Upstate Biotechnology, Millipore

5.1.7.2 Secondary antibodies

Used secondary antibodies were purchased from Invitrogen and used diluted as 1:500.

Table 5-13: Secondary antibodies

Specificity	Host	Fluorochrome
anti-goat	Donkey	Alexa Fluor 350
		Alexa Fluor 488
		Alexa Fluor 568
anti-mouse	Donkey	Alexa Fluor 555
	Goat	Alexa Fluor 350
		Alexa Fluor 488
		Alexa Fluor 555
Alexa Fluor 568		
anti-rabbit	Donkey	Alexa Fluor 488
	Goat	Alexa Fluor 350
		Alexa Fluor 488
		Alexa Fluor 555
Alexa Fluor 568		
anti-rat	Goat	Alexa Fluor 568
		Alexa Fluor 488
Mouse-HRP (Sigma; 1:5.000)		
Rabbit-HRP (Sigma; 1:10.000)		

5.1.8 Bacteria and Plasmids

For plasmid propagation the E. coli strain DH5 α was used.

Table 5-14: Plasmids

Plasmid name	Selection marker	Description	Reference
pEGFP-C1 DN-CLIP	Kan	Dominant negative form of CLIP-170 (aa 1027-1320), removing CLIP-115 and CLIP-170 from microtubules	Komarova et al., 2002
pEGFP-C1 <i>MBD-CLIP</i>	Kan	Microtubule-binding domain of CLIP-115 and CLIP-170 (aa4-596)	Komarova et al., 2002
pEGFP-N2	Kan	control vector (GFP)	Clontech
pEGFP-N1-EB3	Kan	End-binding protein 3 bound to GFP	Stepanova et al., 2003
mCherry-2-EB3	Kan	End-binding protein 3 bound to mCherry	
Lifeact-pEGFP-N1	Kan	17-amino-acid peptide staining F-actin structures, bound to GFP	Riedl et al., 2008
Lifeact-RFP	Kan?	17-amino-acid peptide staining F-actin structures, bound to RFP	Riedl et al., 2008
shRNA scrambled	Amp	GTGCGTTGCTAGTACCAAC; backbone was RNAi-Ready pSIREN-RetroQ-ZsGreen	Oligonucleotides from Metabion, Martinsried, Germany; vector from BD Biosciences
shRNA CLIP-115	Amp	ACAAAGCTGAATGGCGGATAA; backbone was RNAi-Ready pSIREN-RetroQ-ZsGreen	Oligonucleotides from Metabion, Martinsried, Germany; vector from BD Biosciences
shRNA CLIP-170	Amp	CTAGATTACCAGCACGAAATA; backbone was RNAi-Ready pSIREN-RetroQ-ZsGreen	Oligonucleotides from Metabion, Martinsried, Germany; vector from BD Biosciences
IQGAP 1537	Amp	CLIP-170 binding domain of IQGAP1	Brandt et al., 2007

pEGFP-C1 DN170, pEGFP-C1 MBD170 and pEGFP-N1-EB3 were provided by A. Akhmanova (Erasmus Medical Center, Rotterdam, Netherlands). mCherry-EB3 was a gift from V. Small (Institute of Molecular Biotechnology of the Austrian Academy of Sciences, Vienna, Austria).

5.2 Methods

5.2.1 Cell culture

5.2.1.1 Primary culture of hippocampal neurons

Glass coverslips for culturing neurons were treated before as described in De Hoop et al., 1998. In brief, glass coverslips were bathed in nitric acid ($\geq 65\%$) overnight, washed in distilled water, sterilized at $220\text{ }^{\circ}\text{C}$ for 6 hours and distributed to 6cm petridishes under sterile conditions. Coverslips were equipped with paraffin dots and coated with poly-L-lysine (1mg/ml poly-L-lysine in borate buffer) overnight, washed with water and incubated with minimal essential medium (MEM) and 10% heat-activated horse serum at $36\text{ }^{\circ}\text{C}$.

Primary hippocampal neurons derived from E18 rat embryos were cultured as described before (Witte et al., 2008). Briefly, hippocampi of E18 rats were dissected, trypsinized for 15 min with 0.05% Trypsin-EDTA at $36\text{ }^{\circ}\text{C}$, washed with warm HBSS and 7 mM HEPES, and dissociated in HBSS with a fire-polished Pasteur pipette. 110×10^3 neurons were plated on poly-L-lysine coated glass coverslips in 6cm petridishes containing MEM and horse serum. Dishes were kept in 5% CO_2 at $36\text{ }^{\circ}\text{C}$. After 6-8 hours, coverslips were transferred to a 6 cm dish containing cultured astrocytes in MEM and N2 supplements.

5.2.1.2 Primary culture of astrocytes

Astrocytes were obtained from hippocampus in essentially the same way as described for culturing hippocampal neurons. However, to obtain astrocytes, in addition to the hippocampus, the surrounding cortex can also be used. Approximately 2 million astrocytes were plated into tissue culture flasks containing MEM and horse serum and kept at $36\text{ }^{\circ}\text{C}$ with 5% CO_2 . The next day, the medium was exchanged to remove cell debris. At a confluency of 80% , cells were trypsinized with 0.05% Trypsin-EDTA containing 10 mM HEPES and afterwards split either to new flasks or 6 cm petridishes.

5.2.1.3 Transfection of hippocampal neurons

Hippocampal neurons were transfected before plating with highly purified (endogen-free) DNA using the Amaxa Nucleofector system. Per transfection, 500.000 cells were spun down for 5 min at 630 rpm and the cell pellet resuspended in 100 μ l of the Amaxa rat nucleofector solution. 3 μ g of plasmid DNA was added to the solution and transferred to the Amaxa cuvette. To electroporate rat hippocampal neurons, the program O-003 was used. Directly after electroporation, 500 μ l of warm MEM-HS was added to the suspension and distributed into 2 dishes containing poly-L-lysine coated coverslips in MEM-HS and further cultured as above.

5.2.1.4 Drug treatment

For long term experiments, cultured neurons were treated with 3 nM taxol, 1 μ M cytochalasin D, 1 μ M blebbistatin, 1 μ M latrunculin B, 1 μ M ML7, 10 μ M Y27632, or 3.3 μ M nocodazole directly after flipping the cells into the dishes containing MEM-N2 and further kept at 36 °C with 5 % CO₂.

For short term experiments, neurons, cultured on custom-made glass bottom dishes, were treated with 5 μ M cytochalasin D or 5 μ M blebbistatin and directly imaged in the presence of the drug.

Nocodazole precipitates in aqueous solutions. To ensure homogenous distribution of this drug, 1 ml of the medium of the cells to be treated was transferred to a 2 ml Eppendorf tube, the drug was added to the tube and vortexed immediately after addition. The medium was transferred back to the dish and mixed by swirling.

5.2.2 Microscopy

5.2.2.1 Live cell imaging and image acquisition

Images of fixed cells or time-lapse recordings were captured using an Axiovert 135/135TV inverted microscope (Carl Zeiss, Oberkochen, Germany), and standard filters for GFP, Texas Red, and DAPI, using a high performance CCD camera 4912

(COHU) and Scion Image Beta 4.0.2 software for Microsoft Windows. Images or recordings were obtained by mounting the coverslips on HBSS/HEPES-containing closed metal chambers and images were taken at 37 °C.

Time-lapse recordings of short term treatments with blebbistatin or cytochalasin D were obtained by using custom-made glass bottom dishes and acquired using a life cell imaging set up (Delta vision RT; Applied Precision).

5.2.2.2 Image analysis and quantification

Length, area and intensity measurements were performed using Scion Image Beta 4.0.2 for Microsoft Windows, ImageJ and Metamorph analysis software.

To analyze movement of fluorescence particles in EB3-transfected neurons, fluorescence images were acquired in 3-5 second intervals during the experiment. Subsequently, kymographs from the regions of interest were made from the individual images using a purpose-written program. To calculate microtubule growth speeds, the slopes of lines drawn on kymographs from the beginning to the end of individual EB3-movements were measured.

The ratio of acetylated versus tyrosinated α -tubulin was determined from the mean fluorescence intensity of both channels in a square of 3 x 3 to 5 x 5 pixels in the medial part of each process after background subtraction with Photoshop (Adobe). For ratio-quantifications, axons were defined as a process at least 40 μ m long.

In all other experiments, axons were identified by Tau-1 staining.

To quantify splayed microtubule-length, the distance from microtubule-tips to the area where microtubules appeared in a bundled formation, was measured.

Actin dynamics were quantified for a time period of 50 s by measuring changes of growth cone area every 10 s. Growth cones were outlined manually using Metamorph software. Growth-cone outlines were pasted onto the following images

and changes of growth cone area between the single images were added together for a total growth cone area change over time.

For analyzing actin retrograde flow, images of Lifeact-transfected neurons were taken every 5 s during the experiment. Retrograde flow was measured as the slope of diagonal lines in kymographs that were acquired by using Metamorph software.

5.2.3 Immunohistochemistry

5.2.3.1 Fixation methods

PFA-fixation

To stain for Tau-1, MAP-2 and Synapsin 1, cells were fixed with 4 % paraformaldehyde, 4 % sucrose in PBS for 20 min and quenched with 50mM ammonium chloride in PBS for 10 min to inactivate residual formaldehyde. After quenching, cells were permeabilized with 0.1 % Triton X-100 in PBS for 5 min.

PHEM-fixation

To assess acetylated, tyrosinated, and total tubulin integrated in microtubules without unpolymerized tubulin subunits, cells were simultaneously fixed and permeabilized in PHEM buffer (60 mM Pipes, 25 mM HEPES, 5 mM EGTA and 1 mM MgCl) containing 0.25 % glutaraldehyde, 3.7 % paraformaldehyde, 3.7 % sucrose and 0.1 % Triton X-100 (as described in Witte et al., 2008), and quenched as above.

Methanol/PFA-fixation

For CLIP- and Cortactin-staining, the effects of transfected constructs were assessed by plating the cells after transfection on coverslips with a relocation grid. After image acquisition of GFP positive cells, the cells were fixed with icecold MeOH for 30 s,

followed by 20 min 4 % paraformaldehyde, 4 % sucrose in PBS, quenched and extracted as above.

5.2.3.2 Immunostaining

For immunostaining, the quenched coverslips were blocked at room temperature for 1 h in a solution containing 2 % fetal bovine serum, 2 % bovine serum albumin, and 0.2 % fish gelatin in PBS. Cells were then incubated with primary antibodies diluted in 10 % blocking solution for at least 1 hour at R or overnight at 4 °C. Then the coverslips were washed 3x with PBS and incubated with secondary antibodies diluted in 10 % blocking solution for at least 30 min at RT. After the incubation time, coverslips were washed 3x with PBS and 3x with distilled water to remove traces of salts. Wax dots attached to the coverslips were removed manually and coverslips were mounted with Gelmount on slides and dried for ~1 hour and kept in the dark.

5.2.4 Molecular Biology

5.2.4.1 Culturing E. coli

E. coli was cultivated at 37 °C under aerobic conditions either in liquid LB-media with vigorous shaking (220 rpm) or on LB-plates. Cultures were inoculated from single colonies. For plasmid selection, media or plates containing appropriate antibiotics were used.

5.2.4.2 Transformation of competent *E. coli* cells

10 to 100 µl of chemical competent bacteria were gently thawed on ice and mixed with the plasmid to be transformed in a 1.5 ml Eppendorf tube. The tube was incubated on ice for 10 min. Bacteria were heat-shocked by incubation at 42 °C for 1 min and then chilled on ice for 2 min. 1 ml of plain LB medium was added to the

cells, incubated at 37 °C for 60 min with shaking at 225-250 rpm. 50 to 100 µl of the transformation were plated on LB agar plates containing the appropriate antibiotic for plasmid selection and incubated at 37 °C overnight. Alternatively, when few transformants were expected, the transformation was spun down at maximum speed for 10 s in a table top centrifuge and 900 µl of the supernatant discarded. The bacterial pellet was resuspended in the remaining liquid, plated and cultured as described above.

5.2.4.3 Preparation of plasmid DNA

Plasmid DNA was purified from large-scale (100 ml, maxipreparation) bacterial cultures. LB medium containing 100 µg/ml ampicillin or 50 µg/ml kanamycin was inoculated from single colonies of transformed bacteria, starter cultures or bacterial glycerol stocks and incubated overnight at 37 °C with vigorous shaking. The bacterial suspension was pelleted by centrifugation at 4.000 rpm for 20 min at 4 °C and frozen down. Maxipreparation of plasmid DNA were carried out according to the Qiagen protocol employing alkaline lysis of the cells and binding of the plasmid DNA to an anion exchange resin. After washing, elution and precipitation the plasmid DNA was redissolved in a suitable volume of TE buffer. DNA concentration was analyzed using the Nanodrop System.

5.2.5 Biochemistry

5.2.5.1 Protein extraction and Western Blotting

For Western Blotting, either 300.000 untransfected neurons or 400.000 transfected neurons were plated on poly-L-lysine coated 6cm petridishes containing MEM-N2 and cultured up to 5 DIV at 36 °C with 5 % CO₂. Protein extracts were collected from 3 dishes per condition. Therefore, dishes were rapidly rinsed once in room temperatured PBS and SDS sample preparation buffer (Laemmli, 1970) was added to the dish and distributed equally. By using a cell scraper, protein extracts were collected in a 1.5 ml eppendorf tube, heated to boiling for 5 min, and precipitated

with 1.8 ml acetone. Protein concentration was determined applying the Bio-Rad Protein-Assay (Bio-Rad Laboratories GmbH, München, Germany) based on the method of Bradford (Bradford, 1976). SDS-PAGE was performed on 8% polyacrylamide gels (4 ml 30 % acrylamide/0.8 % bisacrylamid, 3.75 ml 4x Tris-Cl/SDS (pH 8.8), 7.25 ml H₂O, 50 µl 10 % ammonium persulfate, 10 µl TEMED) and run at 200 V. Proteins were transferred on polyvinylidene difluoride membranes using a semi-dry system (150 mA for 1 hour). Membranes were blocked for 1 hour at RT, incubated with first antibodies overnight at 4 °C and afterwards incubated with horse radish peroxide-linked secondary antibodies for 1 hour at RT. For protein detection, the membrane was incubated with enhanced chemiluminiscence (ECL) solution.

6 References

- Akhmanova, A., C.C. Hoogenraad, K. Drabek, T. Stepanova, B. Dortland, T. Verkerk, W. Vermeulen, B.M. Burgering, C.I. De Zeeuw, F. Grosveld, and N. Galjart. 2001. Clasps are CLIP-115 and -170 associating proteins involved in the regional regulation of microtubule dynamics in motile fibroblasts. *Cell*. 104:923-35.
- Akhmanova, A., A.L. Mausset-Bonnefont, W. van Cappellen, N. Keijzer, C.C. Hoogenraad, T. Stepanova, K. Drabek, J. van der Wees, M. Mommaas, J. Onderwater, H. van der Meulen, M.E. Tanenbaum, R.H. Medema, J. Hoogerbrugge, J. Vreeburg, E.J. Uringa, J.A. Grootegoed, F. Grosveld, and N. Galjart. 2005. The microtubule plus-end-tracking protein CLIP-170 associates with the spermatid manchette and is essential for spermatogenesis. *Genes Dev*. 19:2501-15.
- Al-Bassam, J., N.A. Larsen, A.A. Hyman, and S.C. Harrison. 2007. Crystal structure of a TOG domain: conserved features of XMAP215/Dis1-family TOG domains and implications for tubulin binding. *Structure*. 15:355-62.
- Allen, C., and G.G. Borisy. 1974. Structural polarity and directional growth of microtubules of *Chlamydomonas* flagella. *J Mol Biol*. 90:381-402.
- Amos, L., and A. Klug. 1974. Arrangement of subunits in flagellar microtubules. *J Cell Sci*. 14:523-49.
- Andersen, S.S., and G.Q. Bi. 2000. Axon formation: a molecular model for the generation of neuronal polarity. *Bioessays*. 22:172-9.
- Arimura, N., and K. Kaibuchi. 2007. Neuronal polarity: from extracellular signals to intracellular mechanisms. *Nat Rev Neurosci*. 8:194-205.
- Arnal, I., C. Heichette, G.S. Diamantopoulos, and D. Chretien. 2004. CLIP-170/tubulin-curved oligomers coassemble at microtubule ends and promote rescues. *Curr Biol*. 14:2086-95.

- Arregui, C., J. Busciglio, A. Caceres, and H.S. Barra. 1991. Tyrosinated and detyrosinated microtubules in axonal processes of cerebellar macroneurons grown in culture. *J Neurosci Res.* 28:171-81.
- Baas, P.W. 1998. The role of motor proteins in establishing the microtubule arrays of axons and dendrites. *J Chem Neuroanat.* 14:175-80.
- Baas, P.W., J.S. Deitch, M.M. Black, and G.A. Banker. 1988. Polarity orientation of microtubules in hippocampal neurons: uniformity in the axon and nonuniformity in the dendrite. *Proc Natl Acad Sci U S A.* 85:8335-9.
- Bai, J., R.L. Ramos, M. Paramasivam, F. Siddiqi, J.B. Ackman, and J.J. LoTurco. 2008. The role of DCX and LIS1 in migration through the lateral cortical stream of developing forebrain. *Dev Neurosci.* 30:144-56.
- Barnes, A.P., and F. Polleux. 2009. Establishment of axon-dendrite polarity in developing neurons. *Annu Rev Neurosci.* 32:347-81.
- Binker, M.G., D.Y. Zhao, S.J. Pang, and R.E. Harrison. 2007. Cytoplasmic linker protein-170 enhances spreading and phagocytosis in activated macrophages by stabilizing microtubules. *J Immunol.* 179:3780-91.
- Bito, H., T. Furuyashiki, H. Ishihara, Y. Shibasaki, K. Ohashi, K. Mizuno, M. Maekawa, T. Ishizaki, and S. Narumiya. 2000. A critical role for a Rho-associated kinase, p160ROCK, in determining axon outgrowth in mammalian CNS neurons. *Neuron.* 26:431-41.
- Bradke, F., and C.G. Dotti. 1997. Neuronal polarity: vectorial cytoplasmic flow precedes axon formation. *Neuron.* 19:1175-86.
- Bradke, F., and C.G. Dotti. 1999. The role of local actin instability in axon formation. *Science.* 283:1931-4.
- Bradke, F., and C.G. Dotti. 2000. Establishment of neuronal polarity: lessons from cultured hippocampal neurons. *Curr Opin Neurobiol.* 10:574-81.
- Brandt, D.T., S. Marion, G. Griffiths, T. Watanabe, K. Kaibuchi, and R. Grosse. 2007. Dia1 and IQGAP1 interact in cell migration and phagocytic cup formation. *J Cell Biol.* 178:193-200.

- Brunner, D., and P. Nurse. 2000. CLIP170-like tip1p spatially organizes microtubular dynamics in fission yeast. *Cell*. 102:695-704.
- Buck, K.B., and J.Q. Zheng. 2002. Growth cone turning induced by direct local modification of microtubule dynamics. *J Neurosci*. 22:9358-67.
- Burack, M.A., M.A. Silverman, and G. Banker. 2000. The role of selective transport in neuronal protein sorting. *Neuron*. 26:465-72.
- Burnette, D.T., L. Ji, A.W. Schaefer, N.A. Medeiros, G. Danuser, and P. Forscher. 2008. Myosin II activity facilitates microtubule bundling in the neuronal growth cone neck. *Dev Cell*. 15:163-9.
- Busch, K.E., and D. Brunner. 2004. The microtubule plus end-tracking proteins mal3p and tip1p cooperate for cell-end targeting of interphase microtubules. *Curr Biol*. 14:548-59.
- Caceres, A., and K.S. Kosik. 1990. Inhibition of neurite polarity by tau antisense oligonucleotides in primary cerebellar neurons. *Nature*. 343:461-3.
- Caceres, A., J. Mautino, and K.S. Kosik. 1992. Suppression of MAP2 in cultured cerebellar macroneurons inhibits minor neurite formation. *Neuron*. 9:607-18.
- Carvalho, P., M.L. Gupta, Jr., M.A. Hoyt, and D. Pellman. 2004. Cell cycle control of kinesin-mediated transport of Bik1 (CLIP-170) regulates microtubule stability and dynein activation. *Dev Cell*. 6:815-29.
- Cassimeris, L., and C. Spittle. 2001. Regulation of microtubule-associated proteins. *Int Rev Cytol*. 210:163-226.
- Chien, C.B., D.E. Rosenthal, W.A. Harris, and C.E. Holt. 1993. Navigational errors made by growth cones without filopodia in the embryonic *Xenopus* brain. *Neuron*. 11:237-51.
- Conde, C., and A. Caceres. 2009. Microtubule assembly, organization and dynamics in axons and dendrites. *Nat Rev Neurosci*. 10:319-32.
- Coquelle, F.M., M. Caspi, F.P. Cordelieres, J.P. Dompierre, D.L. Dujardin, C. Koifman, P. Martin, C.C. Hoogenraad, A. Akhmanova, N. Galjart, J.R. De Mey, and O. Reiner. 2002. LIS1, CLIP-170's key to the dynein/dynactin pathway. *Mol Cell Biol*. 22:3089-102.

- Craig, A.M., and G. Banker. 1994. Neuronal polarity. *Annu Rev Neurosci.* 17:267-310.
- De Zeeuw, C.I., C.C. Hoogenraad, E. Goedknecht, E. Hertzberg, A. Neubauer, F. Grosveld, and N. Galjart. 1997. CLIP-115, a novel brain-specific cytoplasmic linker protein, mediates the localization of dendritic lamellar bodies. *Neuron.* 19:1187-99.
- Dehmelt, L., F.M. Smart, R.S. Ozer, and S. Halpain. 2003. The role of microtubule-associated protein 2c in the reorganization of microtubules and lamellipodia during neurite initiation. *J Neurosci.* 23:9479-90.
- Dent, E.W., and F.B. Gertler. 2003. Cytoskeletal dynamics and transport in growth cone motility and axon guidance. *Neuron.* 40:209-27.
- Dent, E.W., A.V. Kwiatkowski, L.M. Mebane, U. Philippar, M. Barzik, D.A. Rubinson, S. Gupton, J.E. Van Veen, C. Furman, J. Zhang, A.S. Alberts, S. Mori, and F.B. Gertler. 2007. Filopodia are required for cortical neurite initiation. *Nat Cell Biol.* 9:1347-59.
- DiTella, M.C., F. Feiguin, N. Carri, K.S. Kosik, and A. Caceres. 1996. MAP-1B/TAU functional redundancy during laminin-enhanced axonal growth. *J Cell Sci.* 109 (Pt 2):467-77.
- Dotti, C.G., C.A. Sullivan, and G.A. Banker. 1988. The establishment of polarity by hippocampal neurons in culture. *J Neurosci.* 8:1454-68.
- Drechsel, D.N., A.A. Hyman, M.H. Cobb, and M.W. Kirschner. 1992. Modulation of the dynamic instability of tubulin assembly by the microtubule-associated protein tau. *Mol Biol Cell.* 3:1141-54.
- Dujardin, D., U.I. Wacker, A. Moreau, T.A. Schroer, J.E. Rickard, and J.R. De Mey. 1998. Evidence for a role of CLIP-170 in the establishment of metaphase chromosome alignment. *J Cell Biol.* 141:849-62.
- Evans, L., T. Mitchison, and M. Kirschner. 1985. Influence of the centrosome on the structure of nucleated microtubules. *J Cell Biol.* 100:1185-91.
- Folker, E.S., B.M. Baker, and H.V. Goodson. 2005. Interactions between CLIP-170, tubulin, and microtubules: implications for the mechanism of Clip-170 plus-end tracking behavior. *Mol Biol Cell.* 16:5373-84.

- Forscher, P., and S.J. Smith. 1988. Actions of cytochalasins on the organization of actin filaments and microtubules in a neuronal growth cone. *J Cell Biol.* 107:1505-16.
- Fukata, M., T. Watanabe, J. Noritake, M. Nakagawa, M. Yamaga, S. Kuroda, Y. Matsuura, A. Iwamatsu, F. Perez, and K. Kaibuchi. 2002. Rac1 and Cdc42 capture microtubules through IQGAP1 and CLIP-170. *Cell.* 109:873-85.
- Galjart, N. 2005. CLIPs and CLASPs and cellular dynamics. *Nat Rev Mol Cell Biol.* 6:487-98.
- Gard, D.L., B.E. Becker, and S. Josh Romney. 2004. MAPping the eukaryotic tree of life: structure, function, and evolution of the MAP215/Dis1 family of microtubule-associated proteins. *Int Rev Cytol.* 239:179-272.
- Garvalov, B.K., K.C. Flynn, D. Neukirchen, L. Meyn, N. Teusch, X. Wu, C. Brakebusch, J.R. Bamberg, and F. Bradke. 2007. Cdc42 regulates cofilin during the establishment of neuronal polarity. *J Neurosci.* 27:13117-29.
- Geraldo, S., U.K. Khanzada, M. Parsons, J.K. Chilton, and P.R. Gordon-Weeks. 2008. Targeting of the F-actin-binding protein drebrin by the microtubule plus-tip protein EB3 is required for neuritogenesis. *Nat Cell Biol.* 10:1181-9.
- Goldberg, D.J., and D.W. Burmeister. 1986. Stages in axon formation: observations of growth of *Aplysia* axons in culture using video-enhanced contrast-differential interference contrast microscopy. *J Cell Biol.* 103:1921-31.
- Goldstein, L.S., and Z. Yang. 2000. Microtubule-based transport systems in neurons: the roles of kinesins and dyneins. *Annu Rev Neurosci.* 23:39-71.
- Gomis-Ruth, S., C.J. Wierenga, and F. Bradke. 2008. Plasticity of polarization: changing dendrites into axons in neurons integrated in neuronal circuits. *Curr Biol.* 18:992-1000.
- Goodson, H.V., S.B. Skube, R. Stalder, C. Valetti, T.E. Kreis, E.E. Morrison, and T.A. Schroer. 2003. CLIP-170 interacts with dynactin complex and the APC-binding protein EB1 by different mechanisms. *Cell Motil Cytoskeleton.* 55:156-73.

- Grabham, P.W., G.E. Seale, M. Bennecib, D.J. Goldberg, and R.B. Vallee. 2007. Cytoplasmic dynein and LIS1 are required for microtubule advance during growth cone remodeling and fast axonal outgrowth. *J Neurosci.* 27:5823-34.
- Grigoriev, I., S.M. Gouveia, B. van der Vaart, J. Demmers, J.T. Smyth, S. Honnappa, D. Splinter, M.O. Steinmetz, J.W. Putney, Jr., C.C. Hoogenraad, and A. Akhmanova. 2008. STIM1 is a MT-plus-end-tracking protein involved in remodeling of the ER. *Curr Biol.* 18:177-82.
- Gualdoni, S., C. Albertinazzi, S. Corbetta, F. Valtorta, and I. de Curtis. 2007. Normal levels of Rac1 are important for dendritic but not axonal development in hippocampal neurons. *Biol Cell.* 99:455-64.
- Hakeda-Suzuki, S., J. Ng, J. Tzu, G. Dietzl, Y. Sun, M. Harms, T. Nardine, L. Luo, and B.J. Dickson. 2002. Rac function and regulation during Drosophila development. *Nature.* 416:438-42.
- Hart, M.J., M.G. Callow, B. Souza, and P. Polakis. 1996. IQGAP1, a calmodulin-binding protein with a rasGAP-related domain, is a potential effector for cdc42Hs. *EMBO J.* 15:2997-3005.
- Hasaka, T.P., K.A. Myers, and P.W. Baas. 2004. Role of actin filaments in the axonal transport of microtubules. *J Neurosci.* 24:11291-301.
- Hayashi, I., and M. Ikura. 2003. Crystal structure of the amino-terminal microtubule-binding domain of end-binding protein 1 (EB1). *J Biol Chem.* 278:36430-4.
- Honnappa, S., C.M. John, D. Kostrewa, F.K. Winkler, and M.O. Steinmetz. 2005. Structural insights into the EB1-APC interaction. *EMBO J.* 24:261-9.
- Hoogenraad, C.C., A. Akhmanova, F. Grosveld, C.I. De Zeeuw, and N. Galjart. 2000. Functional analysis of CLIP-115 and its binding to microtubules. *J Cell Sci.* 113 (Pt 12):2285-97.
- Hoogenraad, C.C., B. Koekkoek, A. Akhmanova, H. Krugers, B. Dortland, M. Miedema, A. van Alphen, W.M. Kistler, M. Jaegle, M. Koutsourakis, N. Van Camp, M. Verhoye, A. van der Linden, I. Kaverina, F. Grosveld, C.I. De Zeeuw, and N. Galjart. 2002. Targeted mutation of Cyln2 in the Williams syndrome

- critical region links CLIP-115 haploinsufficiency to neurodevelopmental abnormalities in mice. *Nat Genet.* 32:116-27.
- Huisman, S.M., and M. Segal. 2005. Cortical capture of microtubules and spindle polarity in budding yeast - where's the catch? *J Cell Sci.* 118:463-71.
- Ishikawa, R., and K. Kohama. 2007. Actin-binding proteins in nerve cell growth cones. *J Pharmacol Sci.* 105:6-11.
- Jacobson, C., B. Schnapp, and G.A. Banker. 2006. A change in the selective translocation of the Kinesin-1 motor domain marks the initial specification of the axon. *Neuron.* 49:797-804.
- Jaworski, J., C.C. Hoogenraad, and A. Akhmanova. 2008. Microtubule plus-end tracking proteins in differentiated mammalian cells. *Int J Biochem Cell Biol.* 40:619-37.
- Jaworski, J., L.C. Kapitein, S.M. Gouveia, B.R. Dortland, P.S. Wulf, I. Grigoriev, P. Camera, S.A. Spangler, P. Di Stefano, J. Demmers, H. Krugers, P. Defilippi, A. Akhmanova, and C.C. Hoogenraad. 2009. Dynamic microtubules regulate dendritic spine morphology and synaptic plasticity. *Neuron.* 61:85-100.
- Jimbo, T., Y. Kawasaki, R. Koyama, R. Sato, S. Takada, K. Haraguchi, and T. Akiyama. 2002. Identification of a link between the tumour suppressor APC and the kinesin superfamily. *Nat Cell Biol.* 4:323-7.
- Kato, M., and W.B. Dobyns. 2003. Lissencephaly and the molecular basis of neuronal migration. *Hum Mol Genet.* 12 Spec No 1:R89-96.
- Kawano, Y., T. Yoshimura, D. Tsuboi, S. Kawabata, T. Kaneko-Kawano, H. Shirataki, T. Takenawa, and K. Kaibuchi. 2005. CRMP-2 is involved in kinesin-1-dependent transport of the Sra-1/WAVE1 complex and axon formation. *Mol Cell Biol.* 25:9920-35.
- Kholmanskikh, S.S., H.B. Koeller, A. Wynshaw-Boris, T. Gomez, P.C. Letourneau, and M.E. Ross. 2006. Calcium-dependent interaction of Lis1 with IQGAP1 and Cdc42 promotes neuronal motility. *Nat Neurosci.* 9:50-7.

- Komarova, Y.A., A.S. Akhmanova, S. Kojima, N. Galjart, and G.G. Borisy. 2002. Cytoplasmic linker proteins promote microtubule rescue in vivo. *J Cell Biol.* 159:589-99.
- Konishi, Y., and M. Setou. 2009. Tubulin tyrosination navigates the kinesin-1 motor domain to axons. *Nat Neurosci.* 12:559-67.
- Kunda, P., G. Paglini, S. Quiroga, K. Kosik, and A. Caceres. 2001. Evidence for the involvement of Tiam1 in axon formation. *J Neurosci.* 21:2361-72.
- Kuroda, S., M. Fukata, K. Kobayashi, M. Nakafuku, N. Nomura, A. Iwamatsu, and K. Kaibuchi. 1996. Identification of IQGAP as a putative target for the small GTPases, Cdc42 and Rac1. *J Biol Chem.* 271:23363-7.
- Lansbergen, G., and A. Akhmanova. 2006. Microtubule plus end: a hub of cellular activities. *Traffic.* 7:499-507.
- Lansbergen, G., Y. Komarova, M. Modesti, C. Wyman, C.C. Hoogenraad, H.V. Goodson, R.P. Lemaitre, D.N. Drechsel, E. van Munster, T.W. Gadella, Jr., F. Grosveld, N. Galjart, G.G. Borisy, and A. Akhmanova. 2004. Conformational changes in CLIP-170 regulate its binding to microtubules and dynactin localization. *J Cell Biol.* 166:1003-14.
- Lee, A.C., and D.M. Suter. 2008. Quantitative analysis of microtubule dynamics during adhesion-mediated growth cone guidance. *Dev Neurobiol.* 68:1363-77.
- Lee, H., U. Engel, J. Rusch, S. Scherrer, K. Sheard, and D. Van Vactor. 2004. The microtubule plus end tracking protein Orbit/MAST/CLASP acts downstream of the tyrosine kinase Abl in mediating axon guidance. *Neuron.* 42:913-26.
- Ligon, L.A., S.S. Shelly, M.K. Tokito, and E.L. Holzbaur. 2006. Microtubule binding proteins CLIP-170, EB1, and p150Glued form distinct plus-end complexes. *FEBS Lett.* 580:1327-32.
- Lowery, L.A., and D. Van Vactor. 2009. The trip of the tip: understanding the growth cone machinery. *Nat Rev Mol Cell Biol.* 10:332-43.
- Luders, J., and T. Stearns. 2007. Microtubule-organizing centres: a re-evaluation. *Nat Rev Mol Cell Biol.* 8:161-7.

- Maiato, H., P. Sampaio, and C.E. Sunkel. 2004. Microtubule-associated proteins and their essential roles during mitosis. *Int Rev Cytol.* 241:53-153.
- Marsh, L., and P.C. Letourneau. 1984. Growth of neurites without filopodial or lamellipodial activity in the presence of cytochalasin B. *J Cell Biol.* 99:2041-7.
- Martinez-Lopez, M.J., S. Alcantara, C. Mascaro, F. Perez-Branguli, P. Ruiz-Lozano, T. Maes, E. Soriano, and C. Buesa. 2005. Mouse neuron navigator 1, a novel microtubule-associated protein involved in neuronal migration. *Mol Cell Neurosci.* 28:599-612.
- Mimori-Kiyosue, Y., I. Grigoriev, G. Lansbergen, H. Sasaki, C. Matsui, F. Severin, N. Galjart, F. Grosveld, I. Vorobjev, S. Tsukita, and A. Akhmanova. 2005. CLASP1 and CLASP2 bind to EB1 and regulate microtubule plus-end dynamics at the cell cortex. *J Cell Biol.* 168:141-53.
- Minc, N., S.V. Bratman, R. Basu, and F. Chang. 2009. Establishing new sites of polarization by microtubules. *Curr Biol.* 19:83-94.
- Mitchison, T., and M. Kirschner. 1984. Dynamic instability of microtubule growth. *Nature.* 312:237-42.
- Moores, C.A., and R.A. Milligan. 2006. Lucky 13-microtubule depolymerisation by kinesin-13 motors. *J Cell Sci.* 119:3905-13.
- Muley, P.D., E.M. McNeill, M.A. Marzinke, K.M. Knobel, M.M. Barr, and M. Clagett-Dame. 2008. The atRA-responsive gene neuron navigator 2 functions in neurite outgrowth and axonal elongation. *Dev Neurobiol.* 68:1441-53.
- Nakada, C., K. Ritchie, Y. Oba, M. Nakamura, Y. Hotta, R. Iino, R.S. Kasai, K. Yamaguchi, T. Fujiwara, and A. Kusumi. 2003. Accumulation of anchored proteins forms membrane diffusion barriers during neuronal polarization. *Nat Cell Biol.* 5:626-32.
- Nathke, I. 2006. Cytoskeleton out of the cupboard: colon cancer and cytoskeletal changes induced by loss of APC. *Nat Rev Cancer.* 6:967-74.
- Nathke, I.S. 2004. The adenomatous polyposis coli protein: the Achilles heel of the gut epithelium. *Annu Rev Cell Dev Biol.* 20:337-66.

- Ng, J., and L. Luo. 2004. Rho GTPases regulate axon growth through convergent and divergent signaling pathways. *Neuron*. 44:779-93.
- Ng, J., T. Nardine, M. Harms, J. Tzu, A. Goldstein, Y. Sun, G. Dietzl, B.J. Dickson, and L. Luo. 2002. Rac GTPases control axon growth, guidance and branching. *Nature*. 416:442-7.
- Niccoli, T., A. Yamashita, P. Nurse, and M. Yamamoto. 2004. The p150-Glued Ssm4p regulates microtubular dynamics and nuclear movement in fission yeast. *J Cell Sci*. 117:5543-56.
- Perez, F., G.S. Diamantopoulos, R. Stalder, and T.E. Kreis. 1999. CLIP-170 highlights growing microtubule ends in vivo. *Cell*. 96:517-27.
- Pierre, P., J. Scheel, J.E. Rickard, and T.E. Kreis. 1992. CLIP-170 links endocytic vesicles to microtubules. *Cell*. 70:887-900.
- Pollard, T.D., and G.G. Borisy. 2003. Cellular motility driven by assembly and disassembly of actin filaments. *Cell*. 112:453-65.
- Pryer, N.K., R.A. Walker, V.P. Skeen, B.D. Bourns, M.F. Soboeiro, and E.D. Salmon. 1992. Brain microtubule-associated proteins modulate microtubule dynamic instability in vitro. Real-time observations using video microscopy. *J Cell Sci*. 103 (Pt 4):965-76.
- Reed, N.A., D. Cai, T.L. Blasius, G.T. Jih, E. Meyhofer, J. Gaertig, and K.J. Verhey. 2006. Microtubule acetylation promotes kinesin-1 binding and transport. *Curr Biol*. 16:2166-72.
- Riedl, J., A.H. Crevenna, K. Kessenbrock, J.H. Yu, D. Neukirchen, M. Bista, F. Bradke, D. Jenne, T.A. Holak, Z. Werb, M. Sixt, and R. Wedlich-Soldner. 2008. Lifeact: a versatile marker to visualize F-actin. *Nat Methods*. 5:605-7.
- Rodriguez, O.C., A.W. Schaefer, C.A. Mandato, P. Forscher, W.M. Bement, and C.M. Waterman-Storer. 2003. Conserved microtubule-actin interactions in cell movement and morphogenesis. *Nat Cell Biol*. 5:599-609.
- Sampo, B., S. Kaech, S. Kunz, and G. Banker. 2003. Two distinct mechanisms target membrane proteins to the axonal surface. *Neuron*. 37:611-24.

- Sandblad, L., K.E. Busch, P. Tittmann, H. Gross, D. Brunner, and A. Hoenger. 2006. The Schizosaccharomyces pombe EB1 homolog Mal3p binds and stabilizes the microtubule lattice seam. *Cell*. 127:1415-24.
- Schaefer, A.W., N. Kabir, and P. Forscher. 2002. Filopodia and actin arcs guide the assembly and transport of two populations of microtubules with unique dynamic parameters in neuronal growth cones. *J Cell Biol*. 158:139-52.
- Schaefer, A.W., V.T. Schoonderwoert, L. Ji, N. Mederios, G. Danuser, and P. Forscher. 2008. Coordination of actin filament and microtubule dynamics during neurite outgrowth. *Dev Cell*. 15:146-62.
- Schroer, T.A. 2004. Dynactin. *Annu Rev Cell Dev Biol*. 20:759-79.
- Schwamborn, J.C., and A.W. Puschel. 2004. The sequential activity of the GTPases Rap1B and Cdc42 determines neuronal polarity. *Nat Neurosci*. 7:923-9.
- Shi, S.H., T. Cheng, L.Y. Jan, and Y.N. Jan. 2004. APC and GSK-3beta are involved in mPar3 targeting to the nascent axon and establishment of neuronal polarity. *Curr Biol*. 14:2025-32.
- Slep, K.C., and R.D. Vale. 2007. Structural basis of microtubule plus end tracking by XMAP215, CLIP-170, and EB1. *Mol Cell*. 27:976-91.
- Song, A.H., D. Wang, G. Chen, Y. Li, J. Luo, S. Duan, and M.M. Poo. 2009. A selective filter for cytoplasmic transport at the axon initial segment. *Cell*. 136:1148-60.
- Sonnenberg, A., and R.K. Liem. 2007. Plakins in development and disease. *Exp Cell Res*. 313:2189-203.
- Stepanova, T., J. Slemmer, C.C. Hoogenraad, G. Lansbergen, B. Dortland, C.I. De Zeeuw, F. Grosveld, G. van Cappellen, A. Akhmanova, and N. Galjart. 2003. Visualization of microtubule growth in cultured neurons via the use of EB3-GFP (end-binding protein 3-green fluorescent protein). *J Neurosci*. 23:2655-64.
- Suter, D.M., and P. Forscher. 1998. An emerging link between cytoskeletal dynamics and cell adhesion molecules in growth cone guidance. *Curr Opin Neurobiol*. 8:106-16.

- Tai, C.Y., D.L. Dujardin, N.E. Faulkner, and R.B. Vallee. 2002. Role of dynein, dynactin, and CLIP-170 interactions in LIS1 kinetochore function. *J Cell Biol.* 156:959-68.
- Tanaka, E., T. Ho, and M.W. Kirschner. 1995. The role of microtubule dynamics in growth cone motility and axonal growth. *J Cell Biol.* 128:139-55.
- Tanaka, E.M., and M.W. Kirschner. 1991. Microtubule behavior in the growth cones of living neurons during axon elongation. *J Cell Biol.* 115:345-63.
- Trinczek, B., J. Biernat, K. Baumann, E.M. Mandelkow, and E. Mandelkow. 1995. Domains of tau protein, differential phosphorylation, and dynamic instability of microtubules. *Mol Biol Cell.* 6:1887-902.
- Tsai, J.W., K.H. Bremner, and R.B. Vallee. 2007. Dual subcellular roles for LIS1 and dynein in radial neuronal migration in live brain tissue. *Nat Neurosci.* 10:970-9.
- Waterman-Storer, C., A. Desai, and E.D. Salmon. 1999. Fluorescent speckle microscopy of spindle microtubule assembly and motility in living cells. *Methods Cell Biol.* 61:155-73.
- Westermann, S., and K. Weber. 2003. Post-translational modifications regulate microtubule function. *Nat Rev Mol Cell Biol.* 4:938-47.
- Wieland, G., S. Orthaus, S. Ohndorf, S. Diekmann, and P. Hemmerich. 2004. Functional complementation of human centromere protein A (CENP-A) by Cse4p from *Saccharomyces cerevisiae*. *Mol Cell Biol.* 24:6620-30.
- Williamson, T., P.R. Gordon-Weeks, M. Schachner, and J. Taylor. 1996. Microtubule reorganization is obligatory for growth cone turning. *Proc Natl Acad Sci U S A.* 93:15221-6.
- Winckler, B., P. Forscher, and I. Mellman. 1999. A diffusion barrier maintains distribution of membrane proteins in polarized neurons. *Nature.* 397:698-701.
- Wisco, D., E.D. Anderson, M.C. Chang, C. Norden, T. Boiko, H. Folsch, and B. Winckler. 2003. Uncovering multiple axonal targeting pathways in hippocampal neurons. *J Cell Biol.* 162:1317-28.

- Witte, H., and F. Bradke. 2008. The role of the cytoskeleton during neuronal polarization. *Curr Opin Neurobiol.* 18:479-87.
- Witte, H., D. Neukirchen, and F. Bradke. 2008. Microtubule stabilization specifies initial neuronal polarization. *J Cell Biol.* 180:619-32.
- Wolyniak, M.J., K. Blake-Hodek, K. Kosco, E. Hwang, L. You, and T.C. Huffaker. 2006. The regulation of microtubule dynamics in *Saccharomyces cerevisiae* by three interacting plus-end tracking proteins. *Mol Biol Cell.* 17:2789-98.
- Yap, C.C., D. Wisco, P. Kujala, Z.M. Lasiecka, J.T. Cannon, M.C. Chang, H. Hirling, J. Klumperman, and B. Winckler. 2008. The somatodendritic endosomal regulator NEEP21 facilitates axonal targeting of L1/NgCAM. *J Cell Biol.* 180:827-42.
- Yokota, Y., C. Ring, R. Cheung, L. Pevny, and E.S. Anton. 2007. Nap1-regulated neuronal cytoskeletal dynamics is essential for the final differentiation of neurons in cerebral cortex. *Neuron.* 54:429-45.
- Zhou, F.Q., J. Zhou, S. Dedhar, Y.H. Wu, and W.D. Snider. 2004. NGF-induced axon growth is mediated by localized inactivation of GSK-3beta and functions of the microtubule plus end binding protein APC. *Neuron.* 42:897-912.

Acknowledgements

First of all, I would like to thank my supervisor Dr. Frank Bradke for giving me the opportunity to do my PhD in his lab, for his great support and fruitful discussions.

I wish to thank MD Dr. Michael Sixt and Prof. Dr. Vic Small as members of my thesis committee for their efforts and helpful suggestions.

I would like to thank the Boehringer Ingelheim Fonds for their generous funding of the major part of my thesis. I deeply enjoyed the interesting seminars and the inspiring atmosphere within the BIF-family.

I am very grateful to Michael Stuess and Dr. Shalin Naik for critically reading my thesis and giving helpful suggestions. I am indebted to Liane Meyn for preparing excellent neuronal cultures and for being our caring lab-mom.

In general, I want to thank every single member of the Bradke lab, as each of you makes the Bradke-Lab to what is: a wonderful and motivating working space. My special thanks go to Boyan for his great supervision during my whole PhD, and for his wonderful and unique sense of humor. I want to thank Michi for helpful scientific suggestions, for always "google-ing" every question, for sharing excellent funk-music and all his "horrible" jokes. Big thanks to Sabina for helpful discussions regarding science and personal issues. Thanks to good old Harry, for sharing incredible funny moments with me and for providing very useful support for writing my thesis. Thanks to Farida, Joana and Kevin for being fantastic, helpful and very entertaining Postdocs. I want to thank Claudii for lovely girls-talk, formatting-support and excellent Golf-teaching. Thanks to Jörgl, who always creates action and fun during unlucky lab-days. Thanks to Sonja, Irene and Vanessa for creating a fresh breeze in the lab. Last but not least I want to thank Julia for great laughs and fantastic parties, and for being my personal motivator during all these years. To Frank, I would like to pronounce my respect for having the right touch to always pick great, enthusiastic and interested people for his lab.

Das größte Dankeschön gilt jedoch meiner Familie, insbesondere meinen Eltern. Ihr habt mich immer unterstützt, aufgebaut, und mir mit Eurem Stolz immer die nötige Motivation gegeben. Danke für all Eure Liebe und Hilfe zu jeder Zeit!!! Dem Rest meiner Familie, meinem Bruderherz, meiner Halbschwester Mandy, meiner Schnecke und meiner Britzn möchte ich danken, dass Ihr mir stets die nötige Ablenkung gegeben, mir manchmal die richtige Richtung gewiesen habt und immer für mich da gewesen seid, bei allen Höhen und Tiefen in den letzten Jahren!

Curriculum Vitae

Personal data

Name Dorothee Katharina Hildegard Neukirchen
Date of birth October 10th 1978 in Wertheim, Germany

Education

Since 09/2005 PhD thesis with PD Dr. Bradke at the Max Planck Institute for Neurobiology, Martinsried, Germany

11/2004-03/2004 Studies of Immunology at the Walter and Eliza Health Institute of Medical Research, Melbourne, Australia, practical project with Dr. Mireille Lahoud in the Department of Immunology

10/2004 Diploma in Biology

11/2003-09/2004 Diploma Thesis with Prof. Dr. Wesselborg, Section of Molecular Gastroenterology, Department of Internal Medicine, University Clinic of Tübingen

04/1999-11/2003 Studies of Biology at the Johannes Gutenberg University Mainz and the Eberhard-Karls-Universität Tübingen

10-12/1998 Practical course at Siemens in Erlangen, Germany

04/1998 Abitur

Fellowships

08/2006-08/2008 PhD scholarship of the Boehringer Ingelheim Foundation

Publications

Neukirchen and Bradke; **CLIPs regulate neuronal polarization through microtubule and actin dynamics**, *in submission*.

Tahirovic S, Hellal F, Neukirchen D, Hindges R, Garvalov BK, Flynn KC, Stradal TE, Chrostek-Grashoff A, Brakebuch C, Bradke F; **Rac1 regulates axon growth through the WAVE-complex**, *in submission*.

Berg CP, Schlosser SF, Neukirchen DK, Papadakis C, Gregor M, Wesselborg S, Stein GM (2009); **Hepatitis C virus core protein induces apoptosis-like caspase independent cell death**, *Virology*. 2009 Dec 1;6:213.

Riedl J, Crevenna AH, Kessenbrock K, Yu JH, Neukirchen D, Bista M, Bradke F, Jenne D, Holak TA, Werb Z, Sixt M, Wedlich-Soldner R. (2008); **Lifect: a versatile marker to visualize F-actin**, *Nat Methods*. 2008 Jul; 5(7):605-7. Epub 2008 Jun 8.

Witte H, Neukirchen D, Bradke F. (2008). **Microtubule stabilization specifies initial neuronal polarization**, *J Cell Biol*. 2008 Feb 11;180(3):619-32.

Garvalov BK, Flynn KC, Neukirchen D, Meyn L, Teusch N, Wu X, Brakebusch C, Bamberg JR, Bradke F. (2007). **Cdc42 regulates cofilin during the establishment of neuronal polarity**, *J Neurosci*. 2007 Nov 28;27(48):13117-29.